

# Redefining Integrated Assessment Models

An Exploratory Approach Towards  
Robust Climate-Economic Policies

Shajeeshan Lingeswaran

REDEFINING INTEGRATED ASSESSMENT  
MODELS: AN EXPLORATORY APPROACH  
TOWARDS ROBUST CLIMATE-ECONOMIC  
POLICIES

Master thesis submitted to Delft University of Technology  
in partial fulfillment of the requirements for the degree of

Master of Science

in Engineering and Policy Analysis  
Faculty of Technology, Policy and Management

by

Shajeeshan Lingeswaran

August 2019

An electronic version of this thesis is available at  
<http://repository.tudelft.nl/>.

Associated code and models are available at  
<https://github.com/shajeelwn/PyDICE>.

Shajeeshan Lingeswaran: *Redefining Integrated Assessment Models: An Exploratory Approach Towards Robust Climate-Economic Policies* (2019)  
© ⓘ This work is licensed under a Creative Commons Attribution 4.0 International License.



Economics of Technology and Innovation  
Engineering and Policy Analysis  
Faculty of Technology, Policy & Management  
Delft University of Technology

Supervisors: Dr. Servaas Storm  
Dr. Jan Kwakkel  
Prof. Dr. Cees van Beers

## ACKNOWLEDGEMENTS

This manuscript marks the end of my journey at the Delft University of Technology. As such, my main aim in choosing this research topic was not only to contribute to a global grand challenge but also to exemplify the capabilities and strengths of a graduate of the master's program Engineering and Policy Analysis (EPA).

The EPA master's program would not be the same without the diverse range of knowledge holders who were more than willing to share their world views, passions, and expertise with their students. I am very grateful for the opportunity to have worked with two of the most inspiring personalities at EPA.

If a professor can manage to spark the curiosity of his students to a field which she/he was never interested in, it says a lot about the personality, character, and expertise of this person. Servaas is one of these few professors. I am very thankful to not only for your academic guidance but also for your personal advice knowing my personality very well.

At a time, when doubts about modeling and simulation started to creep into my mind, the course Model-based Decision-Making showed me the never-ending potential of the field. Many thanks for your expertise and your inspiration, Jan.

It is the friends, we meet along the way that help us to appreciate the journey. Thus, I am grateful to have met my *EPA Support Group*, Amir, Bramka and Alper, who have helped me in their own individual way to overcome the hurdles of this thesis whether academic or personal. But especially, I want to send my deepest gratitude to Mikhail, Ammar, Yubin, and Merih with whom I have spent almost every second of the last two years. Thank you for everything!

Lastly, I want to thank my family for their unconditional support and love. Without them, I would not be the man who I am today.

Like all great travelers, I have seen more than I remember, and remember more than I have seen.

*Shajeeshan Lingeswaran  
Den Haag, August 2019*

# EXECUTIVE SUMMARY

The Dynamic Integrated Model of Climate and the Economy (DICE) of the Nobel laureate Nordhaus, which can be classified as an Integrated Assessment Models (IAMs), is aiming to shed light on the cost-benefit of climate mitigation's. However, current IAMs are depicted with a wide range of weaknesses [Storm, 2017; Pindyck, 2017; Weyant, 2017]. Next to questionable assumptions of model functions, such as the damage function, IAMs are inadequate at addressing deeply uncertain parameters, such as the equilibrium climate sensitivity (ECS).

Various research has been conducted in addressing these structural and parametric uncertainties by utilizing stochastic dynamic programming or approximate dynamic processing. However, two crucial aspects were not considered in these studies. First, most researchers utilized optimization to determine the optimal policy as their decision analytic method for the risk analysis. Yet optimal strategies are highly sensitive to uncertainties and thus, they lose their prescriptive value in deep uncertain environment like in the field of climate economics. Therefore, it is better to consider robust policies in regards to systems with manifold of deep uncertainties. Second, many economist described the deep uncertainties of IAMs model by a normal distribution, at best by log-normal distribution. However, Weitzman [2009a] has shown in his Dismal Theorem, that deep “uncertainty in the form of fat tails is, at least in theory, capable of swamping the outcome of any CBA”. This research is aimed in overcoming the mentioned issues and thus, the following research question was answered:

## Main Research Question

*What are the repercussions of fat-tailed distributions over uncertain parameters on the outcomes and on the robustness of the policy options of the DICE simulation model?*

To address this research question, the field of decision making under (deep) uncertainty offers a methodological framework, namely multi-scenario Many-Objective Robust Decision Making (MORDM) [Lempert and Collins, 2007; Lempert et al., 2006; Kwakkel et al., 2016b; Kasprzyk et al., 2013; Watson and Kasprzyk, 2017]. Multi-scenario MORDM does not only facilitate a framework to analyze the repercussion of fat-tailed distributions on the outcome space but also to generate robust candidate strategies (see Figure 3.5). However, finding a set of robust candidate strategies requires the evaluation of different policy options against a large ensemble of possible future states of the system. For this purpose, a simulation model is mandatory. Therefore, this study has reconstructed the DICE optimization model into a stochastic simulation model, called PyDICE.

The repercussion of fat-tailed distributions are analyzed through global sensitivity analysis (GSA), exploratory analysis, statistical analysis and scenario discovery. The latter two techniques has been applied on Nordhaus optimal policy to further underline the devastating effects of deep uncertainties on the outcomes. Since the PyDICE is a non-linear and relatively fast model, this study has used variance based GSA to measure the development of sensitivity of outcomes on the identified uncertainties (see Table 4.3). Exploratory analysis is used to generate a initial understanding about the effects of fat-tailed distribution, damage function and the combination of both on the outcomes of interest (see Table 4.1). This first observations are further highlighted by a statistical analysis. Lastly, vulnerable scenarios of Nordhaus optimal policy has been discovered using time series clustering and directed scenario search technique. In time series clustering, the time series are partitioned into “appropriate” number of clusters by applying unsupervised machine learning algorithm on the data set. For each outcome variable, the least “favourable” clusters has been investigated with the aim to identify vulnerable regions in the uncertainty space which led to those outcomes. Lastly, robust policy alternatives has been identified by using multi-objective evolutionary algorithm (MOEA). Further, the robustness of the identified policies has been evaluated against a large number of alternative future states in order to determine their robustness by utilizing the signal-to-noise ratio criterion and the minimax regret criterion.

The results of this study show that the effect of fat-tailed distribution is substantial as the optimal policy of Nordhaus fails in 328 out of 30000 scenarios, in which the failure scenarios comprises of either a Cauchy distributed ECS parameter or log-normal distributed ECS parameter. The high impact of fat-tailed distribution has also been unanimously found in the exploratory analysis, statistical analysis and global sensitivity analysis. Moreover, it has also been shown that as fatter the tail of the distribution becomes, the more severe are the consequences. However, it is important to note that, that disastrous outcomes are only reached in combination with damage function similar to Weitzman. Furthermore, this study has shown that in contrast to Nordhaus optimal policy, the Pareto optimal robust policies set a lower pure rate of social time preference and a far earlier emission control rate target between 2060 and 2070. In addition to this point, it has also been observed that robust policies are located at the edges of the defined policy space. This means to avoid catastrophic outcomes from deep uncertainties (incl. fat-tailed distribution and damage functions), policies must be more radical than suggested by Nordhaus, but much closer to the demands of climate scientists.

Lastly, it can be concluded that as long as scientific ambiguity surrounds parameters such as the equilibrium climate sensitivity parameter or the damage function, one has to explore all possible alternatives to deduct a robust set of policies. The implications of using the traditional method for risk and decision analysis (optimization) instead of methods like multi-scenario MORDM (robust optimization) is that disastrous events in future will be considered in hindsight as “Black Swans” although they were predictable “Grey Swans” all the time.

# CONTENTS

<b>I</b>	<b>Introduction</b>	<b>1</b>
<b>1</b>	<b>INTRODUCTION</b>	<b>2</b>
1.1	Integrated Assessment Models . . . . .	2
1.2	Dynamic Integrated Climate Economic Model . . . . .	3
1.3	Uncertainty Analysis . . . . .	4
1.4	Academic Research Gap . . . . .	5
<b>2</b>	<b>RESEARCH DEFINITION</b>	<b>7</b>
2.1	Research Question . . . . .	7
2.2	Research Methods . . . . .	7
2.3	Thesis Structure . . . . .	9
<b>3</b>	<b>BACKGROUND AND CONTEXT</b>	<b>10</b>
3.1	Uncertainty . . . . .	10
3.2	Fat-Tailed Distribution . . . . .	12
3.2.1	Black Swans . . . . .	12
3.2.2	Epistemic Crisis . . . . .	12
3.3	Dynamic Integrated Model of Climate and Economic . .	13
3.3.1	Model Structure . . . . .	13
3.3.2	Critics . . . . .	17
3.4	Decision Making under Deep Uncertainty . . . . .	21
3.4.1	Optimality vs. Robustness . . . . .	21
3.4.2	Exploratory Modelling and Analysis - Stochastic Optimization . . . . .	22
<b>II</b>	<b>Methods</b>	<b>25</b>
<b>4</b>	<b>MODEL CONCEPTUALIZATION</b>	<b>26</b>
4.1	DICE Simulation Model: PyDICE . . . . .	26
4.2	Verification . . . . .	28
4.3	PyDICE XLRM Structure . . . . .	29
4.3.1	“M”: Outcomes . . . . .	30
4.3.2	“L”: Policy Levers . . . . .	30
4.3.3	“X”: Uncertainties . . . . .	32
4.3.4	“R”: Relations . . . . .	36

<b>5 OPEN EXPLORATION</b>	37
5.1 Sampling Techniques . . . . .	37
5.2 Statistical Analysis . . . . .	38
5.3 Global Sensitivity Analysis . . . . .	39
<b>6 SCENARIO DISCOVERY</b>	42
6.1 PRIM & CART . . . . .	42
6.2 Time Series Clustering . . . . .	43
6.3 Directed Scenario Search . . . . .	45
6.4 Scenario Selection . . . . .	46
<b>7 POLICY DISCOVERY</b>	48
7.1 Directed Policy Search . . . . .	48
7.1.1 Multi-objective evolutionary algorithms . . . . .	48
7.1.2 Pareto-based MOEA: $\epsilon$ -NSGA-II . . . . .	49
7.2 Uncertainty Analysis . . . . .	50
<b>III Results</b>	51
<b>8 OPEN EXPLORATION</b>	52
8.1 Initial Exploration . . . . .	52
8.2 Global Sensitivity Analysis . . . . .	54
<b>9 ANALYSIS OF NORDHAUS OPTIMAL POLICY</b>	59
9.1 Initial Exploration . . . . .	59
9.2 Statistical Analysis . . . . .	66
9.2.1 Effect of Fat-Tailed ECS Parameter . . . . .	66
9.2.2 Effect of Damage Function . . . . .	67
9.2.3 Effect of Damage Function and Fat-Tailed ECS Parameter in Combination . . . . .	68
9.3 Scenario Discovery . . . . .	71
9.3.1 Time Series Clustering . . . . .	71
9.3.2 Directed Scenario Search . . . . .	77
<b>10 POLICY DISCOVERY</b>	79
10.1 Scenario Selection . . . . .	79
10.2 Directed Policy Search . . . . .	80
10.3 Uncertainty Analysis . . . . .	82
<b>IV Discussion</b>	87
<b>11 CONCLUSION</b>	88
11.1 Revisiting the Sub-Research Questions . . . . .	88
11.2 Answering the Main Research Questions . . . . .	93
<b>12 DEBATE</b>	95
12.1 Policy Advice . . . . .	95
12.2 Salvation of Integrated Assessment Models . . . . .	96
12.3 Unbiased Biased Choices . . . . .	99
<b>13 FUTURE AVENUES</b>	101

Appendices	111
A VERIFICATION	112
B OPEN EXPLORATION	115
C GLOBAL SENSITIVITY ANALYSIS	119
D STATISTICAL ANALYSIS	126
E UNCERTAINTY ANALYSIS	133

# LIST OF FIGURES

Figure 3.1	Structure of the DICE Model described in an aggregated hybrid Casual Loop Diagram. . . . .	13
Figure 3.2	Estimates of the probability distribution for climate sensitivity in degrees Celsius [Heal and Millner, 2014]. . . . .	19
Figure 3.3	The variety of different damage functions which can be found in climate economics literature's .	20
Figure 3.4	The XLRM framework adopted from Kwakkel [2017]. . . . .	22
Figure 3.5	Multi-Scenario MORDM Process adopted from Bartholomew [2018] . . . . .	23
Figure 4.1	Comparison between PyDICE and DICE. Left panel: Emissions control rate; Right panel: Savings rate. . . . .	26
Figure 4.2	Comparison between PyDICE and DICE with the optimized outcome of Nordhaus optimal policy for the parameter control rate $t$ and savings rate $srt$ . . . . .	28
Figure 4.3	Comparison between PyDICE and DICE with the integrated functions for emission control rate 4.2 and savings rate 4.2. . . . .	29
Figure 4.4	The damage functions of the PyDICE model. For completeness, the algebraic damage function Newbold and Daigneault is illustrated. . . . .	35
Figure 5.1	Sampling Techniques [Buchheit et al., 2019] . . . . .	37
Figure 5.2	Visualization examples in statistical analysis. a): Boxenplot; b): Pairplot. . . . .	38
Figure 5.3	GSA decision tree. . . . .	41
Figure 6.1	Scenario Discovery using directed search over uncertainties and times series clustering. . . . .	45
Figure 7.1	An illustrative example of epsilon dominance [Woodruff and Herman, 2013]. . . . .	49
Figure 8.1	Time series plots and boxenplots over every outcomes of interests. . . . .	53
Figure 8.2	Sobol indices for the outcome atmospheric temperature: Each cell illustrates the (global) sensitivity of the uncertainties (rows) on the outcome variable for the years 2050, 2100, 2150, 2200, 2300 (columns). . . . .	55
Figure 8.3	Sobol indices for the outcome damages: Each cell illustrates the (global) sensitivity of the uncertainties (rows) on the outcome variable for the years 2050, 2100, 2150, 2200, 2300 (columns).	56

Figure 8.4	Sobol indices for the outcome total output: Each cell illustrates the (global) sensitivity of the uncertainties (rows) on the outcome variable for the years 2050, 2100, 2150, 2200, 2300 (columns).	57
Figure 8.5	Sobol Indices for the outcome utility: Each cell illustrates the (global) sensitivity of the uncertainties (rows) on the outcome variable for the years 2050, 2100, 2150, 2200, 2300 (columns)	57
Figure 9.1	For the year 2050 (a) and 2300 (b), pair plot over the outcome variable is presented. A third dimension is added to the pair plot by colouring each point based on the utilized distribution type for the ECS parameter. Besides the cells in the diagonal axis of the pair plot (which illustrates the distribution of each outcome), each cell illustrates a scatter plot of two different outcomes of interest.	60
Figure 9.2	For the year 2050 (a) and 2300 (b), pair plot over the outcome variable is presented. A third dimension is added to the pair plot by colouring each point based on the damage function. Besides the cells in the diagonal axis of the pair plot (which illustrates the distribution of each outcome), each cell illustrates a scatter plot of two different outcomes of interest.	62
Figure 9.3	For the year 2050 (a) and 2300 (b), pair plot over the outcome variable is presented. A third dimension is added to the pair plot by colouring each point based on the combination of damage function and the distribution type. Besides the cells in the diagonal axis of the pair plot (which illustrates the distribution of each outcome), each cell illustrates a scatter plot of two different outcomes of interest.	64
Figure 9.4	Distributions of the simulation outcomes for the three ECS distribution functions at the time points 2050, 2100, 2150, 2200 and 2300 are illustrated in boxenplots.	66
Figure 9.5	Distributions of the simulation outcomes for the three damage functions at the time points 2050, 2100, 2150, 2200 and 2300 are illustrated in boxenplots.	68
Figure 9.6	Distributions of the simulation outcomes for the nine different combinations between the three damage functions and the three ECS distribution types at the time points 2050, 2100, 2150, 2200 and 2300 are illustrated in boxenplots.	69
Figure 9.7	The average silhouette widths of CID-generated for k amount of clusters ( $k = [2, 13]$ ).	71

Figure 9.8	For the outcome atmospheric temperature: a) Time Series Clustering; b) Input space of the undesired cluster. . . . .	72
Figure 9.9	Clustered space of the outcome damages: a) Time Series Clustering; b) Input space of the undesired cluster. . . . .	74
Figure 9.10	For the outcome total output: a) Time Series Clustering; b) Input space of the undesired cluster. . . . .	75
Figure 9.11	For the outcome cumulative discounted utility: a) Time Series Clustering; b) Input space of the undesired cluster. . . . .	76
Figure 9.12	Uncertainty space of the worst case scenarios from the directed scenario search. . . . .	77
Figure 10.1	Results of the scenario selection algorithm illustrating the K=4 maximum diverse scenarios (coloured in yellow, green, blue, purple) from N=490 policy relevant scenarios (light grey). . . . .	80
Figure 10.2	Epsilon progress for each maximum identified scenarios. . . . .	81
Figure 10.3	Candidate strategies generated for the a) scenario 102, b) scenario 354, c) scenario 467, d) scenario 473. . . . .	81
Figure 10.4	The 10 most robust polices after applying the SNR criterion. . . . .	83
Figure 10.5	Comparison of the SNR policies to Nordhaus optimal policy. . . . .	83
Figure 10.6	The 10 most robust polices after applying the minimax regret criterion. . . . .	84
Figure 10.7	Comparison of the MiniMax policies to Nordhaus optimal policy. . . . .	85
Figure B.1	For the years 2050(a),2100(b),2150(c),2200(d) and 2300(e), pair plot over the outcome variable is presented with the third dimension describing ECS distribution types. . . . .	116
Figure B.2	For the years 2050(a),2100(b),2150(c),2200(d) and 2300(e), pair plot over the outcome variable is presented with the third dimension describing the damage functions. . . . .	117
Figure B.3	For the years 2050(a),2100(b),2150(c),2200(d) and 2300(e), pair plot over the outcome variable is presented with the third dimension describing the combination of damage function and ECS distribution . . . . .	118
Figure C.1	Results of the global sensitivity analysis of the uncertainties on the outcome atmospheric temperature at the time points 2050(a), 2100(b), 2150(c), 2200(d) and 2300(e) (with confidence intervals). .	120

Figure C.2	Results of the global sensitivity analysis with confidence intervals of the uncertainties on the outcome damage at the time points 2050(a), 2100(b), 2150(c), 2200(d) and 2300(e) (with confidence intervals). . . . .	121
Figure C.3	Results of the global sensitivity analysis of the uncertainties on the total output at the time points 2050(a), 2100(b), 2150(c), 2200(d) and 2300(e) (with confidence intervals). . . . .	122
Figure C.4	Results of the global sensitivity analysis of the uncertainties on the outcome utility at the time points 2050(a), 2100(b), 2150(c), 2200(d) and 2300(e) (with confidence intervals). . . . .	123
Figure C.5	Results of the global sensitivity analysis of the levers on the outcomes atmospheric temperature(a), damages(b), total output(c), and utility(d). . . . .	125
Figure E.1	The output space of the ten most robust policies according to the SNR criterion . . . . .	134
Figure E.2	The output space of the ten most robust policies according to the maximum regret criterion . . .	135

# LIST OF TABLES

Table 3.1	Five Levels of Uncertainty (adopted from Walker et al. [2013]) . . . . .	11
Table 4.1	Outcomes of Interest. . . . .	30
Table 4.2	Policy Levers. . . . .	31
Table 4.3	Deep Uncertainties. . . . .	32
Table 4.4	Equilibrium Climate Sensitivity estimation of the IPCC AR5 and [Rogelj et al., 2012]. . . . .	34
Table 4.5	Statistical Sizes of the Equilibrium Climate Sensitivity Distributions. . . . .	35
Table 9.1	Nordhaus Optimal Policy in PyDICE parameters	59
Table 9.2	Number of chosen clusters for the outcome parameter . . . . .	72
Table 10.1	Selected scenario based on diversity and policy relevance for alternative policy determination. . . . .	79
Table A.1	Comparison of the PyDICE and the DICE on the parameters emission control rate, per period utility, emission, atmospheric temperature, damage and total output with the optimized outcome of Nordhaus optimal policy for the parameter control rate $s_t$ and savings rate $sr_t$ . . . . .	113
Table A.2	Comparison of the PyDICE and the DICE on the parameters emission control rate, per period utility, emission, atmospheric temperature, damage and total output with the integrated functions (4.1) and (4.2) for emission control rate 4.2 and savings rate 4.2 . . . . .	114
Table D.1	Descriptive statistics of the simulation outcomes for the three ECS distribution functions at the time points 2050, 2100, 2150, 2200 and 2300. . . . .	127
Table D.2	Descriptive statistics of the simulation outcomes for the three damage function at the time points 2050, 2100, 2150, 2200 and 2300. . . . .	128
Table D.3	Descriptive statistics of the outcome atmospheric temperature for the nine different combinations between the three damage functions and the three ECS distribution functions at the time points 2050, 2100, 2150, 2200 and 2300. . . . .	129
Table D.4	Descriptive statistics of the outcome damages for the nine different combinations between the three damage functions and the three ECS distribution functions at the time points 2050, 2100, 2150, 2200 and 2300. . . . .	130

Table D.5	Descriptive statistics of the outcome total output for the nine different combinations between the three damage functions and the three ECS distribution functions at the time points 2050, 2100, 2150, 2200 and 2300. . . . .	131
Table D.6	Descriptive statistics of the outcome utility for the nine different combinations between the three damage functions and the three ECS distribution functions at the time points 2050, 2100, 2150, 2200 and 2300. . . . .	132

## LIST OF ALGORITHMS

6.1 Complexity-Invariant Distant (CID) measure for time se- ries . . . . .	44
---	----



# **Part I**

## **Introduction**

“Economists set themselves too easy, too useless a task, if in tempestuous seasons they can only tell us, that when the storm is long past, the ocean is flat again.” -

John Maynard Keynes

# 1

## INTRODUCTION

In October 2018, the [IPCC \[2018\]](#) has released a landmark report which emphasized that the world community has only 12 years to keep the global warming at a maximum of 1.5°C. Even a half-degree difference would mean the eradication of our coral reefs. This would increase the pressure on the Arctic sheets and thus would accelerate global warming. These predictions became truly real by the fact that the record-breaking summer of 2019 led to an increased ice sheet melt and thaw lakes equal to the worst recorded melt year in 2012 [[Borunda, 2019](#)]. Furthermore, the 2019 heatwave is different from the heatwave in 2012 as it has occurred in the absence of El Niño. An international consortium of climate scientist concluded that the 2019 heatwave would have been extremely unlikely without human-caused global warming, with a chance of only once in a thousand years [Vautard et al. \[2019\]](#). To make the matter worse, climatologists predict that these weather patterns will occur almost every summer by 2050 [[Borunda, 2019](#)]. As has been seen with the extreme wildfire in Siberia due to the 2019 heatwave, human-induced global warming increases substantially the risk of natural catastrophes like droughts, wildfires and floods all around the world. According to a variety of sources, including the United Nations Office for Disaster Risk Reduction (UNISDR) and big insurance companies such as the Munich RE, the losses from natural catastrophes amounted to US\$ 334bn just in 2017 [[United Nations, 2018; Straub, 2018](#)]. Losses of this magnitude lead to the question of common sense: Why has the international community not invested yet in climate mitigation to prevent future massive economic losses?

### 1.1 INTEGRATED ASSESSMENT MODELS

The calculation of the cost-benefits of large-scale preventative investment demands models capable of capturing the complex interaction between economy, climate system and earth system. Conventionally, these models are captured under the umbrella term “Integrated Assessment Model” (IAM). IAMs can be distinguished between simple IAMs and detailed IAMs. Whereas simple IAMs estimate mitigation costs and future climate damages based on relatively simple assumptions, complex IAMs comprises complete energy system models, land use models as well as detailed population models. Although the structure and the transparency of the assumptions underlying the IAM have been challenged, IAMs are an essential tool to support the decision-making of policy makers [[Pachauri and Mayer, 2014; Metcalf and Stock, 2015; Weyant, 2017](#)].

Critics have attributed a wide range of weaknesses to IAMs. Former co-chair of the Intergovernmental Panel on Climate Change (IPCC) working group and current senior advisor of the European Climate Foundation (ECF), Dr. Bert Metz, argues while IAMs “can paint a reasonable picture of what the future would look like... they are based on assumptions. So, the strength of that picture depends on the strength of your assumptions.” [Carbon Brief, 2018]. Moreover, Dr. Céline Guivarch, senior researcher at Centre International de Recherche sur l’Environnement et le Développement (CIRED), states accurately that “fundamentally, the issue of climate change is a question of decisions under deep uncertainty, which we have to accept and embrace. We have to make decisions that are robust against uncertainty” [Carbon Brief, 2018]. In contrast, IAMs often adopt deterministic estimates about variety of deeply uncertain parameters which results often in policy proposals with no/little action. Although some structural as well as parametric uncertainties will be outside of the realm of our expectation, a robust decision under uncertainty requires the assessment of all plausible scenarios [Walker et al., 2013].

## 1.2 DYNAMIC INTEGRATED CLIMATE ECONOMIC MODEL

This also applies to the family of models of the Nobel Prize winner Dr. William Nordhaus, the Dynamic Integrated Model of Climate and the Economy (DICE)/ Regional Integrated Model of Climate and the Economy (RICE) [Nordhaus, 2008a]. Whereas the DICE model takes a global perspective, the RICE model is grouped into 12 regions. The DICE is mainly utilized to estimate the Social Cost of Carbon (SCC). The SCC is “the cumulative economic impact of the global warming caused by (or attributed to) each tonne of the pollutant sent into the atmosphere” [Nature, 2018]. Nordhaus DICE model is suggesting that the optimal pathway<sup>1</sup> of the carbon price ascends from \$21.2/t CO<sub>2</sub> in 2020 to about \$51.5/t CO<sub>2</sub> in 2050 [Nordhaus, 2014]. However, this optimum is reached with an increase of the global mean temperature around 3.5°C above pre-industrial levels [Nordhaus, 2014]. It conflicts with the prevailing consensus among climate scientist that the increase in global mean temperature has to be kept below 1.5°C to 2°C [IPCC, 2014, 2018]. However, this has the consequence that policy-makers, such as the Obama administration [Bell and Callan, 2011], line-up behind the results of the DICE model, as it gives them the “scientific” evidence that government intervention to limit the mean temperature to already 2.5°C would make them - in the context of economic growth - worse off [Nordhaus, 2014].

Further, recent literature argues that the DICE model includes improbable assumptions on climate damage functions, economic growth and climate risks which does not represent the possibility of a catastrophic climate outcome. IAMs ignore the non-zero probability of calamitous warming. This lead to a distorted picture of the cost-benefit estimation [Weitzman, 2009a, 2011; Pindyck, 2017; Millner, 2013; Heal and Millner, 2014; Weyant, 2014; Rosen and Guenther, 2015; Moore and Diaz, 2015].

---

<sup>1</sup>The optimal pathway is a climate policy scenario, that optimizes the time path of emission reductions and investment.

However, various researchers from different fields made attempts to adjust the DICE model of Nordhaus. For instance, Weitzman [2009a] has proposed an alternative climate damage function that put more emphasis on the climate change impacts for larger temperature increases. It displays the structural uncertainty of the DICE model. Moreover, Roe and Baker [2007] argued that the climate sensitivity parameter is deeply uncertain and that the right-hand tail of its distribution is even “fat”.

### 1.3 UNCERTAINTY ANALYSIS

The evaluation of such exogenous parameters is generally well fitted for an approach called uncertainty propagation. In this approach, the optimization model is executed over many possible parameter combinations. The outcomes of those runs may be combined in a weighted-average if a probability distribution is identified [Golub et al., 2014]. This Monte Carlo type of approach is very popular in literature [Nordhaus, 2008a; Dietz, 2011; Ackerman et al., 2010]. However, this approach has its limits in analyzing endogenous uncertainties such as the damage function or the development of technology. The literature has illustrated different alternative approaches [Shayegh and Thomas, 2015; Chang, 2014; Traeger, 2014; Ackerman et al., 2010]. However, due to computational limitations of linear optimization models, these models just comprise two-stages and a couple of scenarios. A further approach to include uncertainties is stochastic dynamic programming [Chang, 2014]. The outcomes of these approaches show a steady increase in the expected abatement path and thereby support the claims of climate scientist for stricter climate mitigation policy [Chang, 2014]. Another research covered the uncertainty aspect by using the Approximate Dynamic Processing for the DICE model [Traeger, 2014]. The approximation model utilized basic functions to approximate future states on a continuing or a finite horizon. The model was later extended by Shayegh and Thomas [2015]. Their research aimed at the uncertain property of the climate sensitivity parameter in relation to the risk of hitting a climate tipping point. Since Shayegh and Thomas [2015] focus on the result of tipping points, they did not include the “pure” continuous response of the model to uncertainty in the climate sensitivity parameter.

Furthermore, Wagner and Weitzman [2018] highlighted the importance of conceptualizing climate policy from the perspective of risk management. Moreover, they supported the claim of Tol [2003], that there is a sound logic that the uncertainties about the shocks of climate change are fat-tailed [Weitzman, 2009a, 2011, 2013]. More specifically, if there is a reasonably large body of empirical evidence for a parameter, then the best estimate of this distribution might be a normal distribution or other “thin-tailed” distribution. But then again, in a complex uncertain system such as in the field of climate economic, sufficient knowledge about certain parameters are limited. Therefore, Weitzman argues that the best available estimate for parameters with a small number of observations are fat-tailed distribution, with relatively high probabilities of extreme values. However, Nordhaus points out that it is in contrast to the axiom of decision-making under uncertainty as it leads theoretically to

infinite large preventative investment. Weitzman is aware of this and emphasizes that the “infinite limit in [his] Dismal Theorem is a formal mathematical way of saying that structural uncertainty in the form of fat tails is, at least in theory, capable of swamping the outcome of any cost-benefit analysis (CBA) that disregards this aspect.” [Weitzman, 2009b]. Moreover, Weitzman points out that the worrisome part of a fat-tailed probability density function (PDF) is not that it is long but rather that it is fat. Thus, he is more concerned about how fast the probability of a catastrophe declines relative to the welfare impact.

To overcome the issue raised by Weitzman’s Dismal Theorem, several concepts have been explored in implementing uncertainties and fat-tailed distributions into IAMs. For instance, Newbold and Daigneault [2009] impose a lower bound on consumption whereas Costello et al. [2010] put an upper bound on temperature rise. Furthermore, Pindyck [2011] places an upper bound on marginal utility. Ikefuji et al. [2014] utilize a bounded utility function instead of the constant relative risk aversion (CRRA) function. Ackerman et al. [2010] draws a sample from key parameters based on fat-tail distribution and then simulate the model. Hwang et al. [2014] analyzed the impacts of tails with the curvature of carbon-tax function according to uncertainty.

## 1.4 ACADEMIC RESEARCH GAP

Multiple research was conducted in adopting uncertainties into the DICE model without altering the nature of it as an optimization model. However, Pindyck [2011, 2013, 2017], Heal and Millner [2014], and Boyce [2017] have argued that Integrated Assessment Models such as the DICE/RICE model are not accurate enough to be used for predictions and calculating the optimal outcomes. They argue that IAMs should be rather utilized to first analyze the behaviour of the complex and uncertain system of climate economics, and to derive answers to the “what-if” questions. Furthermore, Lempert et al. [2006] puts forward that in deep uncertain systems, analyst should rather search for the most robust solution rather than the optimal solution. Therefore, the research aims to transform the model from a non-linear optimization model into a discrete simulation model. By utilizing the simulation model the details of the current system become less important while the variety of multiple possible paths becomes more essential. Especially the very presence of deep uncertainties indicates the need to compare several alternative paths and their end states based on diverse assumptions. Although, Ackerman et al. [2010], Hwang et al. [2014] and others have replaced the deterministic assumption of uncertain parameters in IAMs with a normal distribution or at best with a log-normal distribution to cope with Weitzman’s Dismal Theorem, it is still worth conducting research around this topic for the following reasons. First of all, every reviewed literature so far has used a different methodology to integrate and to analyze the effects of the fat-tailed distribution in Integrated Assessment Models. This demonstrates that there is still a dissent in the academic community around the subject matter of decision-making under uncertainty. Second, we have seen that within the research community there is dissonance

about the usefulness of integrating fat-tailed distributions into the DICE/RICE model. At last, to the best knowledge of the author, there is no work done in understanding the implication of fat-tailed uncertainties on the robustness of climate-economic policies.

# 2 | RESEARCH DEFINITION

## 2.1 RESEARCH QUESTION

The detected academic research gap, in Section 1.4, is the driving force behind this research. This research is proposed as a master thesis for Engineering and Policy Analysis program at the Delft University of Technology. This master thesis is aimed at clarifying the distorted picture of Integrated Assessment Models by exploring the effect of fat-tailed uncertainties on the outcomes of a stochastic simulation version of the DICE model. Thus, the following research question is raised:

### Main Research Question

*What are the repercussions of fat-tailed distributions over uncertain parameters on the outcomes and on the robustness of the policy options of the DICE simulation model?*

## 2.2 RESEARCH METHODS

The following research methods are utilized to enlighten the before defined research question. In the following, the methods and its sub-research questions are presented:

Earlier, we acknowledged that the DICE model comprises uncertain parameters. As climate change models are built on numerous uncertainties, the use of a simulation model over an optimization model is preferred [Pindyck, 2013; Heal and Millner, 2014]. With transforming the linear optimization model into a simulation model, there is often a significant amount of ambiguity on how to describe the parameters of the objective function in a simulation model. Since many of the analysis tools is written in the high-level programming language, Python, the simulation model is also implemented in Python to ensure an easy integration. In the next research step, the crucial uncertainties are described by either a uniform distribution, when there is no prior knowledge about its probability, or a fat-tail distribution using empirical data from literature, i.e. Ackerman et al. [2010]; Wagner and Weitzman [2018]; Hwang et al. [2013]. After the deep uncertainties and stochastic uncertainties has been defined, this will be integrated to the DICE model.

**SQ1:** *Which fat-tailed distributions are used to describe the uncertain parameter and how are they integrated into the DICE simulation model?*

Once the model conceptualization, formalization and implementation are done and the DICE model is extended by the ability to characterize uncertainties by fat-tailed distribution. At first, the model is explored over large set of scenarios and a dozen policies to illustrate the different pathways and behaviours of the model outcomes. Next, a global sensitivity analysis (GSA) is conducted. A GSA allows us to rank how uncertainties in output are attributed to different sources, i.e. to determine from where the uncertainty is coming from. In addition, the sensitivity analysis is also run over policy levers to provide similar insights. The goal of this GSA is to identify the most important components of the model that will have the greatest effect on the anticipated outcome. This allows us to focus on the most important uncertainties. Furthermore, the intent is to provide insight into uncertainty interactions within the model and if any uncertainties can be selected specifically to mitigate potential adverse consequences [Cariboni et al., 2007]. In this research, a variance-based GSA, namely the Sobol method, is applied.

**SQ2:** *How sensitive are the outcomes of the DICE simulation model to the identified uncertainties?*

In the next research step, Nordhaus optimal policy is evaluated over different future states of the world. Hereby, the outcomes are statistically analyzed. At this point, it is attempted to reach a conclusion about the effect of fat-tails on the outcomes. The research is limited to determine normatively the rightfulness of Weitzman's Dismal Theorem instead of conducting an extended mathematical proof. Subsequently, a scenario discovery in the form of time series clustering is applied on the optimum policy to illuminate its vulnerabilities. Note that in contrast to optimization modelling, in which scenarios are selected a-priori, in simulation modelling scenario discovery is used to reason backwards from intriguing future states to the combinations of uncertainties and levers that generated those states. Time series clustering is complemented by using Many-Objective Evolutionary Algorithm (MOEA) to identify worst case scenarios for the optimized policy by Nordhaus. From the identified scenarios from scenario discovery, a subset of four maximum diverse scenarios are selected as reference scenarios to discover robust policies. To attain a policy which minimizes the atmospheric temperature and damages and at the same time maximizes total output and utility, MOEA is used. In summary, this research follows the multi-scenario many-objective robust decision making (MORDM) framework (see Section 3.4). The results of the entire process are then reviewed with particular focus on the political and scientific ramifications of the identified measures. With the mentioned methods, the following sub-questions can be answered:

**SQ3:** *For which scenarios is the optimal policy of the DICE optimization model vulnerable?*

**SQ4:** *What are the robust set of policies for the DICE simulation model and how does they differ to optimal policy of the DICE optimization model?*

## 2.3 THESIS STRUCTURE

This master thesis is structured as follows: In the remainder of Part I, the fundamental concepts of the thesis of uncertainty, fat-tailed distributions, and decision-making under deep uncertainty are presented to the reader. Next, the internal dynamics and the main points of criticism of the DICE model are illustrated in 3. Part II of this manuscript provides an extensive description and justification of the chosen methods. It also presents, in 4, the conceptualization of the stochastic simulation version of the DICE model, PyDICE. The chosen methods and the formalized model are applied in Part II. Here the system behavior of PyDICE and the robustness of Nordhaus optimal policy under deep uncertainty is analyzed in detail. In the final chapter of Part III, a set of robust policies are determined and compared to Nordhaus optimal policy. Part IV connects the various results from Part III and thereby answers the main research question of this research. Furthermore, the implications of the findings for decision-makers, the use of Integrated Assessment Models and future avenues are discussed.

# 3 | BACKGROUND AND CONTEXT

In this chapter, background information around the key subjects of the thesis is presented. This is essential to understand the main body of the thesis. In that regard, this also illustrates the scope of the thesis. Section 3.1 presents the definition of uncertainty. Section 3.2 explores the socioeconomic and mathematical concept around fat-tailed distribution. In Section 3.3, the DICE model is introduced in detail as it forms the foundation of the thesis. Lastly, Section 3.4 introduces a methodological framework to cope with deep uncertainties.

## 3.1 UNCERTAINTY

In the earlier section, it was made clear that the climate economic systems are plagued with various types of uncertainties. However, the literature in the field of climate economics does not make any effort to differentiate between the uncertainties. As a result, the research community in the field of climate economics lacks the right methodology or understanding to treat the different types of uncertainties respectively. Therefore, this subsection is dedicated to clarify the term uncertainty and the various types.

In general, uncertainty describes an epistemic state of incomplete or unknown information [uncertainty, nd]. Knight [1921] was the first one to distinguish uncertainty between: known probabilities, “risk”, and unknown probabilities, “uncertainty”. Similar to the Knightian definition, Quade and Carter [1989] introduced also two categories of uncertainty: stochastic and real. Stochastic uncertainty is akin to Knightian risk whereas the real uncertainty is akin to Knightian uncertainty. This already shows that there is fundamental difference between stochasticity and uncertainty.

Later Walker et al. [2013] further distinguished uncertainties into five levels as described in Table 3.1. In addition, they have provided a set of methodologies for each level of uncertainty. The first level can be tackled with a simple sensitivity analysis of the model parameters. The sensitivity analysis will determine the impact of small perturbation of the input parameters on the output of the model. The second level uncertainty are stochastic uncertainties and thus can be addressed by statistical analysis. The analysis can be done using a forecast with a confidence interval, or several forecasts with associated probabilities. The third level is addressed via trend-based scenarios that are based on the different assumptions about the driving forces. The scenarios are later ranked depending on the perceived likelihood. Note that, no prob-

abilities are assigned to the scenarios. The four and fifth level uncertainties are the product of insufficient amount of information/knowledge. However, in a model with Level 4 uncertainty, there is a range of plausible scenarios which can be specified well enough to select a scenario with a possible acceptable outcome. Furthermore, different scenarios can be compared based on basic conditions that are believed to be true, and rule out the less favourable scenarios. This method is known as Exploratory Modelling and Analysis (EMA). Level 5 can be addressed by creating adaptive policies over time which in turn will change to adapt the possible scenarios based on new data over time, this method is called Adaptive Foresight.

**Table 3.1:** Five Levels of Uncertainty (adopted from [Walker et al. \[2013\]](#))

Level	Description
<b>Level 1</b>	occurs in a system with a clear enough future. However, the situation is not absolute certain.
<b>Level 2</b>	occurs in a system with alternate probable futures. The parameters are described sufficiently in statistical terms.
<b>Level 3</b>	occurs in a system in which alternate futures can be ranked. It is possible to enumerate alternatives and to rank them in terms of their likelihood.
<b>Level 4</b>	occurs in a system with a multiplicity of plausible futures. However, there is not enough information to rank those scenarios.
<b>Level 5</b>	occurs in a system with completely unknown futures. The system contains of various unknown “unknowns” which possibly have a high impact on the system.

[Walker et al. \[2013\]](#) subsumes Level 4 and Level 5 uncertainty under the term “deep uncertainty” akin to the Knightian uncertainty or Quades real uncertainty. Deep uncertainty is defined more specific by [Lempert et al. \[2006\]](#) as a situation when the analysts do not know (Level 5) or the parties to a decision cannot settle on (Level 4)

- the appropriate conceptual models that characterize the relationships among the key driving forces that shape the long-term future,
- the probability distributions used to perform uncertainty about key variables and parameters in the mathematical representations of these conceptual models, and/or
- how to value the desirability of alternative results.

## 3.2 FAT-TAILED DISTRIBUTION

### 3.2.1 Black Swans

Events resulting from systems with deep uncertainties (i.e., Level 5 uncertainty) can be called “Black Swans” [Taleb, 2010]. A Black Swan event is characterized by three main properties. First, a Black Swan event is outside of the realm of our expectations. Second, the occurrence of these events are only explainable in hindsight. And lastly, a Black Swan event has an extremely widespread effect on potentially other fields as the world becomes more complex. It is generally assumed that examples of Black Swan events ranges from the global financial crisis in 2008, the level 9.1 Tōhoku earthquake in 2011, the oil crisis in 2014 to the BREXIT in 2016. However many events such as the financial crisis in 2008 could have been predicted but experts in their respected fields have erroneously assigned a very low probability on the particular scenario and discarded from their forecasts. Such events are called “Grey Swans”. Moreover, Taleb [2010] reasons that the main reason that experts have underestimated the probability of those high impact event is due to their high confidence in Gaussian models. However, Mandelbrot [1997] has shown that many random variables observed from real-world processes, such as stock returns or daily river levels, follow fat-tailed distributions. Defining fat-tailed distributions with certainty is very difficult, as various authors use the terms fat-tailed and heavy-tailed (and sometimes even long-tailed distribution) interchangeably whereas others distinguish between fat-tailed and heavy-tailed. The following paragraph is dedicated to clarifying this malapropism.

### 3.2.2 Epistemic Crisis

Heavy-tailed distributions are probability distributions in which the tails of those distributions are not exponentially bounded. Hence, they consist of “heavier” tails than the exponential distribution. Distributions can be one-tailed or two-tailed. The same applies for tails, heavy-tailed distribution can be “heavy” on one tail or on two tails. Moreover, heavy-tailed distributions can be divided into three sub-classes: the fat-tailed distributions, the long-tailed distributions and the subexponential distributions. Thus, by definition, a fat-tailed distribution has the same attribute as the heavy-tailed distribution in terms of the large skewness and kurtosis. Further, every heavy-tailed distribution is a fat-tailed distribution but not every fat-tailed distribution is a heavy-tailed distribution [Taleb, 2006, 2015; Taleb et al., 2019].

According to Taleb [2010], there are three types of fat-tails:

1. any distribution with fatter tails than the normal distribution with more observations within one sigma and with a kurtosis  $Kurt[X] > 3$ ;
2. any distributions with a power-law decay in the tail of the distribution but not at every point along the distribution;
3. power-law distributions.

However, this thesis is not differentiating between the three types but rather regards them homogeneously. Thus, distributions are identified as fat-tailed if the kurtosis is leptokurtic:  $Kurt[X] > 3$ .

### 3.3 DYNAMIC INTEGRATED MODEL OF CLIMATE AND ECONOMIC

In 1992, Nordhaus published one of the first IAM models, the DICE model. In general, the DICE model is a simplified analytical and empirical model, that represents the optimal time path of emission reductions and associated carbon taxes in a fully dynamic Ramsey-type optimal growth model. Technically speaking, the DICE model is a non-linear, inter-temporal optimization model. Over the past years, the DICE model has gone through several revisions. Although the latest version of the model was updated in 2016 (DICE-2016R), this thesis uses the DICE-2013R version. The reason for this is that some parameters of the 2016 version were adjusted from the earlier version without any further explanations. In addition, the DICE-2013R version is well documented in the User's Manual online [Nordhaus, 2013] and thus the author is comfortable in utilizing the 2013 version for his study. Starting at year 2010, the model is solved in discrete time for sixty-time intervals of five years.

### 3.3.1 Model Structure

The DICE model consists of three sub-models: carbon, climate and economy. As stated earlier, the DICE model translates the effects of the climate change into a standard neoclassical optimal growth model, the Ramsey–Cass–Koopmans (RCK) model.

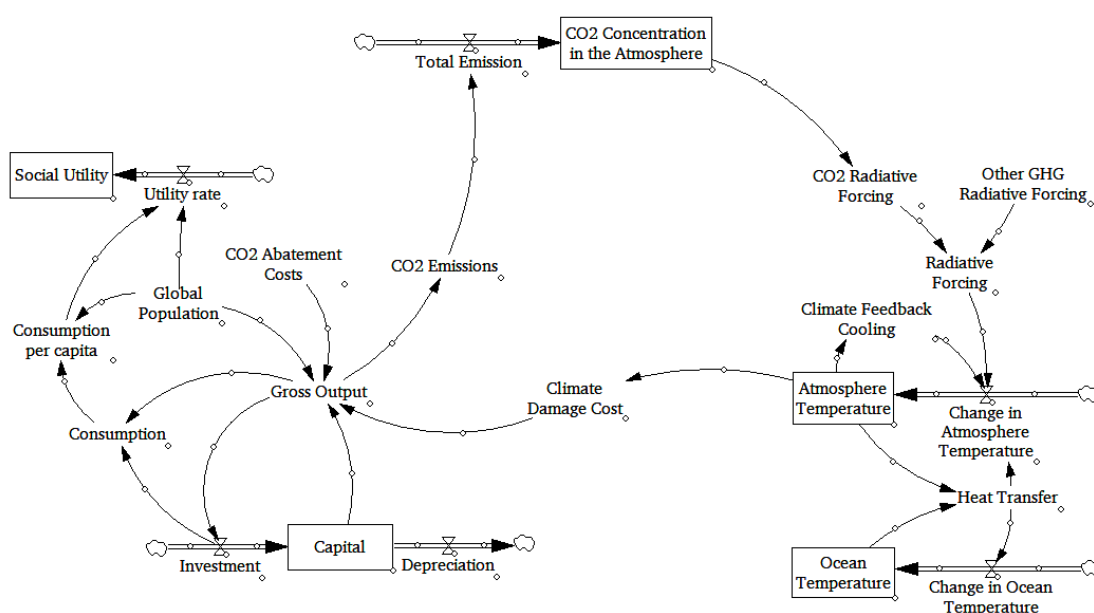


**Figure 3.1:** Structure of the DICE Model described in an aggregated hybrid Casual Loop Diagram.

In the RCK growth model, the key equation is the social planners' problem of maximizing social welfare function. The welfare is expressed as the discounted sum of all future utilities from consumption. Consumption is again a function of the world economic output. The output function is expressed as a Cobb-Douglas function and thus it only increases when there is a rise in the labour force and/or the productivity becomes efficient. With the increase in economic activity, Nordhaus assumes that more  $CO_2$  is emitted into the atmosphere. However, the  $CO_2$  in the atmosphere is passed through the upper ocean to the lower ocean, which reduces the  $CO_2$  concentration in the atmosphere. The remnant  $CO_2$  adds to the accumulated  $CO_2$  concentration in the atmosphere so that more "heat" is trapped which results in an increase in atmospheric temperature. The resulting climate damage costs from the increasing temperature reduces the world economic output. Climate damages can be abated using current investments. This fundamental interaction of the three sub-models of DICE is represented in Figure 3.1.

In the following paragraphs, the three sub-models are explored in detail and the mathematical representations of those model parameters are introduced.

### **Economic Sub-Model**

The economic sub-model is based on a standard neoclassical economic growth theory, namely the Ramsey–Cass–Koopmans (RCK) growth theory. The RCK model consists of two agents, households and firms. To maximize the present and future flow of discounted utilities,  $U_t$ , the households consume the world gross output,  $Y_{gross}$ , and invest in firms. The output itself is produced by similar firms which sell their products in a competitive market. Since all firms are held by households, the generated profits flow back to the households. The world gross output is expressed by the common Cobb-Douglas production function. The Cobb-Douglas production function exhibits constant returns to scale:

$$Y_{gross,t} = A_t L_t^{1-\gamma} K_t^\gamma \quad (3.1)$$

where:  $A_t$  : total factor productivity<sup>1</sup>  
 $L_t$  : population & labour force  
 $K_t$  : capital stock  
 $\gamma$  : output elasticity of capital.

The output elasticity of capital,  $\gamma$ , describes the responsiveness of output to a change in capital. The capital stock is accumulated by investment,  $I_t$ , and at the same time, it is reduced by depreciation rate of capital,  $\delta$ :

$$K_{t+1} = I_t T_{step} + (1 - \delta)^{T_{step}} K_t \quad (3.2)$$

where:  $T_{step}$  : time step.

The investment,  $I_t$ , is equal to the difference between total income,  $Y_t$ , and consumption,  $C_t$ :

$$I_t = Y_t - C_t. \quad (3.3)$$

A certain fraction of gross output is lost to damages and another to the cost of abatement. Thus, the resulting, total output is determined by:

$$Y_t = Y_{gross,t} * (1 - \Lambda_t - \Omega_t). \quad (3.4)$$

Although finding a reliable projection of the damages from climate change over the long-run seems to be extremely difficult [Pindyck, 2013], a damage function is imperative for the decision-making of finding the right balance between abatement costs and climate damages. Nordhaus attempt to express the damage function by,  $\Omega_t$ :

$$\Omega_t = \psi_1 T_{ATM,t} + \psi_2 (T_{ATM,t})^{\psi_3} \quad (3.5)$$

where:  $T_{ATM,t}$  : atmospheric temperature  
 $\psi_{1,2,3}$  : estimation parameters.

The damage function is calibrated using the estimation parameters,  $\psi_{1,2,3}$ , for damages between 0°C and 3°C Nordhaus [2013]. On the other hand, abatement function,  $\Lambda$ , which describes the ratio of abatement cost to output, increases exponentially to the emission control rate,  $\mu$ :

$$\Lambda_t = \Theta_1 \mu_t^{\Theta_2}. \quad (3.6)$$

Here, the backstop technology is expressed by the calibration parameters,  $\Theta_1$  and  $\Theta_2$ . Moreover, Nordhaus assumes that technological advancement will lead to an increase in efficiency of the backstop technology until the cost of abatement eventually reaches zero. The backstop technology is defined as a technology with the capability to remove carbon from the atmosphere or as an environmentally friendly zero-carbon energy technology.

With the above determined parameters, the households (social planner) are maximizing the social welfare function,  $W$ , or in economic terms, the discounted sum of utilities from consumption per capita:

$$W = \sum_{t=1}^{T_{max}} U(c_t) L_t R_t \quad (3.7)$$

where:  $c_t$  : consumption per capita  
 $L_t$  : population & labour force  
 $R_t$  : social discount factor  
 $U(c_t)$  : per-period utility function.

The per-period utility function,  $U(c_t)$ , is expressed by a Constant Relative Risk Aversion (CRRA) utility function:

$$U(c_t) = \frac{c_t^{(1-\alpha)} - 1}{1 - \alpha} - 1, \quad \text{for } \alpha < 1. \quad (3.8)$$

This function requires a constant elasticity of the marginal utility of consumption,  $\alpha^2$ . It is better described as the degree of relative generational inequality aversion. Simply put,  $\alpha$  depicts the diminishing social valuations of consumption of future generations. Further, the social discount factor is determined by:

$$R_t = \frac{1}{(1 + \rho)^t}. \quad (3.9)$$

The pure rate of social time preference,  $\rho$ , gives welfare weights on the utilities of different generations.

### ***Carbon Sub-Model***

The carbon sub-model calculates the radiative forcing on the basis of the carbon cycle which consists of three-reservoirs: atmospheric level, upper ocean level and deep ocean level. However, prior to this, the model first defines the total emission,  $E$ , which is defined by the sum of the endogenous industrial emissions,  $E_{Ind}$ , and the exogenous emissions from deforestation,  $E_{Land}$ :

$$E_t = E_{Ind,t} + E_{Land,t}. \quad (3.10)$$

The industrial emissions,  $E_{Ind}$ , are reflected in the economic activity of the world and it only can be reduced by the emission control rate,  $\mu_t$ :

$$E_{Ind,t} = \sigma_t Y_t (1 - \mu_t) \quad (3.11)$$

where:  $\sigma_t$  : emissions output ratio.

The total carbon emissions,  $E_t$ , feeds into the atmospheric reservoir of carbon and results in an increase of  $CO_2$  concentration. From there, a certain portion of the total emission is transferred to the carbon reservoirs of the lower and deeper ocean. This has a dampening effect on the  $CO_2$  concentration in the atmosphere. This mechanism is described by the following matrix equation:

$$\begin{pmatrix} MAT_{t+1} \\ MU_{t+1} \\ ML_{t+1} \end{pmatrix} = \begin{pmatrix} 1.36 \\ 0 \\ 0 \end{pmatrix} E_t + \begin{pmatrix} \phi_{11} & \phi_{12} & 0 \\ \phi_{21} & \phi_{22} & \phi_{32} \\ 0 & \phi_{23} & \phi_{33} \end{pmatrix} \begin{pmatrix} MAT_t \\ MU_t \\ ML_t \end{pmatrix}. \quad (3.12)$$

Once  $CO_2$  emissions are added to the carbon cycle, it stays there. The depreciation of carbon is not considered in the model. If now the carbon concentration in the

---

<sup>2</sup>When  $\alpha = 1$ , the utility function is logarithmic due to l'Hôpital's rule.

atmosphere,  $MAT_{t+1}$ , exceeds the pre-industrial equilibrium concentration  $MAT_{EQ}$ , the temperature will rise due to radiative forcing,  $FORC$ . This is illustrated by the following equation:

$$FORC_t = \eta \left[ \log_2 \left( \frac{M_{ATM,t}}{M_{EQ,t}} \right) \right] + FORC_{EX,t} \quad (3.13)$$

As shown in 3.13,  $FORC$  is also affected by greenhouse gases (GHG) other than  $CO_2$ , which is added exogenous ( $FORC_{EX,t}$ ) to the model.

### **Climate Sub-Model**

The climate sub-model is also illustrated as a cycle, in which thermal energy is transferred between the atmosphere and the oceans. As explained earlier, higher radiative forcing  $FORC$  warms the atmospheric layer which again warms the ocean layer. This mechanism is described in the following matrix equation.

$$\begin{pmatrix} T_{ATM,t+1} \\ T_{OCEAN,t+1} \end{pmatrix} = \begin{pmatrix} \xi_1 \\ 0 \end{pmatrix} FORC_t + \begin{pmatrix} 1 - \xi_1 \xi_2 - \xi_1 \xi_3 & \xi_1 \xi_3 \\ \xi_4 & 1 - \xi_4 \end{pmatrix} \begin{pmatrix} T_{ATM,t} \\ T_{OCEAN,t} \end{pmatrix} \quad (3.14)$$

where:  $\xi_1$  : climate equation coefficient for upper stratum  
 $\xi_2$  : climate sensitivity parameter  
 $\xi_3$  : heat transfer coefficient between upper and lower stratum  
 $\xi_4$  : climate equation coefficient for lower level.

The most critical model parameter is the climate sensitivity parameter,  $\xi_2$ . It is determined by the following equation:

$$\xi_2 = fco22x / t2xco2 \quad (3.15)$$

where:  $fco22x$  : forcings of equilibrium  $CO_2$  doubling  
 $t2xco2$  : equilibrium climate sensitivity [dC per doubling  $CO_2$ ].

The estimation of the equilibrium climate sensitivity parameter has been proven to be difficult. Based on a systematic survey on “The equilibrium sensitivity of the Earth’s temperature to radiation changes” of Knutti and Hegerl [2008], Nordhaus estimates the equilibrium climate sensitivity at  $2.9^\circ C$ .

#### **3.3.2 Critics**

Nordhaus and his DICE model made an enormous contribution to the field of environmental economics, as it was the first cost-benefit analysis of policies to mitigate GHG emissions. Nevertheless, it has become increasingly evident that the model outcomes

are in contrast to scientific consensus. In particular, [Nordhaus \[2014\]](#) derives to the conclusion that the world economy can cope with a temperature increase of 3-3.5°C above pre-industrial level whereas prior to the COP24 conference in Poland, 91 climate scientist from 41 countries have warned in the special report “Global Warming of 1.5°C” about devastating consequences of climate change by an increase of half a degree, from 1.5°C to 2°C [[IPCC, 2018](#)]. The DICE model has been criticized for several reasons, but the most important shortcomings can be outlined in the following paragraphs.

### *Pure Rate of Social Time Preference*

The DICE model consists of input parameter values which are subjective in nature. The most prominent one is the pure rate of social time preference,  $\rho$ . There is no consensus among economists about a legitimated value for this parameter, as such, it is the choice of the modeller. [Stern \[2006\]](#) has argued in his review that a high “pure” time discounting is discriminating life by the birth date. To be more specific, if we consider two identical lives in every aspect but their date of birth, the one born later has a lower value considering a high  $\rho$ . Moreover, he has shown that different input values for  $\rho$  will lead to a different conclusion regarding the optimal policy. On this occasion, one point must be stressed. There is a strict distinction between discounting and pure rate of social time preference. The one is partly a function of expected future consumption paths,  $R_t$ , and the later one is the rate of devaluation of future generations through time,  $\rho$ . This mistake was even made by [Nordhaus \[2007\]](#) in his response to Stern: “An examination of the Review’s radical revision of the economics of climate change finds, however, that it depends decisively on the assumption of a near-zero time discount rate combined with a specific utility function.” Stern never applied a near-zero discount rate but a near-zero rate of time preference. It is essential to understand that the modelling approach in the DICE model can be utilized to generate almost any outcomes of interest which can legitimize subjective opinions.

### *Climate Sensitivity*

Another critic point in the DICE model is the climate sensitivity parameter. The equilibrium climate sensitivity (ECS) describes the temperature increase that would result from a sustained doubling of the atmospheric equivalent CO<sub>2</sub> concentration. However, the strengths and even the sign of the feedback loops that determine the ECS are to a large extent unknown [[Pindyck, 2017](#); [Heal and Millner, 2014](#); [Wagner and Weitzman, 2018](#)]. Numerous attempts have been made to decrease the uncertainty, but the likely range has been between 1.5°C to 4.5°C (high confidence), extremely unlikely less than 1°C (high confidence), and very unlikely greater than 6°C (medium confidence) for 40 years [[Charney, 1979](#); [IPCC, 2018](#)].

To make the matter worse, like many IAMs, DICE is a deterministic model. Thus, it is utilizing best estimates over a speculative probability distribution in order to address uncertainties about future costs and benefits [[Newbold and Daigneault, 2009](#); [Stanton et al., 2009](#)]. This approach would not be an issue if the best estimate was

derived from a single agreed-upon climate model for estimating climate sensitivity. However, this is not the case. Figure 3.2 illustrates the different estimates of the ECS parameter illustrating huge disagreement in climate science on describing the ECS. Many studies have tried to implement stochasticity into the DICE optimization model using normal distribution. However, they did not consider the wide variety of normal distribution in those analyses, but rather they have utilized some kind of meta-analysis or have engaged in informal cherry picking to determine a posterior distribution. In addition, Tol (2003) raised the issue that the ECS parameter cannot be described by a normal distribution. This was further explored by [Weitzman \[2009a\]](#). Weitzmann suggests in his theoretical work that climate policy is highly sensitive to fat-tailed risks of catastrophic outcomes. This new dimension of uncertainty turns ECS into a deep uncertainty (see Section 3.1).

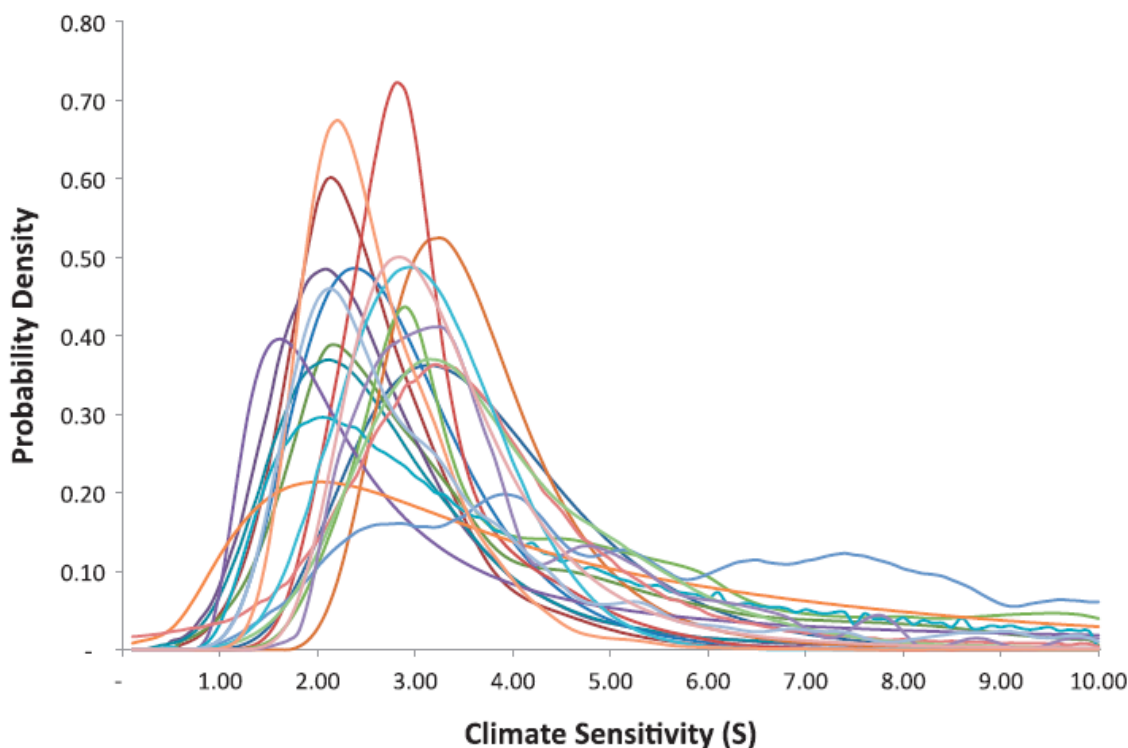


**Figure 3.2:** Estimates of the probability distribution for climate sensitivity in degrees Celsius [[Heal and Millner, 2014](#)].

### *Damage Function*

Nordhaus stated already in his latest manual that “the thorniest issue in climate-change economics” [[Nordhaus, 2013](#)] is the damage function. While it was possible to deduct distribution for the ECS on the basis of atmospheric physical science, we have no idea when it comes to damage function. There is no data or theory to base the choice of a certain damage function [[Pindyck, 2017](#); [Wagner and Weitzman, 2018](#)]. However, IAM modellers try to estimate the damage function using studies of climate damage at specific degrees of global warming ( $T_{ATM} = 2.5 - 3^{\circ}\text{C}$ ). In the case of DICE model, Nordhaus tried to estimate the coefficients  $\psi_1$  and  $\psi_2$  of a quadratic damage function (3.5) on the basis of data points from studies, such as crop losses

and heating. Since  $T_{ATM} = 3^{\circ}\text{C}$  has not been seen on the planet for around 3 million years and thus the consequences of this are unknown, these “quasi” data points are, to be honest, useless. It is even more difficult to make an assumption on the damage function for  $T_{ATM} \geq 3^{\circ}\text{C}$ , due to the complete lack of knowledge, understanding and evidence. Moreover, the quadratic term for damage function (3.5) results in unrealistic low damages at high temperatures [Stern, 2006; Dietz and Stern, 2015; Weitzman, 2011; Hwang et al., 2014]. Nordhaus damage function, for instance, assumes that a  $10^{\circ}\text{C}$  increase in temperature leads to a damage cost of 26.7% of the gross world output (see Figure 3.3).

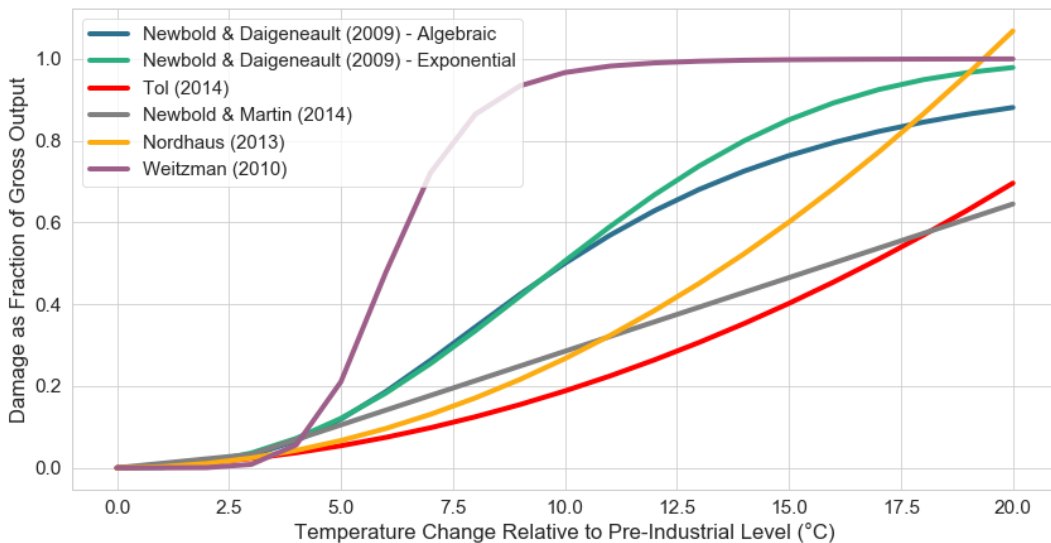


**Figure 3.3:** The variety of different damage functions which can be found in climate economics literature’s

### Methodology

Regarding the methodology, the DICE model is a deterministic non-linear, inter-temporal optimization model. The greatest shortcoming of traditional deterministic optimization is that it can only consider a very small subset of possible scenarios [Better et al., 2008]. Some developers/users of the DICE model are fully aware of the limitation of the methodology and also about the considerable uncertainty over the ECS and the damage function. Nonetheless, they presume that uncertainties can be managed by assigning probability distributions on those parameters and to run a Monte Carlo simulation afterwards [Pindyck, 2017]. For instance, Weitzman [2009a] argues that estimates of the economic impacts of climate change are better derived through probabilistic studies, in which, crucially, the key parameters like climate sensitivity and the damage function are better described by distributions with a fat-tail. However, the issue is that there is a fundamental lack of knowledge about the correct probability distribution (e.g ECS), or the correct functional form of parameters (e.g damage function). Thus, the presence of uncertainties makes the identification of an optimal policy extremely difficult.

In light of the above-mentioned critics, the question arises whether the DICE model can be actually used for forecasting or even for storytelling. “Can IAMs be salvaged

as a tool for policy analysis if we somehow account for lack of knowledge about key relationships and parameter values?” [Pindyck, 2017]. This thesis, to some extent, is dedicated to answering this question by the means of the methodology presented in the following section.

## 3.4 DECISION MAKING UNDER DEEP UNCERTAINTY

### 3.4.1 Optimality vs. Robustness

#### *Traditional Decision Analytic Method*

Hitherto, optimization was traditionally utilized as decision-analytic methods for risk and decision analysis, as well as in the field of climate economics. Optimization models were designed to identify optimal strategies based on the given constraints and uncertainties. With a single set of strategies and a single set of probability distribution over the uncertainties, these approaches generated single best outcomes [Lempert et al., 2006]. This approach is well suited to determine the best possible strategy when the uncertainties can be described by probability distributions (i.e Level 2 uncertainties). If there are additional uncertainties over the optimization model, professionals of traditional decision-analytic methods employ sensitivity analyses to test the dependence of their optimum strategy on those uncertainties [Saltelli, 2008]. This method is adequate if the chosen optimum strategy is relatively robust to these key assumptions. However, if the optimal strategy is sensitive to those assumptions, optimum strategies lose their prescriptive value [Walker et al., 2013]. Consequently, it can be stated with certainty that traditional decision-analysis is unsuitable for decision-making under deep uncertainty. As a result, the scientific community has realized that any policy recommendation in a complex system, such as in the field of climate economics, must be robust in regards to the manifold of the deep uncertainties of those systems [Lempert and Collins, 2007; Giuliani and Castelletti, 2016; Kwakkel et al., 2016b; Herman et al., 2015]. But what does robustness actually mean in the context of policy analysis?

#### *Robustness*

Robustness is defined differently from one field to another. However, in principle, most of those definitions agree upon that robustness is only reached when it is able to maintain its functionality despite external or internal distresses. In policy analysis, this definition can be applied on a system level as well as a policy level. On a system level, a system is defined as robust when the main functionality can be maintained despite changes in their state. Similarly, a policy is considered robust when it performs well across a variety of possible future states of a system [Herman et al., 2015; Kasprzyk et al., 2013; Lempert and Collins, 2007; Giuliani and Castelletti, 2016; McPhail et al., 2018]. Although robustness of candidate strategies can be analyzed from different viewpoints, in general, their calculation consists of three factors: (1) the policy strategies for which robustness is to be calculated, (2) the outcome of in-

terest and (3) plausible future states of the world (scenarios) [McPhail et al., 2018]. The robustness metrics, which was utilized in this research, are presented in Section 7.2. However, it must be noted that robustness does not come without a cost in performance. In the literature, this is called as the “price of robustness” [Bertsimas and Sim, 2004]. This trade-off can be illustrated by comparing the pure rate of social time preference or the social cost of carbon of Nordhaus optimal policy with the set of robust policies of this study in Section 10.3.

### 3.4.2 Exploratory Modelling and Analysis - Stochastic Optimization

Admittedly finding robust policies requires evaluation of different policy options over a large ensemble of possible future states of the system. To answer the “what-if” question and to generate a large number of scenarios, a simulation model is mandatory. As simulation models strive to describe the reality as precisely as possible, it allows the integration of various sources of uncertainty [Better et al., 2008]. Exploratory Modeling and Analysis (EMA) techniques have been used as a foundation for finding robust policies [Bankes et al., 2013]. In EMA, computational experiments of the simulation model are used to systematically explore the behaviour of the complex systems under an ensemble of prior specified uncertainties in response to different policy settings.

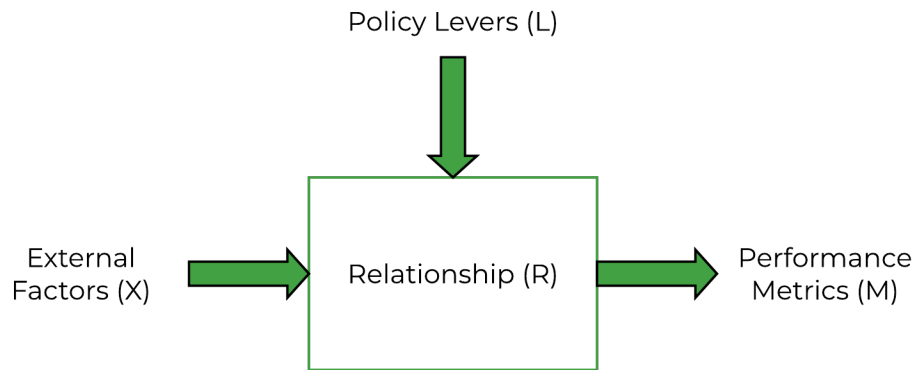


**Figure 3.4:** The XLRM framework adopted from Kwakkel [2017].

As one of the first, Lempert et al. [2006] proposed the robust decision making (RDM) method. The first step of the RDM method is to conceptualize the simulation model according to XLRM framework. The four categories of the framework are the following:

- X: Exogenous uncertainties that are outside of the control of decision makers
- L: Policy Levers that are in the control of the decision makers
- M: Outcomes of interest
- R: Causal relation between X, L and M

From here on in an iterative process, policies/candidate strategies are identified based on expert opinion or traditional sensitivity analysis. Next, a diverse ensemble of scenarios/experiments are built, and subsequently, outcomes are determined on the basis of the generated set of scenarios and the defined policies. This is done by utilizing an exploratory modelling software. In the final step, the information from the computational experimentation is used to calculate the robustness of the policy, but also to discover the vulnerabilities by applying scenario discovery techniques like PRIM or CART. With the knowledge about the robustness and the vulnerability of the policy, the policy can be refined in another iteration [Lempert et al., 2006; Kwakkel, 2017].

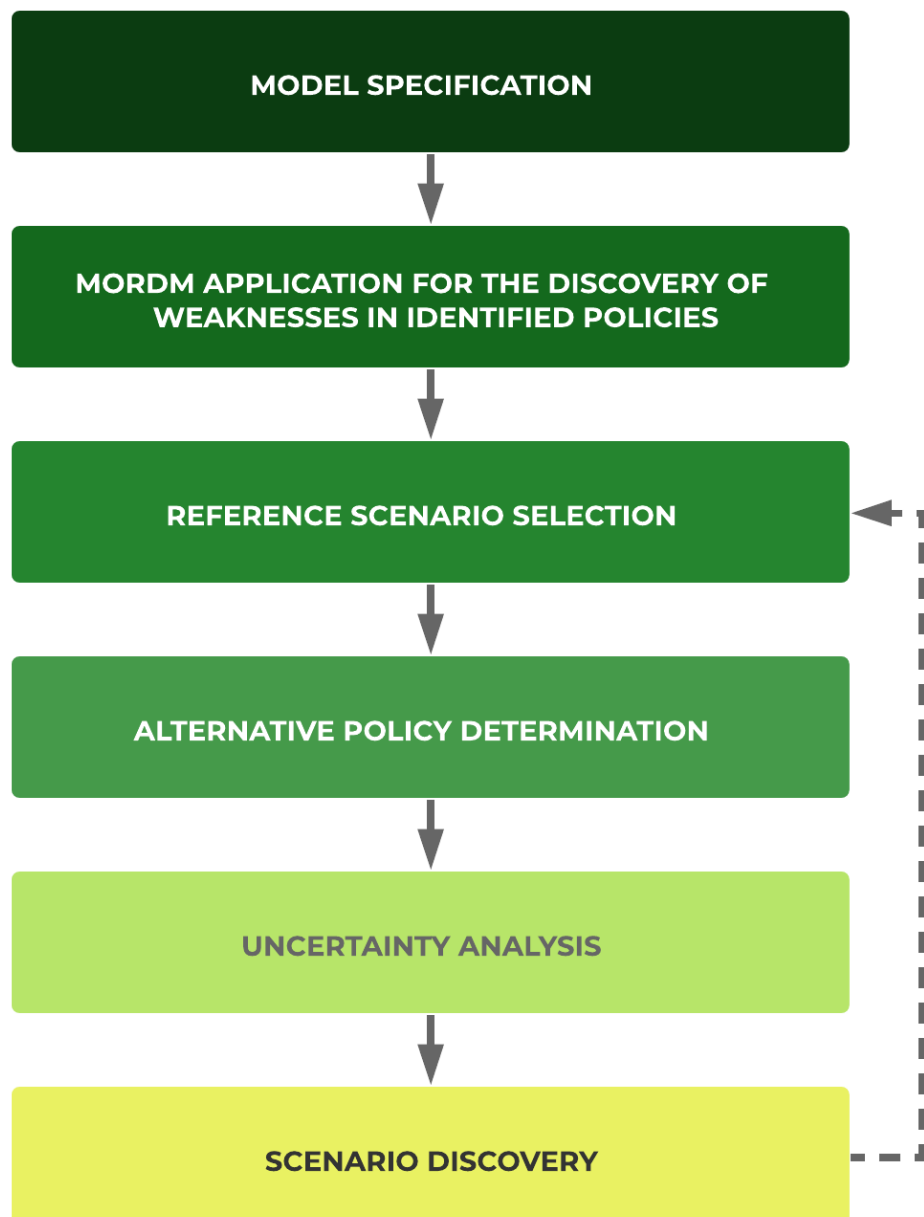


Figure 3.5: Multi-Scenario MORDM Process adopted from Bartholomew [2018]

Kasprzyk et al. [2013] expanded the RDM method to the Many-Objective Robust Decision Making (MORDM) method. The most noteworthy change is the use of multi-objective evolutionary algorithms (MOEA) to identify candidate strategies at base reference point [Hadka et al., 2015]. In addition, MOEA allows addressing conflicting outcomes of interest directly in the search phase. Furthermore, an uncertainty analysis is performed over the ensemble of policy options. For this purpose, a set of scenarios is created by sampling the uncertainty parameters. This new method has already been proven in several cases [Kasprzyk et al., 2013; Herman et al., 2014; Trindade et al., 2017; McPhail et al., 2018].

However, Watson and Kasprzyk [2017] rightfully pointed out that in MORDM the non-dominated set of candidate strategies/policies will be based on a single reference point. This has the consequence that in conditions, which differ from the reference point, will result in a less robust policy set. Thus, they suggested the multi-scenario MORDM method. The crucial difference is the use of MOEA to search for scenarios, based on the identified weakness of the policy through scenario discovery. With multiple reference scenarios, a more diverse and robust set of policies can be determined.

As mentioned many times earlier, the field of climate economics is depicted with deep uncertainties. Traditional decision analytic methods have shown their deficiency in managing uncertainties. The multi-scenario MORDM shows great potential to overcome this shortcoming. Thus, multi-scenario MORDM is used as the key methodological framework of this thesis.

# **Part II**

# **Methods**

“The standard library saves programmers from having to reinvent the wheel.” -  
Bjarne Stroustrup

# 4 MODEL CONCEPTUALIZATION

In order to explore the robustness of Nordhaus optimal policy with regards to deep uncertainty, this study has reconstructed the DICE optimization model into a stochastic simulation model called PyDICE. Section 4.1 illustrates the conceptualization of the PyDICE. Further, the model is verified by comparing the outcomes of the PyDICE to DICE in Section 4.2. Lastly, Section 4.3 presents the model specification of PyDICE according to XLRM framework.

## 4.1 DICE SIMULATION MODEL: PYDICE

In PyDICE, the original model equations of the DICE model are maintained to a large extent. However, as the DICE model aims to maximize the welfare function, optimal values for the two parameters emissions control rate and savings rate are determined at the end of the optimization. Thus, in a simulation version of DICE, these two parameters have to be specifically described in the model, for instance via a function. The global social planner in the RCK growth model chooses his savings rate and emission control rate so that the welfare function is maximized. Thus, in PyDICE, the two parameters are modelled so that they follow the trajectory of each from the “optimal” climate policy scenario.

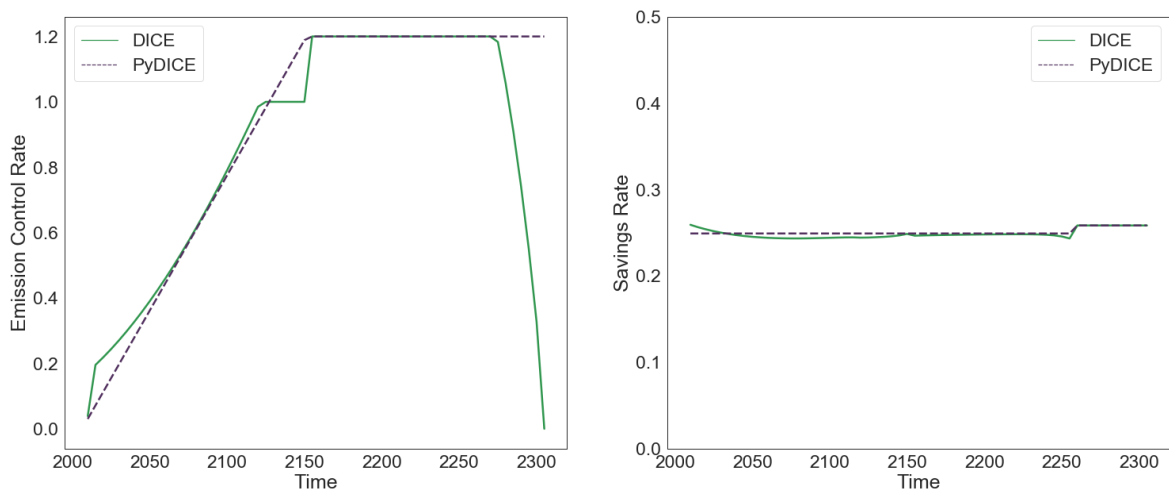


**Figure 4.1:** Comparison between PyDICE and DICE. Left panel: Emissions control rate; Right panel: Savings rate.

Assessing the trajectory of the emission control rate of the DICE model in Figure 4.1, it can be stated that the control rate increases generally linear over time until

a certain control rate maximum is reached. The maximum emission control rate  $\mu_{max}$  can be above 1, since [Nordhaus \[2013\]](#) assumes that a backstop technology, which extracts carbon from the air (i.e., direct air capture technology), will be used on a massive scale in future. Similar to the outcome in DICE, PyDICE adopted the following linear equation to describe the emission control rate,  $\mu_t$ :

$$\mu_t = \mu_{max} * t / t_\mu + \mu_0 \quad (4.1)$$

where:  $\mu_{max}$  : maximum emission control rate

$\mu_0$  : initial emission control rate

$t_\mu$  : emission control rate target

Here, the emission control rate is driven by the emission control rate target  $t_\mu$  of the global community. Figure 4.1 shows that the resulting behaviour from Equation 4.1 mimics to a large extent the trajectory of the control rate in DICE. The drop at the end of the emission control rate was most certainly caused by the end-of-horizon effect, which is an inherent problem of long term optimization.

The savings rate,  $sr_t$ , of the DICE model shows a strong non-linear behaviour. However, these dynamics are restricted to values between 0.244 and 0.258. Thus, the savings rate can be simply approximated by a constant, as it can be seen in the right panel of Figure 4.1. Therefore, the following equation is used to describe the savings rate in PyDICE:

$$sr_t = \begin{cases} sr, & \text{if } t < t_{-10} \\ optlrsav, & \text{otherwise} \end{cases} \quad (4.2)$$

$$optlrsav = \frac{(\delta + 0.004)}{(\delta + 0.004\alpha + \rho)\gamma} \quad (4.3)$$

where:  $\delta$  : depreciation rate of capital

$\alpha$  : elasticity of marginal utility

$\rho$  : pure rate of social time preference

$\gamma$  : capital elasticity

Same as in the DICE model, the optimal long-run savings rate is used in PyDICE for the last 10 time steps of the savings rate in order to fulfil the transversality condition of the RCK growth model.

PyDICE runs in time steps of five years beginning in the year 2010 until 2310 (60 time steps in total). With regard to the Python scripted analysis tools used in this study, PyDICE is written also in Python, a high-level general-purpose programming language.

## 4.2 VERIFICATION

Usually a model development process consists of an extensive validation and verification process of the model. Hereby, modellers perform conceptual, operational and data validity by using for instance expert opinion, historical methods or extreme condition tests [Sargent, 2013]. However, since the PyDICE is a re-implementation of the highly utilized DICE model, a conceptual, operational and data validity is not required. Therefore, this section only focus on the verification of the PyDICE by comparing it to the DICE model. First, it is verified whether the internal functions of the DICE model and their relationship was implemented correctly into the Python environment. To that end, the functions (4.1) and (4.2) with (4.3) are replaced by the optimized value for the emission control rate  $\mu_t$  and savings rate  $sr_t$ . Next to the graphical illustration of the verification in Figure 4.3, the numeric verification can be found in the Appendix A.

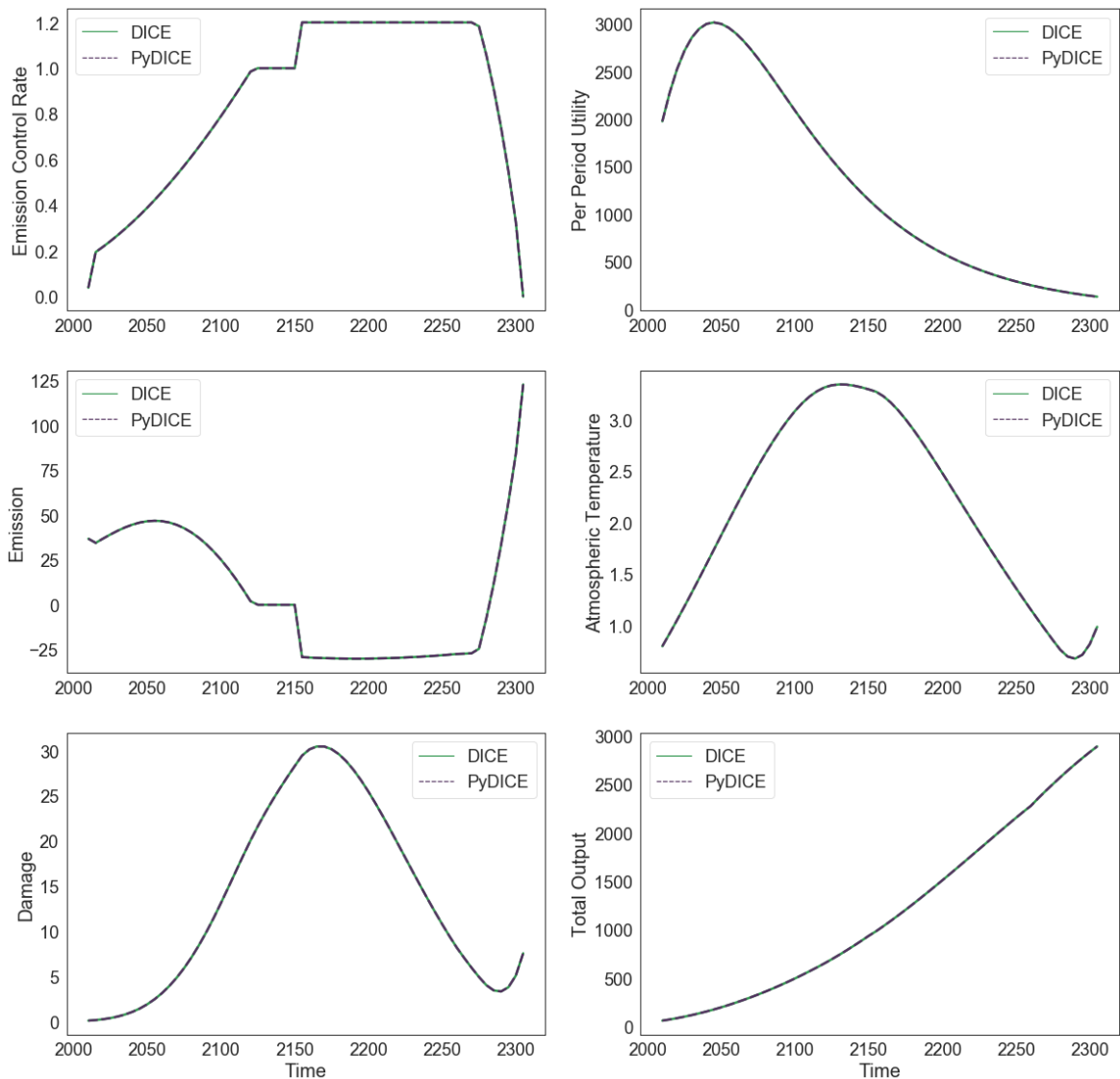


**Figure 4.2:** Comparison between PyDICE and DICE with the optimized outcome of Nordhaus optimal policy for the parameter control rate  $t$  and savings rate  $sr_t$ .

To inspect whether the integration of the new model functions functions (4.1) and (4.2) with (4.3) has a significant effect on the model outcomes, a second verification is done by comparing the model behaviour of the PyDICE with the DICE model. This is visually illustrated in Figure 4.3.

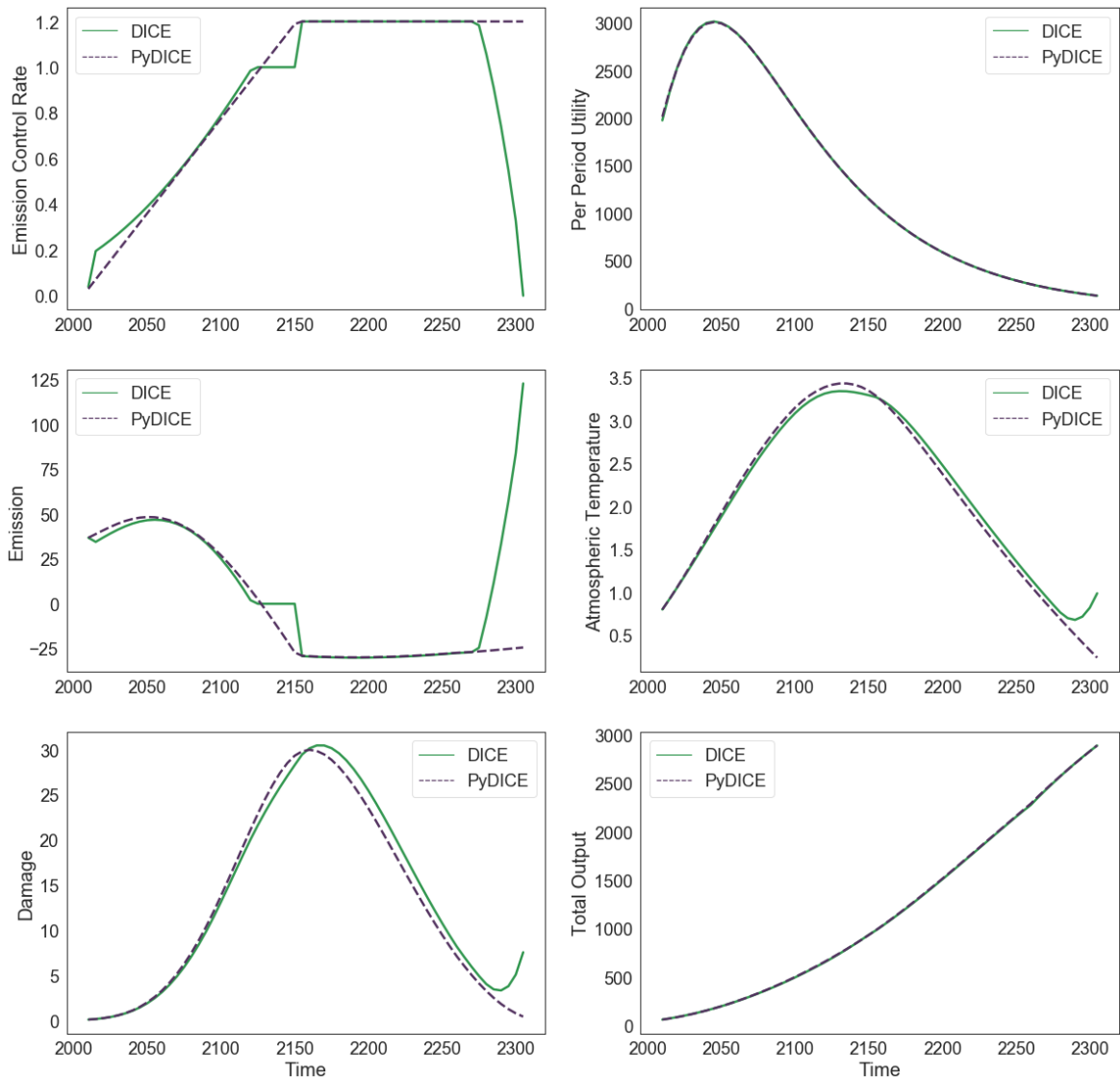


**Figure 4.3:** Comparison between PyDICE and DICE with the integrated functions for emission control rate 4.2 and savings rate 4.2.

Figures 4.2 and 4.3 and Tables A.1 and A.2 show that the outcomes of the PyDICE coincide to a large extent with the outcomes of the DICE model. Therefore, PyDICE can be treated as a discrete stochastic simulation version of the DICE model.

## 4.3 PYDICE XLRM STRUCTURE

In addition to the amendments made in Section 4.1, PyDICE is organized by the XLRM Framework (see Section 3.4.2). Structuring the model into policy levers, out-

comes of interest, exogenous uncertainties and their relationship is the first important step in the multi-scenario MORDM process (see Figure 3.2).

#### 4.3.1 “M”: Outcomes

In complex problem settings with many stakeholders and different interests, the decision-maker, in this case, the global social planner or the international community, have numerous goals, which are sometimes conflicting. As a consequence, finding a strategy, that can realize many objectives, is difficult (and messy). The four main objectives of the decision-maker in PyDICE is summarized in Table 4.1.

**Table 4.1:** Outcomes of Interest.

Name	Equation	Year	Direction of Optimization
Atmospheric Temperature	(3.14)	2050, 2100, 2150, 2200, 2300	Min
Damages	(3.4), (3.5)	2050, 2100, 2150, 2200, 2300	Min
Total Output	(3.4)	2050, 2100, 2150, 2200, 2300	Max
Utility	(3.7)	2300	Max

Since the key economic structure of the model represents the RCK growth theory, it is self-evident that cumulative (discounted) utility over the full period is an outcome of interest. Furthermore, from an economic growth perspective, the total output/income is of interest as it reflects the buying power and the overall economic activity of the world. At the same time, it is also crucial to discover policies which minimize damages to the greatest possible extent. The atmospheric temperature is chosen as an outcome of interest because the main criticism of climate scientists on the optimal policy proposition of Nordhaus is that it allows the temperature to rise up to 3.5 degrees above the pre-industrial level. The outcomes, atmospheric temperature, damages and total output, are only examined at five specific points in time (2050, 2100, 2150, 2200, 2300), since utilizing the whole time series would have not generated greater insights but would have rather yielded in higher computational effort.

#### 4.3.2 “L”: Policy Levers

Simply speaking, policy levers are control parameters that the global social planner has control over to reach the outcomes of interest (see Table 4.1). Based on the literature review in Chapter 3, the levers are chosen in regards to their effectiveness at least on one outcome. The levers are summarized in Table 4.2.

**Table 4.2:** Policy Levers.

Name	Equation	DICE	Range	Unit	Data Type
Savings Rate	(4.2)	0.248	0.1 – 0.5	Dmnl	float64
Emission Control Rate Target	(3.6), (3.11), (4.1)	2150	2060 – 2300	Year	int64
Pure rate of social time preference	(3.9), (4.2)	0.015	0.001 – 0.015	Dmnl	float64
Full Participation Target	(3.7)	0	2060 – 2300	Year	int64

### *Savings Rate*

As already outlined in Section 4.1, the savings rate is chosen by the global social planner to maximize utility. Moreover, the growth theory assumes that by modifying the savings rate, the transitional dynamics between capital and consumption can be affected. Thus, this policy lever would have a direct influence on two outcomes of interest, total output and utility. In PyDICE, the policy lever savings rate can range between 0.1 and 0.5. The baseline value of 0.25 reflects the optimal policy of the DICE model.

### *Emission Control Rate Target*

Extending the RCK growth model by the climate and carbon model in DICE, Nordhaus quantified the effects of man-made greenhouse gases as a damage of the gross output. The emission control rate is the only dirigible factor in the model, which has an impact on the severity of the resulting damage. At the same time, it also determines the abatement costs. Emission control rate has not only a direct effect on damages but also on total output. Therefore, emission control rate target is chosen as one of the four policy levers. As shown in Equation (4.1), it determines how fast the maximum control rate is reached. In other words, the emission control target lever reflects the setting of “net-zero” carbon target<sup>1</sup> by the global community. In PyDICE, this policy target can range between 2060 and 2300. The minimum value of this policy lever displays the call of the UN Global compact for a net-zero target by 2050 [United Nations, 2019]. In addition, the 2060 target still presents a realistic goal since countries like Sweden, Japan and the United Kingdom have already adopted a legally binding net-zero target for 2050 [Carbon Brief, 2019]. In line with the optimal policy of the DICE model, the baseline value of this lever is 2150.

### *Pure Rate of Social Time Preference*

The choice of the pure rate of social time preference has been long debated (see Sub-section 3.3.2). On the one hand, scholars like Stern [2006] argues that a “high” rate of social time preference is ethically unjustifiable and on the other hand, academics

---

<sup>1</sup>If the emission control rate maximum is above 1, the emission control rate target turns into a negative carbon target.

like Nordhaus argues that “near-zero” rate of social time preference leads to paradoxical results. As there is no consensus, it is modelled in PyDICE as a policy decision of the global social planner [Stern, 2006; Nordhaus, 2013]. The careful reader has already noted that this study takes a mediator role in such debates and thus has considered both “extremes” as the boundary values of the policy lever. In line with the optimal policy of the DICE model, the baseline value of this parameter is 0.015.

### 4.3.3 “X”: Uncertainties

The various future states of the world are described by different combinations of uncertain parameters. Although those parameters are outside of the control of the decision-maker, they can be used to systematically test the performance of policies. The deep uncertainties of the PyDICE model are resumed in Table 4.3. They have shown in earlier studies that they have the largest impact on the outcomes [Nordhaus, 2008b; Butler et al., 2014].

**Table 4.3:** Deep Uncertainties.

Name	Equation	DICE	Range	Unit	Data Type
Total Availability of Fossil Fuel	(3.11)	6000	[4000, 13649]	GtC	float64
TFP Growth Rate	(3.1)	0.079	[0.07, 0.09]	$\frac{1}{\text{year}}$	float64
Population Growth Rate	(3.1)	0.134	[0.1, 0.15]	$\frac{1}{\text{year}}$	float64
Initial Growth Rate of Emissions to Output Ratio	(3.7)	-0.01	[-0.012, -0.008]	$\frac{1}{\text{year}}$	float64
Price of Backstop Technology	(3.4)	344	[100, 600]	$\frac{2005\$}{\text{tCO}_2}$	int64
Equilibrium Climate Sensitivity Distribution	(3.14), (3.15)	-	0: Normal	Dmnl	int64
			1: Log-normal		
			2: Cauchy		
Damage Function	(3.4), (3.5)	0	0: Nordhaus	Dmnl	int64
			1: Newbold & Daigneault		
			2: Weitzman		

#### **Total Availability of Fossil Fuel**

The total availability of fossil fuel is the driving factor that determines the growth rate of Hotelling rent<sup>2</sup> to drive the consumption to the backstop technology. This becomes especially crucial for scenarios of fast economic growth or low rates of carbon-reducing technological change. The boundaries of the parameters are chosen based on literature [Bruckner et al., 2014; Rezai and Van Der Ploeg, 2017].

<sup>2</sup>The price of an exhaustible resource must increase over time with the interest rate.

### ***TFP Growth Rate***

According to [Nordhaus \[2008b\]](#), the most important uncertain parameter is the growth rate of total factor productivity. The total factor productivity is one of the main drivers of long-run economic growth (see Equation (3.1)). Subsequently, as industrial emissions are determined by the output, climate damages are propelled by the growth rate of total factor productivity. The extremes of these parameters are chosen based on the literature [\[Nordhaus, 2008b\]](#).

### ***Population Growth Rate***

The other main driver of economic growth is labour force (see Equation (3.1)). Similar to the argument above, it can be assumed that climate damages are also driven by the size of the population. Many population prospects in the past had to revise their projections about the maximum population. In the latest “World Population Projection 2019” of UN DESA shows a population of 10.9 Billion by 2100. This corresponds with the maximum population value of 10.1 Billion (at time period 2100) in the DICE model. However, there is still uncertainty whether this maximum will be reached in 2100. Thus, the population growth rate is chosen as an uncertainty in the PyDICE with a value range between 0.1 (population value of 9.8 Billion in 2100) and 0.15 (population value of 10.2 Billion in 2100).

### ***Initial Growth Rate of Emissions to Output Ratio***

The emission to output ratio describes the carbon intensity of production. In other words, this factor reflects the carbon efficiency of the global economy. Furthermore, the growth rate of the emission to output ratio illustrates the rise/decline of carbon efficiency in production. Thus, an increase in efficiency would reduce the industrial emission and subsequently it would lead to lower climate damages (and vice versa). Acknowledging that the growth rate of emissions to output ratio is an uncertainty, [Nordhaus \[2016\]](#) applied a sensitivity analysis on the DICE2016R version. For this purpose, Nordhaus illustrates the growth rate of emission to output ratio as a normal distribution with a standard deviation of 0.003 and a mean of -0.015. Therefore, PyDICE utilizes the same standard deviation to determine the limits of the scalar parameter. To be more specific, the 25<sup>th</sup> and 75<sup>th</sup> quantiles of the n normal distribution with a mean of -0.01 and a standard deviation of 0.003 has been used to calculate the limits of the model.

### ***Price of Backstop Technology***

The upper limit of the carbon price is determined by the price of the backstop technology, as it presents the economic price of replacing fossil fuels. Thus, a low-cost backstop technology would allow the world to prevent climate damages. Of course, this also works in the other direction, i.e. high-cost backstop technology would lead to high climate damages since replacing fossil fuels with the backstop technology would not be profitable. Furthermore, there is no reliable study which defines the price of backstop technology. That is because there is no consensus about which technology or set of technology should reflect the concept of backstop technology.

Thus, the ranges for the price of backstop technology have been chosen so that it still reflects low-cost and high-cost of backstop technology.

### *Equilibrium Climate Sensitivity*

In Section 3.3.2, it is clearly outlined that the equilibrium climate sensitivity (ECS) parameter is deeply uncertain. For one, there is strong dissonance about the statistical sizes of the ECS distribution (see Figure 3.2) and besides, there is strong evidence, that the ECS is fat-tailed. Since this study aims to answer the question of what are the repercussions of applying fat-tailed distribution over uncertain parameters, the ECS parameter is modelled for three distributions, namely normal distribution, log-normal distribution and Cauchy distribution.

**Table 4.4:** Equilibrium Climate Sensitivity estimation of the IPCC AR5 and [Rogelj et al., 2012].

IPCC AR5		Knutti et. al (2012)	
<b>Cumulative probability at 1°C</b>	0.0 - 0.05	<b>Cumulative probability at 1.5°C</b>	0 to 0.1
<b>Cumulative probability at 1.5°C – 4.5°C</b>	Min. 0.66	<b>Cumulative probability at 2.0°C</b>	0 to 0.33
<b>Cumulative probability at 6 °C</b>	0.9 – 1	<b>Cumulative probability at 4.5 °C</b>	0.66 to 1.0
		<b>Cumulative probability at 6 °C</b>	0.9 – 1
		<b>Most likely value 2.6°C to 3.6°C</b>	0.5

Majority of climate scientists and climate economists have used the normal distribution to estimate the ECS parameter. Furthermore, other scholars like [Hwang et al., 2013] and [Ackerman et al., 2010] have used the log-normal distribution to illustrate the “fat-tailness” of the ECS parameter. Log-normal distribution qualifies as a fat-tailed distribution since the kurtosis  $K^3$  of the log-normal ECS is leptokurtic (see Table 4.5). However, it is also often called as “in-between” distribution due to its mathematical familiarity to normal distribution. Since the log-normal distribution is not an adequate distribution to represent a fat-tailed distribution, this research has also included a Cauchy distribution to describe the ECS parameter.

The probability density function (PDF) of these three ECS distributions were created by the following three steps:

1. Data points for the cumulative density function (CDF) are generated by using the ECS estimation of the IPCC [2014] and Rogelj et al. [2012] (see Table 4.4).
2. CDF of the distribution is fitted over the data points from step 1. R-squared is calculated to assess the goodness of fit.

<sup>3</sup> Kurtosis is calculated using the Pearson formula.

3. If the R-squared is above 0.95, the CDF is translated into a PDF using the corresponding statistical sizes such as mean, variance and/or shape.

In order to prevent absurd extreme cases during the sampling phase like an ECS value of 500°C, the rejection sampling method was used to create truncated distributions between 0°C and 20°C. Moreover, the generated three distributions are enumerated from 0 to 2 (see Table 4.3), so that during the stochastic simulation run, it is already translated into a computer understandable form.

**Table 4.5:** Statistical Sizes of the Equilibrium Climate Sensitivity Distributions.

Equilibrium Climate Sensitivity Distribution	Median	Variance	Skew	Kurtosis
Truncated Normal	3.21	1.98	0.17	2.77
Truncated Log-Normal	3.12	2.34	0.78	4.08
Truncated Cauchy	3.16	4.37	3.21	18.79

### *Damage Function*

A further structural deep uncertainty is the damage function. Also, this deduction has been already explained in detail in Section 3.3.2. To design this structural uncertainty

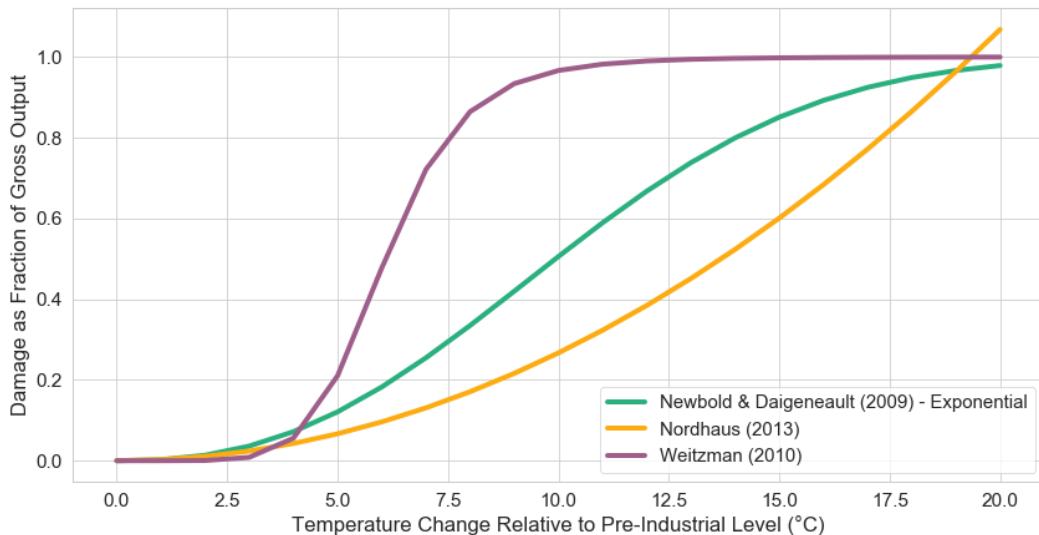


**Figure 4.4:** The damage functions of the PyDICE model. For completeness, the algebraic damage function Newbold and Daigneault is illustrated.

in PyDICE, three different damage function has been chosen. Whereas the damage function of Nordhaus and Weitzman represent the two extremes of the discussion, the exponential damage function of Newbold and Daigneault can be placed in between the two extremes. This is illustrated in Figure 4.4. Similar to the ECS parameter, the damage functions are enumerated from 0 to 2 (see Table 4.3), so that during

the stochastic simulation run, it is already translated in a computer understandable form.

#### 4.3.4 “R”: Relations

The above-described uncertainties, decision levers, and outcomes are connected together through a set of functions, which are described to a large extent in Section 3.3.1 and 4.1. At last, a model is nothing more or less than a set of functions. The PyDICE is developed along the XLRM Framework to connect it to EMA-Workbench, an open-sourced python package for exploratory modelling and analysis. EMA-Workbench consists of various tools like exploratory analysis, global sensitivity analysis and many-objective optimization, which has been used for the following analysis techniques.

# 5

## OPEN EXPLORATION

Open exploration is a technique utilized to generate insights about the variety of dynamics and uncertainties in a model. In other words, it is a methodology to systematically evaluate model parameters to study the entire set of possible behaviours of the outcomes and thereby provides the analyst with a baseline understanding of the outcome space. This method is technically implemented by simulating the model millions of times over an experimental design that samples different combinations of uncertain parameter and tests against a defined set of policies. At the end of this process, a large data set is generated allowing to trace the performance of a policy back to the scenario and its combination of the input parameter. Thus, this method enables the analyst and decision-maker to answers questions like “under which conditions would a specific policy do well/poorly”. This chapter discusses the pitfalls and benefits of various sampling techniques in Section 5.1. Further, in Section 5.2 and 5.3, the use of the two analysis techniques, statistical analysis and global sensitivity analysis are explained in detail.

### 5.1 SAMPLING TECHNIQUES

Sampling strategy plays a crucial role in open exploration, as it is directly correlated with the efficiency and robustness of the statistical analysis. Depending on the use case, sampling methods can vary from Monte Carlo sampling (MC), Latin Hypercube sampling (LHS) to Full Factorial sampling (FF).

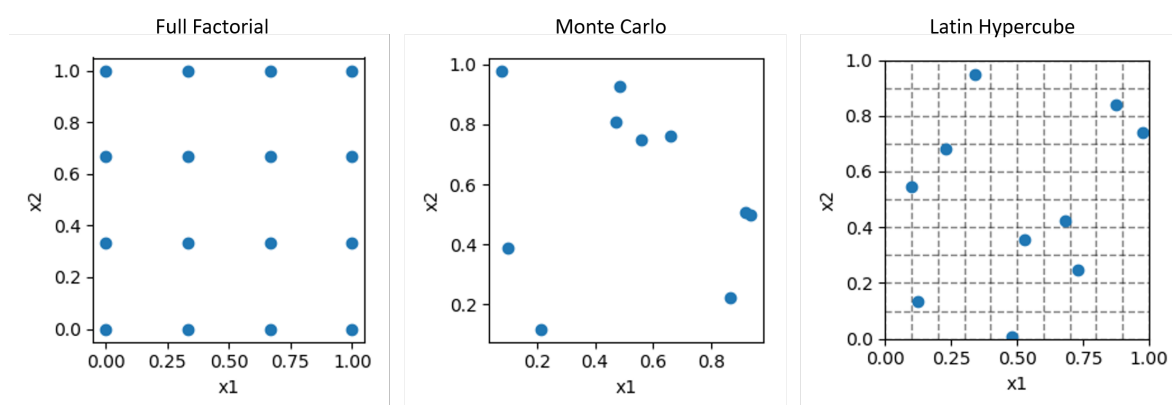


Figure 5.1: Sampling Techniques [Buchheit et al., 2019]

In the context of open exploration, simulation models can be very expensive to run and thus choosing the right sampling strategy is essential for further analysis. Al-

though an FF technique would sample across the whole range of the input space, the computation of the experiment set, which would mean all possible combinations for the specified number of scenarios across all input parameters ( $scenarios^{input\ parameter}$ ), is just not feasible. Therefore, MC technique could give a more reliable inference of the input space. But since it relies on pure randomness, it lacks efficiency. MC can lead to clustering of samples at specific intervals while other points have no samples. Thus, an increase in precision of MC requires a higher sample size.

In contrast, the stratified sampling technique, LHS ensures equal representation of the uncertainty parameters in the experiment set by first dividing the input space uniformly and then selecting one sample from each interval. Moreover, LHS shuffles the sample for each input parameter so that an unbiased experiment set is created. This sampling technique describes the uncertainty space with fewer scenarios and thus LHS is perfectly suitable for open exploration as one usually generates a great number of experiments.

## 5.2 STATISTICAL ANALYSIS

In order to generate the first insights from the experiment set, the outcomes from the open exploration have to be statistically and visually analyzed. In a stochastic simulation model, like the PyDICE, the input space affects the performance of the outcome. Thus, it is assumed that these conditions are representative of the actual system. Subsequently, the population statistics for the described system can be estimated using the sample statistics. This study's statistical analysis focuses mainly on three key measures: mean, standard deviation and quantiles. Hereby, the statistical values are used to compare the subset of scenarios in their inference on the outcomes of interest.

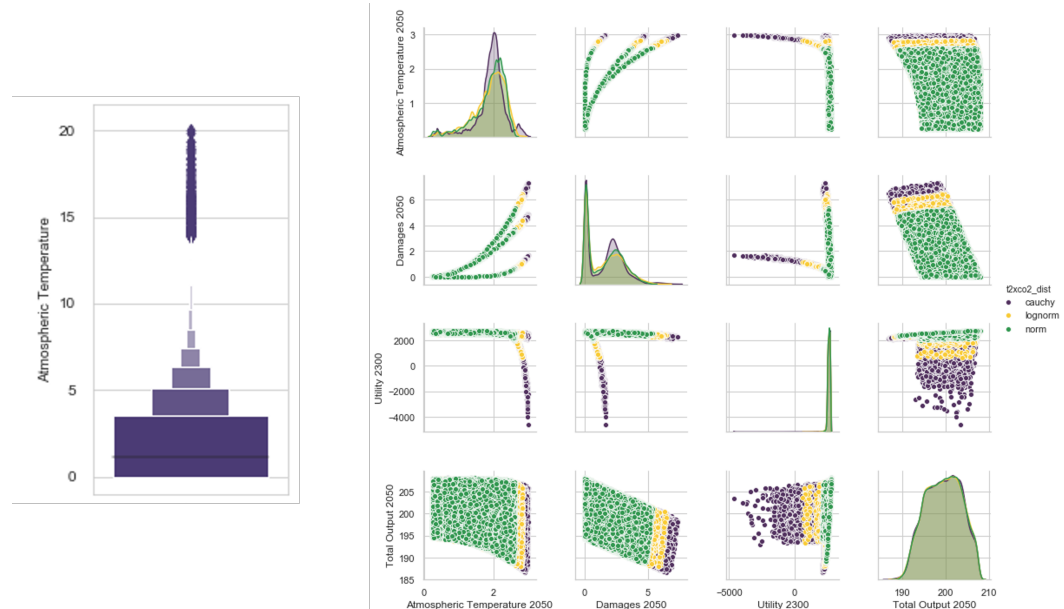


Figure 5.2: Visualization examples in statistical analysis. a): Boxenplot; b): Pairplot.

The measures of the outcome are not only presented in tables but also visually illustrated in boxenplots (or letter value plot). The boxenplot visualisation is similar to boxplot in terms of its non-parametric representation of a distribution in which all characteristics of the plot correspond to actual outcomes of the stochastic simulation model. The major advantage of the boxenplot is its smart intuitive visualization of the quantiles. In particular, this is very convenient when representing the tails of the distribution of the outcomes (see Figure 5.2).

Furthermore, to create a greater understanding of the statistical relation between the output parameter, the correlation is calculated using the Kendall rank correlation coefficient (KRCC). KRCC is chosen over the correlation coefficients such as the Pearson correlation coefficient since this study does not attempt to estimate the population distribution of the outcomes from the experiment set. Visually, the correlation between the parameters is presented in a pairplot. A pairplot is created by a grid of axes so that each outcome variable will be shared in the x-axis across a single column and y-axis across a single row. Thus, each subplot within the pairplot represents a scatterplot. In addition, the diagonal axis represents the distribution of each outcome.

## 5.3 GLOBAL SENSITIVITY ANALYSIS

Another statistic tool, which is also very often used in risk assessment, is the global sensitivity analysis (GSA). It is aimed at the identification of the most influential uncertainty parameter on the outcomes. Thereby, GSA answers questions such as, how much of the uncertainty is epistemic? How much is irreducible? Which uncertain inputs should be a priority for research?

The most prominent GSA methods in the literature are arguably regression analysis, decision tree-based GSA and variance-based GSA. The former fits a linear regression to the model outcome and utilizes the standardized regression coefficients as direct measures of sensitivity. This simple and fast application makes regression analysis a powerful tool in analyzing the sensitivity of the input parameter(s) on the output parameter. However, this tool is only suited for linear model outcomes as otherwise, it is almost impossible to interpret the standardized coefficients [Jaxa-Rozen and Kwakkel, 2018].

A more accurate GSA technique for non-linear models is the decision-tree based GSA. Decision trees are a well-established feature selection approach from statistical learning. They aim to identify the separation criteria which describes the relationship between a set of input parameter and regions of the output space. The resulting variance of individual decision trees can be overcome using ensemble methods, such as random forest or Extra-Trees algorithms. Theoretically, the accuracy performance of this method can be used by increasing the number of trees, however, in practice, the number of trees is limited to the computational capacity. Moreover, “a forest of

[classification and regression] trees is impenetrable as far as simple interpretations of its mechanism go” [Breiman, 2001]. A further pitfall of decision-tree based GSA is its metric (variable importance). It only describes the relative importance of inputs, rather than their direct effect on output variance [Jaxa-Rozen and Kwakkel, 2018].

Better performance and mathematical representation of GSA can be reached when utilizing a variance-based approach. In a variance-based GSA approach, also referred to as Sobol method/technique, the influence of uncertain input parameter on the outcome variable can be determined using setups like factor fixing or prioritizing. Hereby, the method is based on the disintegration of the variance of the model outcome into summands of the model input variances. The Sobol approach can be divided into four steps [Zhang et al., 2015]:

1. the input space is sampled using a Sobol sequence, a quasi-randomized low-discrepancy sequence. In other words, the Sobol sequence covers the unit hypercube with lower discrepancy than a random sampling;
2. the generated experiment set is used to simulate the model outcomes;
3. the whole data set is then used to calculate the first-order indices and total-order indices to mathematically represent the contribution of each input parameter and their interactions to the overall variance of the model outcome<sup>1</sup>;
4. the first-order and total-order indices and their respective confidence bounds are visually presented in a barplot with error bars.

However, the Sobol technique is computationally expensive for models with a large number of input parameters. The model runs N, which is requisite to calculate Sobol indices, increases linearly with the number of input parameters X so that the following mathematical relationship applies:  $N = n(X + 2)$

---

<sup>1</sup>higher-order interactions such as the second-order interaction between two input parameters are not considered in this analysis

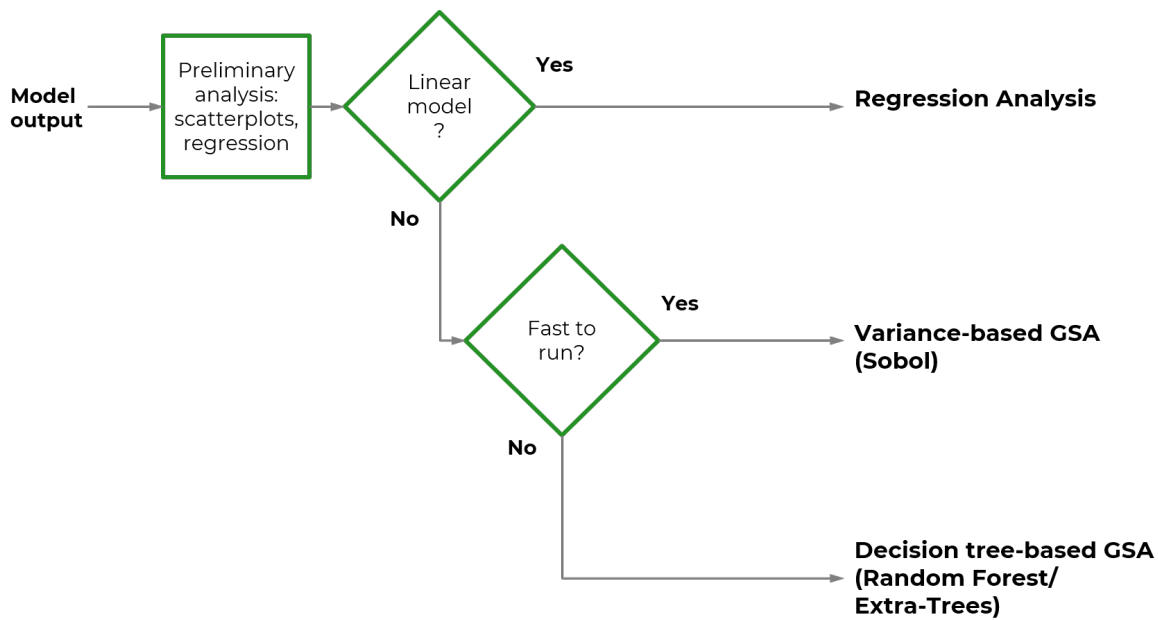


Figure 5.3: GSA decision tree.

This juxtaposition of the different GSA approaches shows clearly that the choice of the “right” GSA method depends on the specific case. To simplify the decision, the choice of the GSA technique will depend on two aspects: linearity and the average speed of a model run. The resulting decision tree is presented in Figure 5.3.

Since the PyDICE is non-linear and fast (one model run takes around 2.7ms), this study chooses to use the Sobol method for the GSA.

# 6 | SCENARIO DISCOVERY

After the stochastic simulation model is run over a carefully chosen set of different combinations of input parameters, which describes sufficiently the input spaces, the resulting set of experiments and their corresponding outcomes are first analyzed with a combination of interactive visualization, statistical analysis, and sensitivity analysis, as shown in Chapter 5. In the following step, a scenario discovery can be conducted to illustrate vulnerable scenarios. It should be noted that scenario discovery differs from more traditional sensitivity analysis because it seeks to describe regions in databases of model results that have particular properties, rather than rank the importance of different inputs in explaining the variance in the model output around a small number of points [Saltelli, 2008].

In Section 6.1, two commonly used supervised machine learning techniques, namely PRIM and CART, for scenario discovery are carefully described to only showcase their shortcomings in a time-based stochastic simulation model. In Section 6.2, an alternative technique, namely time series clustering, is presented. As a complementary technique to time series clustering, directed scenario search technique is proposed in Section 6.3. Lastly, in Section 6.4, a systematic scenario selection method that combines policy relevance and diversity, is illustrated.

## 6.1 PRIM & CART

Scenario discovery can be beneficial to characterize regions in the uncertainty space that demonstrates particular patterns of interest and/or has an impact on the system behaviour. In the framework of multi-scenario MORDM, scenario discovery allows the analyst to define areas in the uncertainty space which remains vulnerable for the defined candidate strategies. Traditionally, statistical or data-mining algorithms are used to find interesting patterns in the multidimensional data set. Lempert et al. [2006] proposed two methods for scenario discovery, the bump-hunting algorithm PRIM and the classification algorithm, CART.

PRIM searches in the multidimensional data set for regions where values of the outcomes are higher or lower than the predefined threshold. PRIM fits “boxes” to these regions and thereby creates hyper-rectangular regions which consist of vulnerable scenarios. Similar to PRIM, CART pursues to divide the space into subspaces. However, CART is “greedier” than PRIM as it splits the data at every step and thus re-

stricting itself to an average of  $\log_2(N)^1$  splits. Thus it is more prone to fail to limit important input parameters before it has utilized the full set of data.

However, there are two major downsides of using the above-mentioned methods for scenario discovery in a time-based stochastic simulation model. First, putting a threshold at a specific time point or a classification criterion like the mean on a time series outcome may confound different model behaviours [Steinmann, 2018]. Moreover, Kwakkel et al. [2013] consider time series outcomes as a thread over time (transient scenario) rather than a state at a specific time. Second, the use of PRIM and CART for scenario discovery presumes that outcomes of the model can be represented by a single orthogonal input space. However, most often this is not the case and this concern is acknowledged by many researchers [Lempert et al., 2006; Steinmann, 2018; Dalal et al., 2013].

To overcome those issues, Kwakkel et al. [2013] suggested using unsupervised machine learning algorithms to cluster the time series output into behavioural subsets.

## 6.2 TIME SERIES CLUSTERING

In contrast to supervised algorithms where it is aimed to predict specific relationship in a labelled data set, unsupervised algorithms are intended to discover interesting aspects in an unlabeled set of data. Naturally, unsupervised algorithms are utilized to organize an unlabeled data set into homogeneous clusters. The aim of unsupervised algorithms is to minimize the similarity within a cluster and at the same time to maximize the distinctness between clusters. Akin, time series clustering seeks to set time series into clusters based on their similarity in behaviour. Thus, by utilizing time-series clustering for scenario discovery, input subspaces, that have generated unfavourable outcomes, can be discovered. Prior to the clustering itself, the pairwise similarity or dissimilarity of the time series data must be computed.

In this research, the complexity-invariant distant (CID) measure for time series is used to calculate the distance between every pair of time series. In CID, the distances between pairs of time series data are calculated using Euclidean distance. In addition, since time series can have a wide diversity of complexities, the Euclidean distance is made complexity-invariant by adding a correction factor. When two-time series are showing two diverging complexities than the correction factor simply increases the Euclidean distance. The complexity of a time series is estimated by “stretching” it into a straight line. Consequently, the time series complexity increases with the length of the line Batista et al. [2014]. The CID is described by the pseudo-code algorithm 6.1.

Clustering can be divided into two styles of clustering, hierarchical clustering and partitional clustering. The former does not specifically know how many clusters are needed for a sufficient clustering and thus clusters are combined to their closest

---

<sup>1</sup> N = Number of points in the data set

---

**Algorithm 6.1:** Complexity-Invariant Distant (CID) measure for time series

---

```

1 def CID(a: array, b: array):
2     //deuc: euclidean distance
3     deuc ← (a1 − b1)2
4     for i ← 2, n do
5         | deuc ← deuc + (ai − bi)2
6     end
7     deuc ←  $\sqrt{d_{euc}}$ 
8     //ce: complexity estimator
9     cea ← (a1 − a2)2
10    ceb ← (b1 − b2)2
11    for i ← 2, n − 1 do
12        | cea ← cea + (ai − ai+1)2
13        | ceb ← ceb + (bi − bi+1)2
14    end
15    cea ←  $\sqrt{ce_a}$ 
16    ceb ←  $\sqrt{ce_b}$ 
17 return d  $\frac{\max(ce_a, ce_b)}{\min(ce_a, ce_b)}$ 

```

---

parent “clusters” from bottom-up (agglomerative). In partitional clustering, the observations are divided into pre-determined clusters. Thus, it can be concluded that hierarchical clustering is an iterative partitional clustering style. This research uses an agglomerative cluster analysis. In the beginning, each time series is first treated as a separate cluster. In each step, the closest clusters are combined into a greater cluster based on the distances between clusters calculated by the CID. The method is terminated if a sufficient number of clusters has been determined.

In the case of scenario discovery, “sufficient” number of clusters is reached when two main criteria can be satisfied: compactness and separability. This is important as policies based on insufficient time series clustering can unintentionally aim outcomes from different input spaces. To determine the appropriate number of clusters which are separable and compact, Rousseeuw [1987] proposes to utilize the overall average silhouette width. The silhouette describes for an observation (*s*(*i*)) the (dis)similarity of co-members of the same clusters (*a*(*i*)) to (dis)similarity of members in other clusters (*b*(*i*)). In other words, *s*(*i*) defines the quality of the clustering of the observation to its cluster:

$$a(i) = \frac{1}{|C_i| - 1} \sum_{j \in C_i, i \neq j} d(i, j) \quad (6.1)$$

$$b(i) = \min_{i \neq j} \frac{1}{|C_i|} \sum_{j \in C_i} d(i, j) \quad (6.2)$$

$$s(i) = \begin{cases} 1 - a(i)b(i), & \text{if } a(i) < b(i) \\ 0, & \text{if } a(i) = b(i) \\ b(i)a(i) - 1, & \text{if } a(i) > b(i) \end{cases} \quad (6.3)$$

The silhouette of an observation  $s(i)$  is above 1, when  $a(i)$  is smaller than  $b(i)$ . If  $s(i)$  is equal to zero, the “within” dissimilarity is approximately equal to the smallest “between” dissimilarity. When the observation lies closer to members of other clusters than to co-members, the  $s(i)$  is below 1. The average silhouette width describes the quality of clustering for all observations of a cluster. To determine the overall quality of the clustering for  $k$  number of clusters over the whole data set, the overall average of  $s(i)$  for all observation  $i$  (overall average silhouette width) can be calculated. Thus, the overall average silhouette width offers an excellent solution for this research to determine the “right” number of clusters.

## 6.3 DIRECTED SCENARIO SEARCH

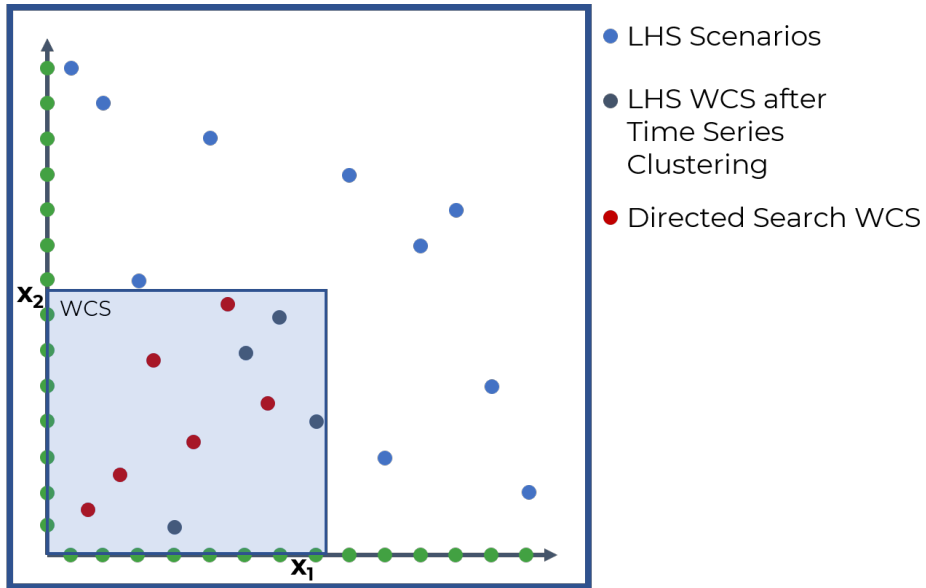


**Figure 6.1:** Scenario Discovery using directed search over uncertainties and times series clustering.

In the previous sections, vulnerable scenarios were selected from a data set that was generated by sampling across a set of uncertainties using LHS. Even though, for open exploration, LHS ensures that the uncertainty set is evenly sampled across the experiment set, it is the cause of a pivotal drawback in scenario discovery. Finding vulnerable scenarios using an LHS sampled data set depends on the analyst choice on the number of scenarios to be considered for the experiment set. With an increasing number of scenarios to be examined, uncertainties in the experiment set become more definite. Theoretically, this intuitive reasoning is correct, however, it is almost

impossible to validate it in practice. Thus, in this research, Time Series Clustering in subsection 6.2 is complemented using the directed search technique over the uncertainties. The directed search technique uses basically evolutionary algorithms to generate Pareto optimal solutions to a many-objective optimization problem. Here, the evolutionary algorithm  $\epsilon$ -NSGA-II is applied to search over the set of uncertainties in finding the worst-case scenarios for the worst optimum outcome.  $\epsilon$ -NSGA-II is explained in more detail in Section 7.1.1.

## 6.4 SCENARIO SELECTION

A very large diverse set of scenarios could generate a more distinct set of robust policies. However, it is crucial to limit the small subset of scenarios for two main reasons: (i) limited users/decision-makers attention to only a small number of scenarios and (ii) the computational constraint of policy evaluation over a larger set of scenarios. Academic research in selecting the right number of scenarios is still at early stages. [Watson and Kasprzyk \[2017\]](#) propose to use at first scenario discovery to determine vulnerable scenarios and afterwards to choose specific values from the uncertain parameter ranges that caused these vulnerabilities. However, this method criticized mainly for the reason that the choice of a few values from the uncertainty ranges is subjective and not subject to a systematic approach that rationalizes the choice. As a consequence, [Eker and Kwakkel \[2018\]](#) introduce a systematic scenario selection method that combines policy relevance and diversity in the search. In their study, they first determine undesirable scenarios based on policy relevance in terms of unwanted scenario conditions determined by the median values of the scenario space/outcomes. In the second step, a small number of scenario is selected from the earlier-defined subset of policy-relevant scenarios on the basis of a diversity criterion as by [Carlsen et al. \[2016\]](#).

The diversity maximization approach of [Carlsen et al. \[2016\]](#) can be divided into two steps:

1. After deciding on the number of to be selected scenarios  $K$  from scenarios  $M$ , the distances between any scenarios  $d_{i,j}$  is determined by applying a distance metric, like Manhatten distance or Euclidean distance, on the normalized outcome variables  $f_{i,(k,j)}$ . Thereby, it is basically assumed that the distances between two scenarios are equidistant to the states of each outcome variable:

$$d_{i,j} = \sqrt{\sum_i (f_{i,j} - f_{i,k})^2} \quad (6.4)$$

2. The diversity of the scenario set  $D_{K_l}$  is defined by the minimal distance and the mean distance between the scenarios of the set  $K_l$  given the weight  $w$ . After having calculated the diversity for each scenario set out of  $(M)_K$  possible combinations, the scenario set  $S_K^*$  with the maximum diversity value is chosen:

$$D_{K_l} = (1 - w) \min(d_{j,k}) + w \text{mean}(d_{j,k}) \quad (6.5)$$

$$S_K^* = \max[D_{K_l}] \quad \text{where: } l = 1 \dots \binom{M}{K} \quad (6.6)$$

Similar to the approach of Eker and Kwakkel [2018] and Carlsen et al. [2016], this study first exploits time series clustering and directed scenario search to discover policy-relevant future states of the world. From this subset of scenarios  $M$ , four maximal diverse scenarios ( $K = 4$ ) are selected based on the diversity criterion by Carlsen et al. [2016].

# 7

# POLICY DISCOVERY

This chapter is divided into two sections. Section 7.1 illustrates the search algorithm,  $\epsilon$ -NSGA-II, that is used in this study to find alternative candidate strategies. Next, two different robustness criterion's for comparing these strategies is discussed in Section 7.2.

## 7.1 DIRECTED POLICY SEARCH

### 7.1.1 Multi-objective evolutionary algorithms

In most cases, complex systems consist of many conflicting objectives. This means that there is no single optimal policy but rather a set of policy alternatives, which are Pareto efficient/optimal. This means that each policy of the set is non-dominant to any other policy in the set. The most renowned search algorithms to discover a set of non-dominated solutions are the many-objective evolutionary algorithm. Many-objective evolutionary algorithms (MOEA) use evolutionary computing (such as genetic algorithms or evolutionary strategies) to optimize over many conflicting objectives and gradually to reach a set of Pareto efficient solutions. The inner workings of the algorithms can be simply described as follows [Reed et al., 2013; Emmerich and Deutz, 2018]:

1. A set of options are initialized on the basis of the objective target.
2. A generational loop is repeated as long as the termination criterion is met.
  - 2.1 Within the loop, the most qualified options from the set is used to determine the next generation of alternative options.
  - 2.2 A selection process takes place in which the least qualified options of the current set are replaced by better performing options from the newly generated set.

Furthermore, MOEAs can be distinguished into three main paradigms: Pareto-based MOEAs, indicator-based MOEAs and decomposition-based MOEAs. The main difference between those classes is the applied selection operator during the selection process. Since Pareto-based algorithms are not only the largest class but also very prominent within the MOEA community [Li, Yang and Liu, 2018], this study just focuses on Pareto-based MOEAs.

### 7.1.2 Pareto-based MOEA: $\epsilon$ -NSGA-II

A typical algorithm within the Pareto-based MOEA paradigm is the NSGA-II algorithm. Instead of replacing the whole population at each search iteration, NSGA-II was one of the first algorithms to utilize Pareto dominance and diversity preservation<sup>1</sup> to search and to rank alternative options to determine a new population for the next search iteration [Reed et al., 2013; Emmerich and Deutz, 2018]. The main advantages of the NSGA-II algorithm are that it only uses a few configuration parameters and it can handle larger numbers of objectives without any issues. However, the drawback of using NSGA-II algorithm is that convergence can neither be guaranteed nor measured.

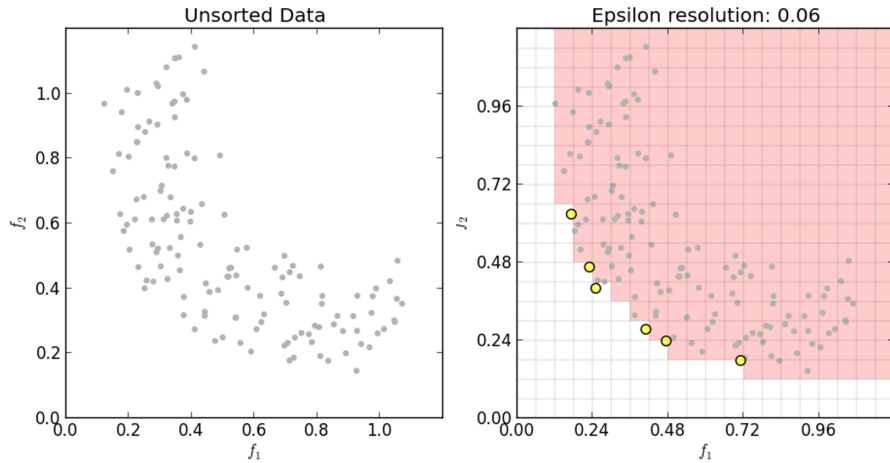


**Figure 7.1:** An illustrative example of epsilon dominance [Woodruff and Herman, 2013].

To make the search process more efficient, the NSGA-II algorithm was extended by two features: the integration of the epsilon dominance in the sorting process and the use of adaptive population sizing [Ward et al., 2015]. The accuracy level of solutions can now be determined by utilizing Epsilon dominance. Subsequently, this feature promotes diversity as it eliminates any alternative solution outside of the space of epsilon dominance (see Figure 7.1). The efficiency of the search process is also enhanced as adaptive population sizing allows to test alternative options with a smaller option. If a more stable set is found, the population size can be increased to ensure that better approximated Pareto optima can be discovered in each generation. The resulting algorithm is called  $\epsilon$ -NSGA-II. This research utilizes this algorithm to not only to find Pareto efficient policies but also, as already mentioned in Section 6.3, to discover Pareto efficient worst-case scenarios.

<sup>1</sup> Crowding distance criterion: the crowding distance is determined by the “empty” space around a solution.

## 7.2 UNCERTAINTY ANALYSIS

After having discovered a non-dominated set of policies using  $\epsilon$ -NSGA-II, an uncertainty analysis is conducted to evaluate the robustness of the policies across a large number of possible scenarios. Like in open exploration (see Section 5.1), Latin Hypercube Sampling is used to sample efficiently and evenly over the uncertainty space. The resulting experiment set is used to calculate the robustness of the policies.

In this research, robustness is defined as the ability to maintain its function despite unexpected external shocks or unpleasant external conditions. In line with this definition, a robust policy is defined as one that is able to perform well across a range of possible scenarios [Kasprzyk et al., 2013; Walker et al., 2013; Herman et al., 2015; Walker et al., 2001]. Further, metrics are used to operationalize the concept of policy “robustness” and facilitate comparison of proposed policy options, that perform strongly under a range of plausible conditions. Further, it is suggested to chose more than one metric as it may disclose different aspects in the robustness of the policy [Kwakkel et al., 2016b]. In this study, two robustness metrics are used: minimax regret and signal-to-noise ratio (SNR).

The minimax regret criterion, also known as Savage criterion, strives to minimize the regret with respect to the worst-case. This metric is considered as conservative, that has a high level of risk aversion. The outcome of the metric ranges between 0 and 1, where 0 indicates high robustness of the policy on the outcome and 1 indicates low robustness. In contrast, the SNR criterion, derived from signal theory, uses the full set of scenarios to provide a balanced perspective, which presents neither a low nor high level of intrinsic risk aversion. To be more specific, the SNR criterion determines the mean and the corresponding variance of a policy option over a set of different scenarios. The outcome of the SNR criterion ranges between 0 and 1, where 1 indicates high robustness of the policy on the outcome and 0 indicates low robustness.

## **Part III**

## **Results**

“Things that have never happened before, happen all the time.” — Scott D. Sagan

# 8 | OPEN EXPLORATION

The goal of this chapter is to first explore the input space and the out space of PyDICE before analyzing the impact of fat-tailed uncertainty on Nordhaus optimal policy in Chapter 9. The results of the open exploration are presented in two stages: initial exploration, indicating the possible range of the outcome space, in Section 8.1 and global sensitivity analysis in Section 8.2.

## 8.1 INITIAL EXPLORATION

To create an initial understanding of the dynamics and the effects of the implemented uncertainties on the outcome space, the open exploration technique is utilized. In particular, this is done by generating time series plots for each outcome. In addition, a boxenplot is added along the y-axis of each time series plot. This boxenplot describes the statistical distribution of the outcomes in the year 2300. The design of experiment (DOE) for this analysis is generated using Latin Hypercube Sampling (LHS) to create an equal representation of the input space. Furthermore, to ensure good coverage of the input space, PyDICE is simulated over 10000 different scenarios and 50 different policies. This results in an experiment count of 500000. This set of experiments was used to chart the time series plots and boxenplots in Figure 8.1. In the following, we will analyze each outcome in more detail.

Figure 8.1a presents the time series outcome of the atmospheric temperature between 2010 and 2300. In general, it can be observed that for most cases, the atmospheric temperature increases over time. Although the atmospheric temperature at the year 2300 is dispersed between 0°C and 20°C, the boxenplot shows that in only very few experiments, the temperature rises above 7.5°C. The boxenplot also displays rare extreme cases where atmospheric temperature ends up between 14°C and 20°C.

The time series outcome of the annual damages is displayed in Figure 8.1b. In general, it can be observed that until 2060 annual damages are relatively robust. However, after 2060, the different annual damages show not only high dispersion but also some non-linear behaviours. Moreover, the boxenplot shows that 25% of all experiments result in annual damage of \$300 trillion and above. This indicates a high variance in the outcomes of the annual damages. The boxenplot also displays rare extreme cases where annual damages end up around \$1300 trillion. Furthermore, between the year 2250 and 2300, a small dip can be observed for multiple scenarios.

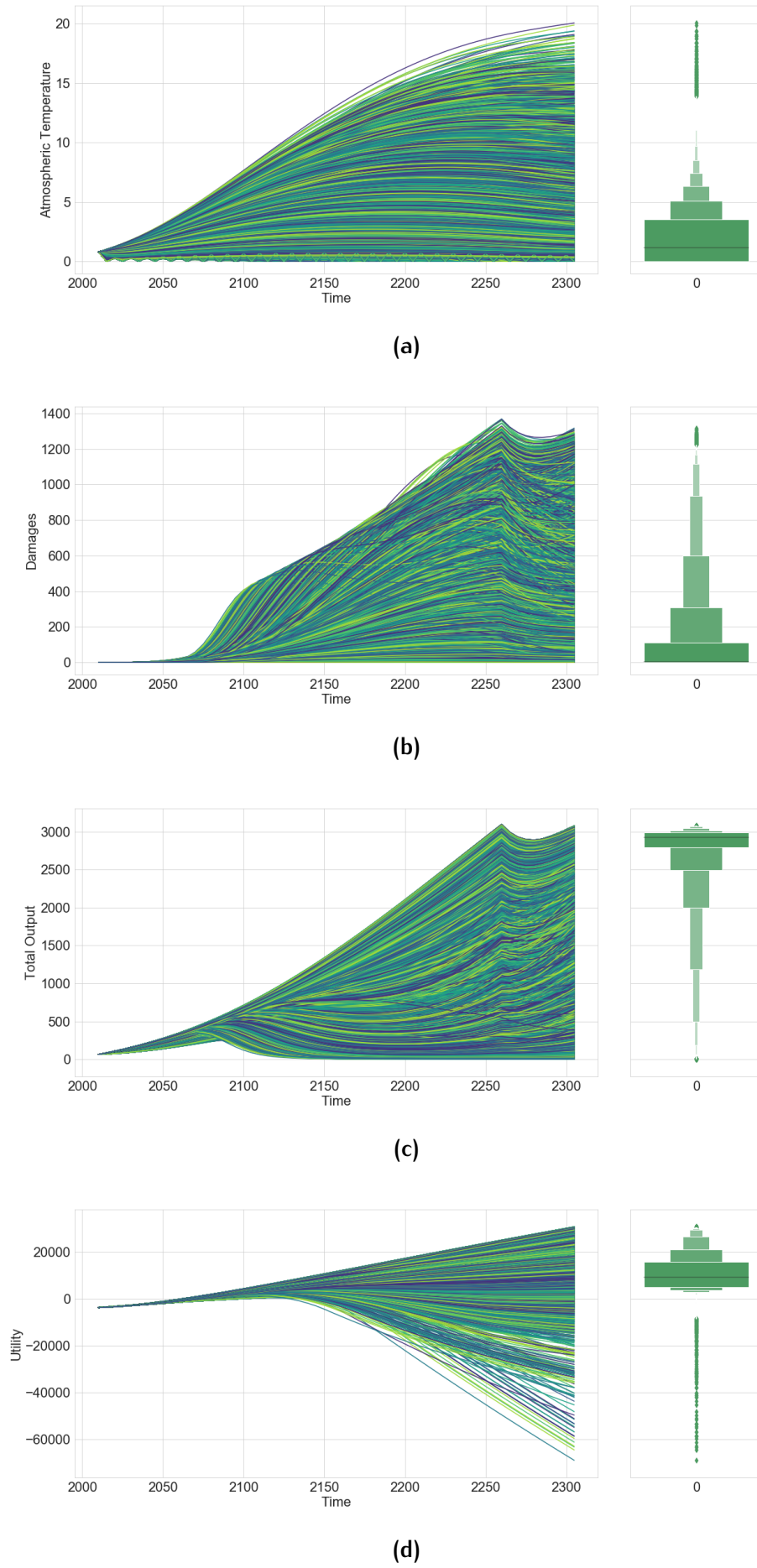


**Figure 8.1:** Time series plots and boxenplots over every outcomes of interests.

This dip is due to the optimal long-run savings rate (see Equation (4.2)) which is used as a savings rate for the last 50 years.

Further, Figure 8.1c illustrates the time series outcome of the total output. Until 2070, the total output is relatively robust. However, from 2070 on, the pathways of the experiments diverges. Although 75% of the runs rises above \$2700 trillion in 2300, there are some rare cases where the value of the total output is below \$250 trillion. Moreover, for some extremely rare cases, the total output is at \$0. A zero total output indicates that the whole world economy has collapsed. Please note, that these values could have gone negative, but in order to reflect the real world, PyDICE and DICE put a lower bound at \$0.

Figure 8.1d illustrates the cumulative (discounted) utility over the full period. Thus, the final year 2300 is of interest. Here, almost every experiment run returns a utility value higher than \$0 (and up to \$30 trillion). However, there are still a few extremely rare cases in which the utility is between \$0 and -\$60 trillion. These extremely low values can only be explained by the fact that the world economy collapsed (total output = \$0) very early in time.

### Summary

The embedded uncertainties in the PyDICE model trigger a wide range of different results for the outcomes of interest. Moreover, this initial exploration has shown that catastrophic outcomes are possible even though they are present in only a few experiment runs. One of the main objective of this research is to determine a set of robust policies on the basis of the precautionary principle and thus each outcome is of equal importance.

## 8.2 GLOBAL SENSITIVITY ANALYSIS

Following the initial exploration, this section aims to identify the most influential uncertainty parameter or combinations of uncertainty parameters on the outcomes of interest. For this purpose, a variance-based global sensitivity analysis (GSA), namely the Sobol method, is utilized. Hereto, the first-order indices  $S1$  and total order indices  $ST$  give a detailed mathematical representation of the contribution of each uncertainty parameter and their interactions to the overall variance of the model outcome. Since the Sobol method only enables sensitive analysis of the uncertainty parameter on the outcomes at a specific point in time, the years 2050, 2100, 2150, 2200 and 2300 have been chosen to sufficiently represent the time axis. Although in theory, Sobol scores can never be negative, in practice, negative values can occur. Subject to the condition that the negative values are relatively small and have confidence intervals that overlap zero, they can be interpreted as zero (see the confidence intervals of the GSA in the Appendix C). Note that, the scores for the ECS distribution must be interpreted with caution. The presence of the ECS distribution alone won't

have an effect on the outcome, because it only affects the model outcomes via the sampled ECS value. Thus, the  $S1$  score will be at all times zero. To determine the relative influence of the ECS distribution on the outcome, the total order indices  $ST$  is used. Moreover, the individual samples from the ECS distributions are also tracked to analyze the impact of the real values on the outcomes of interest. For a more nuanced discussion, each outcome is examined individually.

### Atmospheric Temperature

The GSA on the outcome, atmospheric temperature, in Figure 8.2 shows that neither the total availability of fossil fuel nor the TFP growth rate has a substantial impact. Furthermore, the effects of the uncertainties price of backstop technology, damage function and population growth rate are negligible, as the  $S1$  and  $ST$  scores are below 0.001 over the whole time period. In contrast, the ECS value dominates the outputs of atmospheric temperature. The  $S1$  and  $ST$  scores for this uncertainty parameter is respectively 0.49 and 1 for all time points besides the year 2300. This dominance is no surprise, as the ECS parameter describes the temperature rise that would result from a sustained doubling of the atmospheric equivalent  $CO_2$  concentration. For any experiment run at any time point in which the emission is not equal to zero, the ECS parameter will have a significant effect on the atmospheric temperature. At the year 2300, the atmospheric temperature is more sensitive to the initial growth rate of carbon intensity than the ECS parameter. The implication is that for multiple cases in the experiment set, the carbon efficiency is 100% (i.e., emission to output ratio is zero.) at the year 2300. The second most influential factor is the ECS distribution. This indicates already our prior assumption based on Weitzman Dismal Theorem that fat-tailed distributions have a substantial effect on the outcomes of interest.

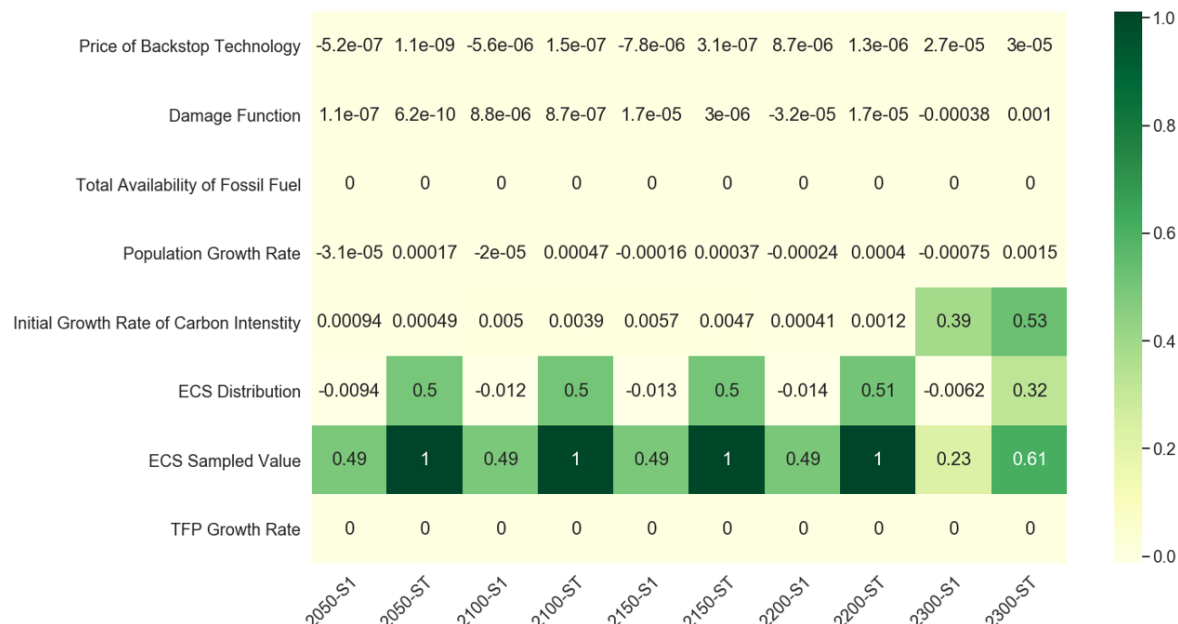


**Figure 8.2:** Sobol indices for the outcome atmospheric temperature: Each cell illustrates the (global) sensitivity of the uncertainties (rows) on the outcome variable for the years 2050, 2100, 2150, 2200, 2300 (columns).

## Damages

The GSA for the damage outcome is presented in Figure 8.3. Similar, to the GSA of the atmospheric temperature, the damage outputs are most sensitive to the ECS parameter and the initial growth rate of carbon intensity. Moreover, the sensitivity for these parameters show the same trends as the GSA on the atmospheric temperature outcome. Thus, many earlier conclusion can be applied to this GSA. What is different though is the marginal higher impact of the applied damage function on the damage outcome. Although the S1 score is only ranges between 0 and 0.13 over the whole time period, the effect of the damage function in interaction with other uncertainty parameters is relatively higher (up to 0.21).

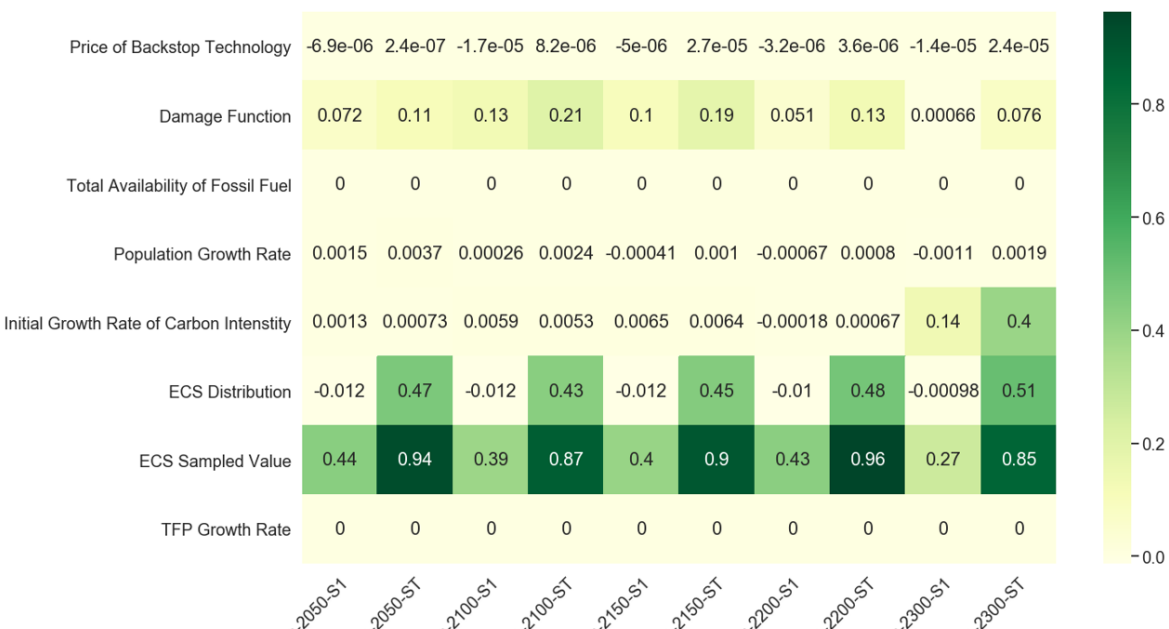


**Figure 8.3:** Sobol indices for the outcome damages: Each cell illustrates the (global) sensitivity of the uncertainties (rows) on the outcome variable for the years 2050, 2100, 2150, 2200, 2300 (columns).

## Total Output

Figure 8.4 illustrates the GSA for the outcome parameter, total output. The Sobol scores for the year 2050 indicates that the total output is solely dominated by the population growth rate. However, after this time point, the preeminence of the population growth rate declines rapidly whereas the total output becomes more and more sensitive to the ECS parameter, the damage function and the initial growth rate of carbon intensity. This shift in dominance between 2050 and 2100 is also reflected in the time series plot earlier (see Figure 8.1c). Otherwise, the sensitivity of the total outcome to the uncertainties is very similar to the two previous GSAs.

## Utility

Lastly, the GSA for the utility outcome is illustrated in Figure 8.5. Although the discounted utility at year 2300 is of interest for the decision-maker, analyzing the



**Figure 8.4:** Sobol indices for the outcome total output: Each cell illustrates the (global) sensitivity of the uncertainties (rows) on the outcome variable for the years 2050, 2100, 2150, 2200, 2300 (columns).

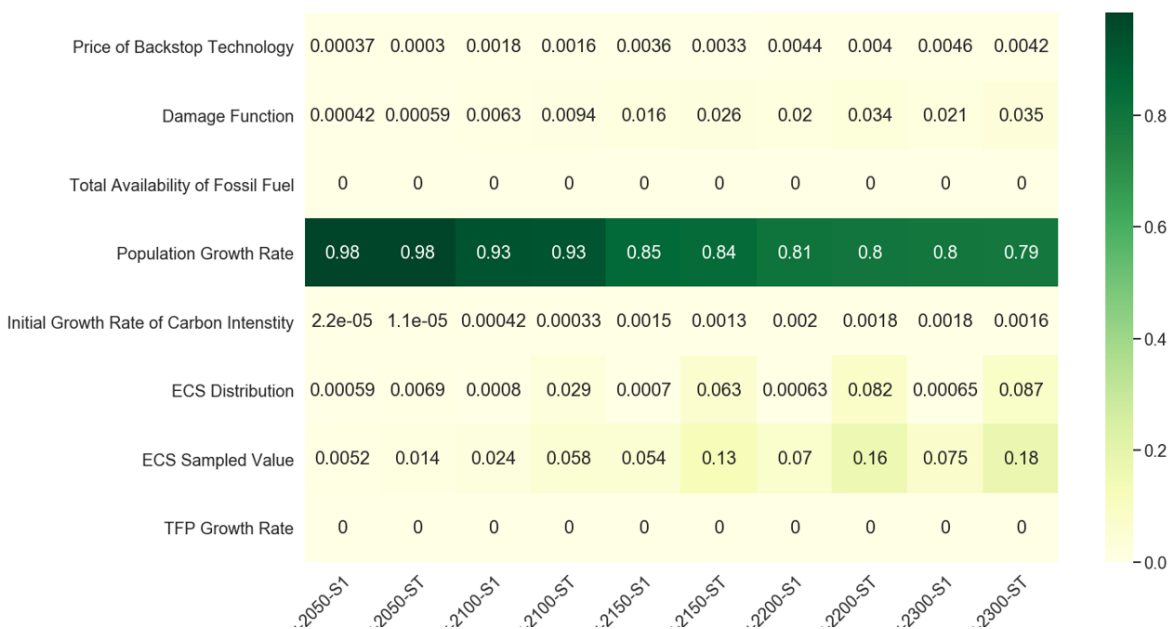


**Figure 8.5:** Sobol Indices for the outcome utility: Each cell illustrates the (global) sensitivity of the uncertainties (rows) on the outcome variable for the years 2050, 2100, 2150, 2200, 2300 (columns)

utility over the full-time period can still present some interesting insights. The Sobol scores for utility shows that the outcome is predominately influenced by the population growth rate (*S1* and *ST* ranges between 0.79 and 0.98). That is because the utility function is population-weighted. Furthermore, it can be observed that the utility becomes over time marginally more sensitive to the ECS parameter, the damage

function and the initial growth rate of carbon intensity and the same time marginally less sensitive to the population growth rate.

## Summary

The variance-based GSA has presented the reader with an overview of the impact of uncertainties on the four outcomes. Overall, the atmospheric temperature, the damages and the total output are mainly sensitive to the ECS parameter and the damage function whereas the cumulative discounted utility is predominantly affected by the population growth rate. Three main insight can be derived from this GSA:

1. The two uncertain parameters, total availability of fossil fuels and TFP growth rate have no effect on any of the four outcomes. The latter is in particular surprising since [Nordhaus \[2008b\]](#) believed it to be the most important uncertainty since it is one of the main drivers of long-run economic growth (see Equation (3.1)). When moving to further analysis, these two uncertain parameters are neglected.
2. In most of the GSAs above, it was also observed that the effect of the initial growth rate of carbon intensity was substantially higher in the final year in contrast to previous time points. The obvious implication of this observation is that a faster improvement in carbon efficiency could yield lower atmospheric temperatures and thus also lower damages.
3. For three out of four outcomes of interest, the GSA has shown that the distribution of the ECS parameters is highly influential. In other words, fat-tailed distributions can have a substantial impact on the outcomes of interest.

In the Chapter 7, the input space and the outcome space of the PyDICE model was explored using global sensitivity analysis (GSA) and open exploration respectively. The reader should have now a sound understanding of the various behaviours of the model. Moreover, they are the first indications that fat-tail distributions can have a significant impact on the outcomes. The following chapter is exploring further this presumption by utilizing Nordhaus optimal policy as the baseline policy. To this end, Nordhaus optimal policy from the DICE model was converted into PyDICE variables. The savings rate and control were approximated using the equations (4.1) and (4.2). The following table displays the chosen input parameter in PyDICE to adequately represent Nordhaus optimal policy:

**Table 9.1:** Nordhaus Optimal Policy in PyDICE parameters

Savings Rate	Emission Control Rate Target	Pure rate of social time preference
0.248	2150	0.015

The effectiveness of these policies levers on the total outcome has been verified by utilizing a GSA over the these levers on the outcomes. The results of this GSA can be found in Appendix C.

## 9.1 INITIAL EXPLORATION

In order to create an underlying understanding of the implications of Nordhaus optimal policy on the outcome, an experiment set is generated by simulating over 540000 different scenarios.

The experiment set is used to create pair plots. Pair plots are a great visualization tool to illustrate the statistical relationship between multiple parameters. Figures 9.1, 9.2 and 9.3 present such a pair plot for the year 2050 and 2300 in which the relationship between the outcomes of interest are displayed in designated scatter plots. A third dimension has been added to the pairplots by coloring each point based on the utilized distribution type for the ECS parameter (see Figure 9.1a,b), the damage function (see Figure 9.2a,b) and the combination of damage function and the distribution type (see Figure 9.3a,b). In the following, the relationship between each outcome is systematically analyzed:

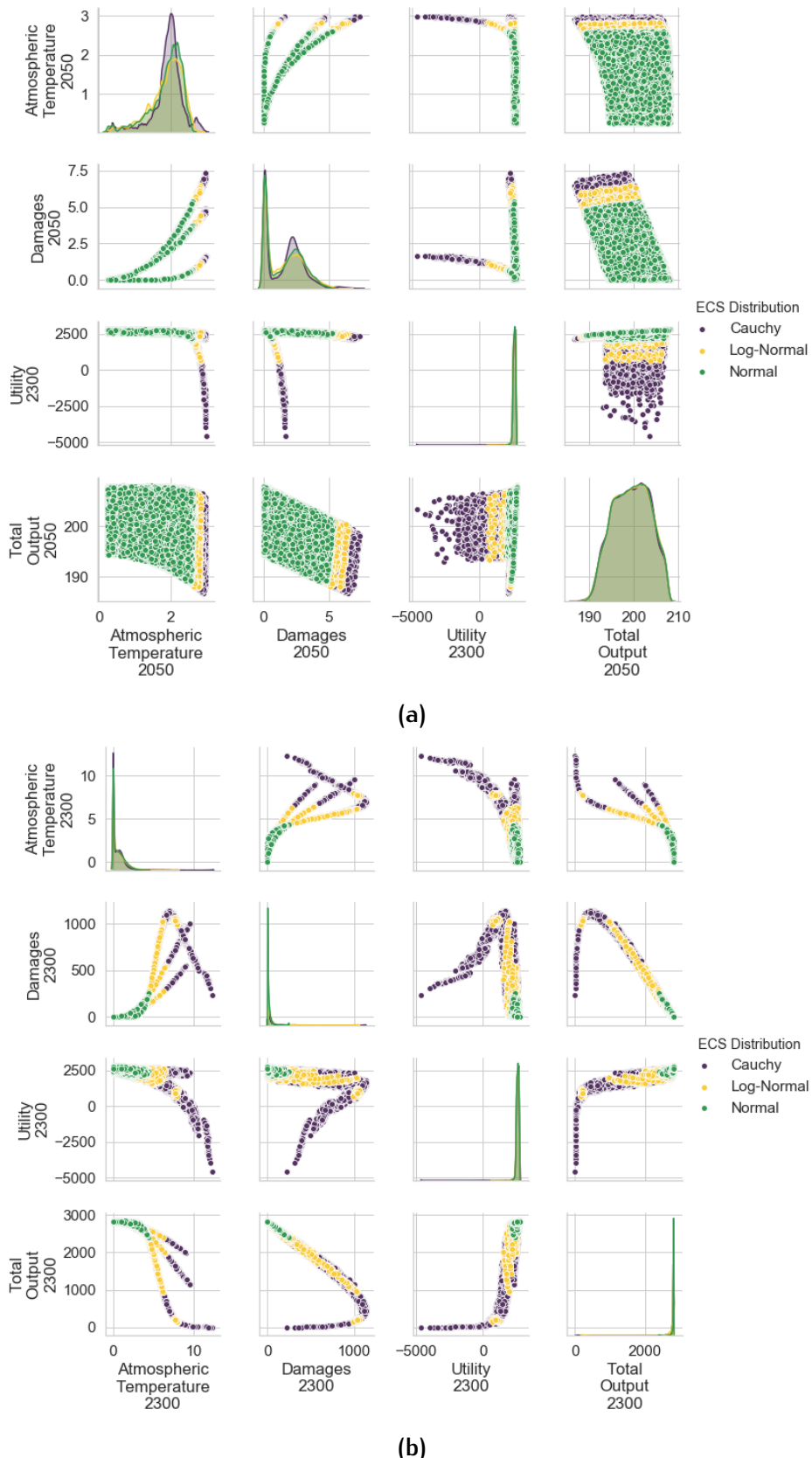


**Figure 9.1:** For the year 2050 (a) and 2300 (b), pair plot over the outcome variable is presented. A third dimension is added to the pair plot by colouring each point based on the utilized distribution type for the ECS parameter. Besides the cells in the diagonal axis of the pair plot (which illustrates the distribution of each outcome), each cell illustrates a scatter plot of two different outcomes of interest.

### ***Atmospheric Temperature - Damages***

From the scatter plot “Atmospheric Temperature - Damages” (TATM-D) in Figure 9.3a, one is able to observe that, as the temperature in the atmosphere rises that the annual damage grows exponentially. Furthermore, TATM-D reveals that the rise in damages can follow three different trajectories. According to the TATM-D in Figure 9.1a, these trajectories are caused by the three damage functions which are specified in PyDICE. At the year 2050, where the atmospheric temperature ranges between 0°C and 3°C, the curve with the highest slope has been induced by the damage function of Newbold, whereas, at the same time, Weitzman damage function has the least impact on the annual damages. But with rising atmospheric temperature over the course of time, Weitzman damage function has the greatest repercussion on the annual damages (see Figure 9.2a).

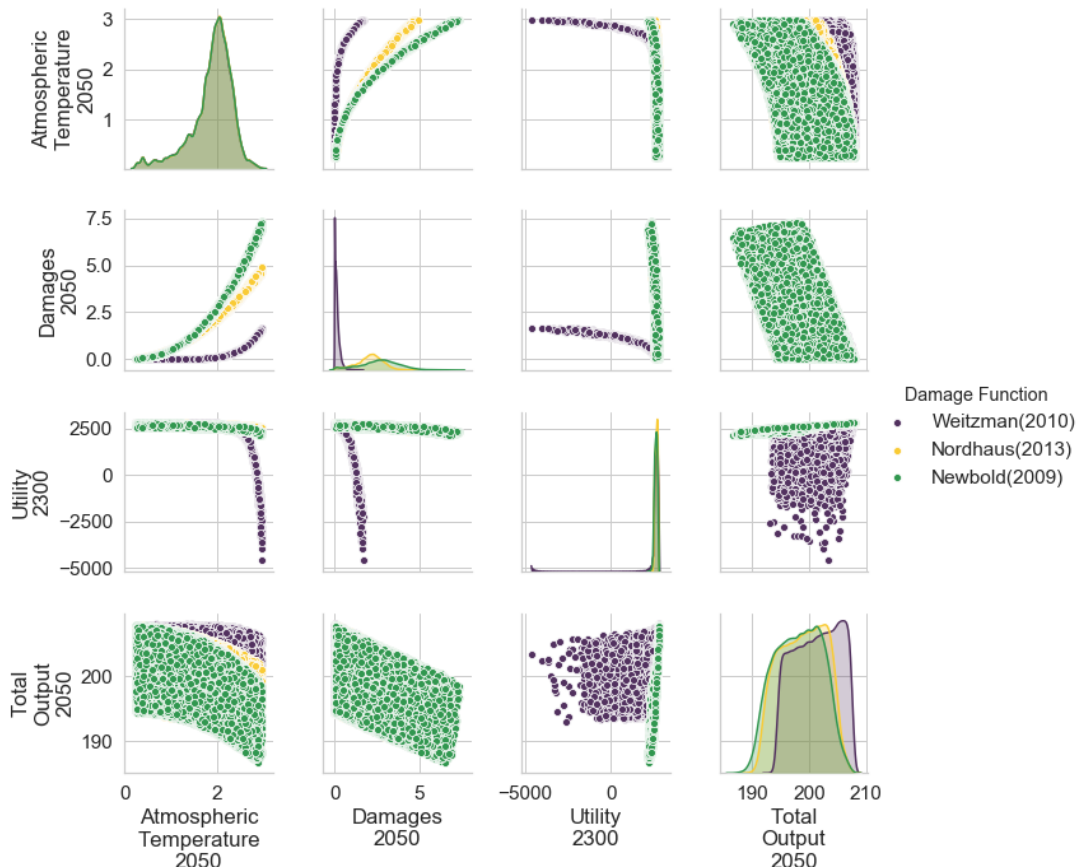
Further, the highest points of all three curves are due to the Cauchy distribution. The remaining points are caused by the log-normal distribution and the normal distribution in descending order (see Figure 9.1a). Additionally, it is also striking to observe that catastrophic damages are attained when Weitzman damage function is combined with the Cauchy distribution (see Figure 9.3a). Lastly, in the year 2300, some scatter points demonstrate at higher temperature respectively lower damages. That is, in these specific future states of the world, the world economy has collapsed (total output has reached zero) or at the verge of collapse. Although in these scenarios, zero-carbon is emitted, some damages will still occur as the accumulated carbon in the atmosphere depreciate slowly over time (see Figure 9.3b).

### ***Damages - Total Output***

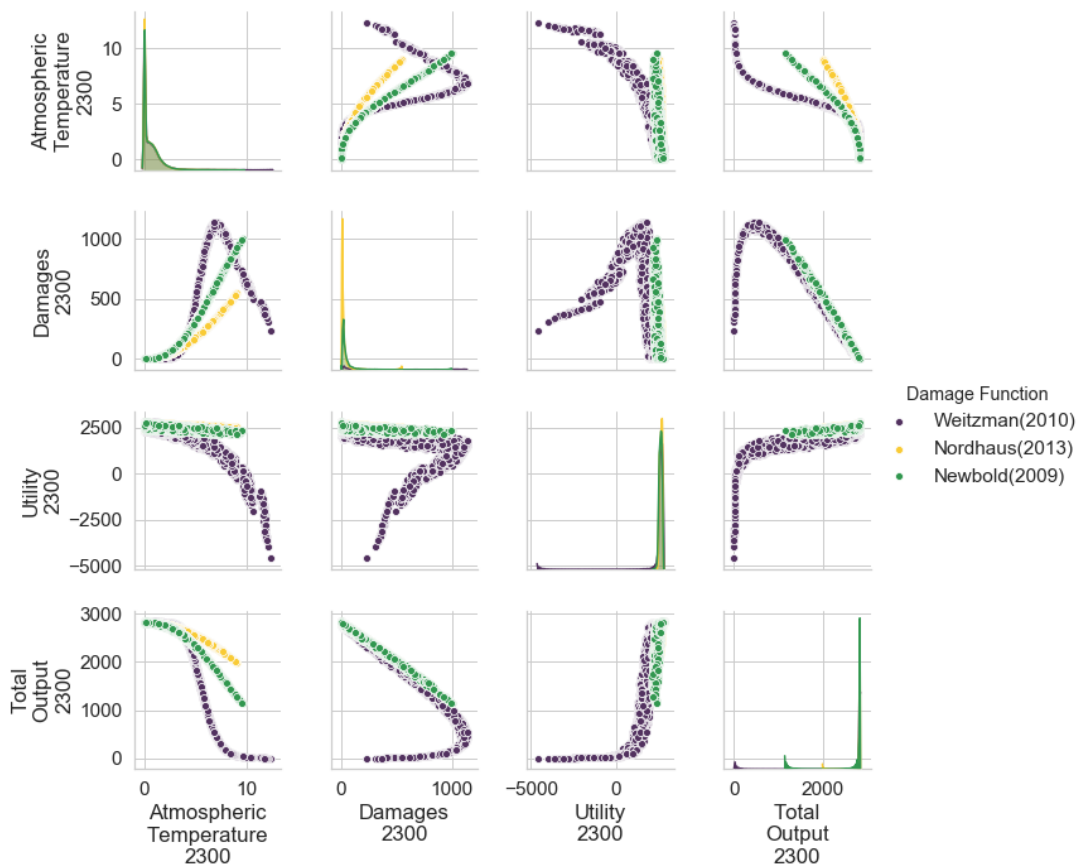
In Figures 9.1, 9.2 and 9.3 it is observed that, as the annual damage rises, the total output declines. But when total output is on the verge of collapse, the damages gradually regress. Furthermore, the highest damages and lowest total output is predominately reached with the Cauchy distribution and for some few cases with the log-normal distribution. Furthermore, as seen in TATM-D, the D-TO reveals that the Newbold damage function has the highest impact in the first few decades when Damages are small due to relatively low atmospheric temperature. From the year 2100 onwards, Weitzman damage function is the most influential factor in the outcomes of total output (see Figure B.2 of the Appendix B). Similar to the description above, catastrophic outcomes (high damages and low to zero total output) are attained when the Weitzman damage function is combined with the Cauchy distribution (see Figure 9.3).

### ***Atmospheric Temperature - Total Output***

The scatter plots “Atmospheric Temperature - Total Output” (TATM-TO) in Figures 9.1, 9.2 and 9.3 shows that rising temperature leads to a decline in total output. How fast the output declines depends largely upon the applied damage function from Weitzman (highest impact), Newbold or Nordhaus (lowest impact). The TATM-TO



(a)



(b)

**Figure 9.2:** For the year 2050 (a) and 2300 (b), pair plot over the outcome variable is presented. A third dimension is added to the pair plot by colouring each point based on the damage function. Besides the cells in the diagonal axis of the pair plot (which illustrates the distribution of each outcome), each cell illustrates a scatter plot of two different outcomes of interest.

in Figure 9.1b shows a further interesting observation. The total output appears to be very robust for the normal distribution. This is mainly because the maximum atmospheric temperature of using a normally distributed ECS parameter is around 5°C and thus not high enough to trigger disastrous outcomes in the model world. However, it can also be observed in the TATM-TO of Figure 9.3b, that the Cauchy distribution nor the log-normal distribution alone have a substantial impact on the total output but only in combination with damage function of Weitzman or Newbold.

### ***Atmospheric Temperature - Utility***

From the scatter plot “Atmospheric Temperature - Utility” (TATM-UTIL) in Figures 9.1, 9.2 and 9.3, one is able to observe that, the utility can follow atmospheric temperature on two different trajectories. The first trajectory is very stable around the cumulative discounted utility of \$2 trillion. However, in the case of the second trajectory, the cumulative discounted utility declines as the atmospheric temperature rises. The second curve is solely caused by the Weitzman damage function whereas the first trajectory is mainly due to the damage function of Nordhaus and Newbold. To be more specific, values below \$2 trillion for the cumulative discounted utility is only reached in conjunction with Cauchy or log-normal distribution (see Figure 9.3).

### ***Damages - Utility***

Once again two different trajectories for the cumulative discounted utility is discovered in the scatter plot “Damages - Utility” (D-UTIL) in Figures 9.1, 9.2 and 9.3. The first trajectory is very stable around the cumulative discounted utility of \$2 trillion. In the case of the second trajectory, the cumulative discounted utility declines as the damage rises. However, in the year 2300, some scatter points demonstrate at lower damages respectively lower utility. That is, in these specific future states of the world, the world economy has collapsed at a certain point in time. Hence, the expected utility in these scenarios for Nordhaus optimal policy is naturally alarming. In fact, this second trajectory is triggered by the Weitzman damage function in combination with the Cauchy or log-normal distribution (see Figure 9.3).

### ***Utility - Total Output***

The scatter plot “Utility - Total Output” (UTIL-TO) of Figure 9.3b shows an exponential relation between utility and total output. As long as the total output is around zero, the expected cumulative discounted utility ranges between around -\$4 trillion and \$0. But from the moment, the expected utility becomes positive, the total output increases exponentially to the utility. Furthermore, the scenarios, in which total output at the year 2300 is lower than \$1.2 trillion, comprises Weitzman damage function in conjunction with Cauchy or log-normally distributed ECS parameter.

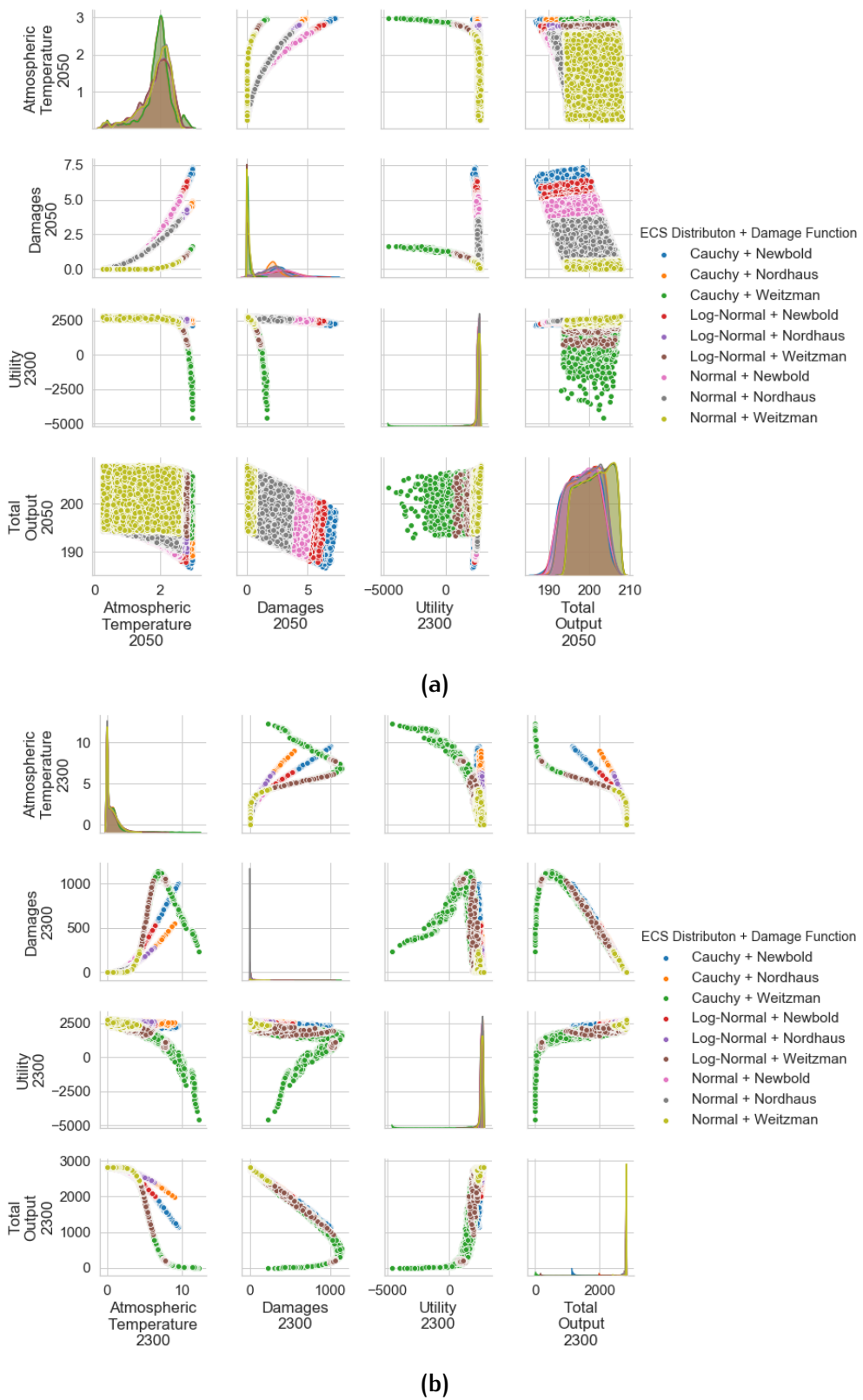


**Figure 9.3:** For the year 2050 (a) and 2300 (b), pair plot over the outcome variable is presented. A third dimension is added to the pair plot by colouring each point based on the combination of damage function and the distribution type. Besides the cells in the diagonal axis of the pair plot (which illustrates the distribution of each outcome), each cell illustrates a scatter plot of two different outcomes of interest.

## Summary

The analysis has illuminated the relationship between the outcomes of interest in great detail. The most intriguing insight from this exploration is that catastrophic outputs in any of the four outcomes are only attained for scenarios which comprise of Weitzman damage function and fat-tailed ECS parameter. It can also be derived as fatter the tail of the distribution becomes, the more severe are the consequences. Lastly, this analysis has also shown that the optimal policy of Nordhaus is not robust for a set of scenarios.

## 9.2 STATISTICAL ANALYSIS

Using a simulation approach has the main advantage that the generated data set can be used to quantify the effects of input parameter on the outcome. In this research, the generated data set is specifically used to understand the effects of the fat-tailed ECS parameter and the different damage functions on the outcomes at the time points 2050, 2100, 2150, 2200, and 2300. The statistics of the data set, namely mean, standard deviation and percentiles/quantiles, are given in the tables of the Appendix D as well as visualized in boxenplots (see Figures 9.4, 9.5 and 9.6). From a risk management perspective, the 1st and 5th percentile for the outcomes, total output and utility, is of interest, since both percentiles can be used to describe the risk of the particular treatment by means of a single descriptive key figure. Further, to allow a better reading experience, the Cauchy, log-normal and normal distributed data set are abbreviated to Cauchy, Log-normal and Normal. Similarly, the data sets that are treated by damage function of Nordhaus, Newbold and Daigneault, and Weitzman will be abbreviated to Nordhaus, Newbold and Weitzman, respectively.

### 9.2.1 Effect of Fat-Tailed ECS Parameter



**Figure 9.4:** Distributions of the simulation outcomes for the three ECS distribution functions at the time points 2050, 2100, 2150, 2200 and 2300 are illustrated in boxenplots.

It is observed that the distributions with high kurtosis for the ECS parameter exhibits a respective high tail in atmospheric temperature. Further, it is interesting to note that the inclusion of a fat-tailed distribution on the ECS parameter has a significant effect on the “tailedness” of the other outcomes. This findings coincides with the discoveries in Section 9.1. Furthermore, Figure 9.4 shows that the tail for all outcomes is increasing with time. The magnitude of the fat-tailed parameter can be quantified by using the statistical description of the generated data set (see Table D.1).

### ***Total Output***

Table D.1c) displays that the average outcome of the total output parameter is very similar for all three distribution. Moreover, there is no significant difference in the 5th percentile of the total output between the different types of distributions. However, there is a substantial difference in the 1% risk. For the year 2100, the 1% value at risk for Cauchy is \$100 trillion lower than for Normal. As the world economy grows, the 1% risk threshold further diverges between Cauchy and Normal (up to 80% in year 2200). The same patterns can also be observed by comparing the statistics of Log-normal and Normal. For the year 2100, the 1% value at risk decreases by \$23 trillion.

### ***Utility***

Table D.1d) reveals that the choice of distribution has in average a negligible effect on the cumulative discounted utility (utility at the year 2300). Moreover, there is not a significant difference in the 5th percentile of the utility between the three distributions. On the other hand, the distribution type has a significant impact on the value at 1% risk. The 1% value at risk for Cauchy is \$659 trillion (27%) lower than for Normal. In the case of Log-normal, the difference in utility at the 1st percentile is “only” \$85 trillion (3% lower).

#### **9.2.2 Effect of Damage Function**

The statistical analysis shows that depending on the utilized damage function, higher damage is generated by the model. However, it is interesting to note that the impact of the damage function also traverse through the other outcomes. This findings coincides with the discoveries in section 9.1. To quantify the effect of damage function, the statistical description of the generated data set is utilized (see Table D.2).

### ***Total Output***

Table D.2c) reveals that the average outcome of the total output parameter is for all three damage function more or less the same. However, there are substantial differences between the damage function for the 1% and 5% value at risk. For the year 2150, the 5% risk of total output for Weitzman is 41% lower than for Nordhaus. In case of Newbold, the total output is 11% lower. When comparing the 1% risk of total output, the influence of the damage function on the total output is even greater.

For instance, in 2150, the 1% risk of total output for Weitzman is 81% lower than Nordhaus.

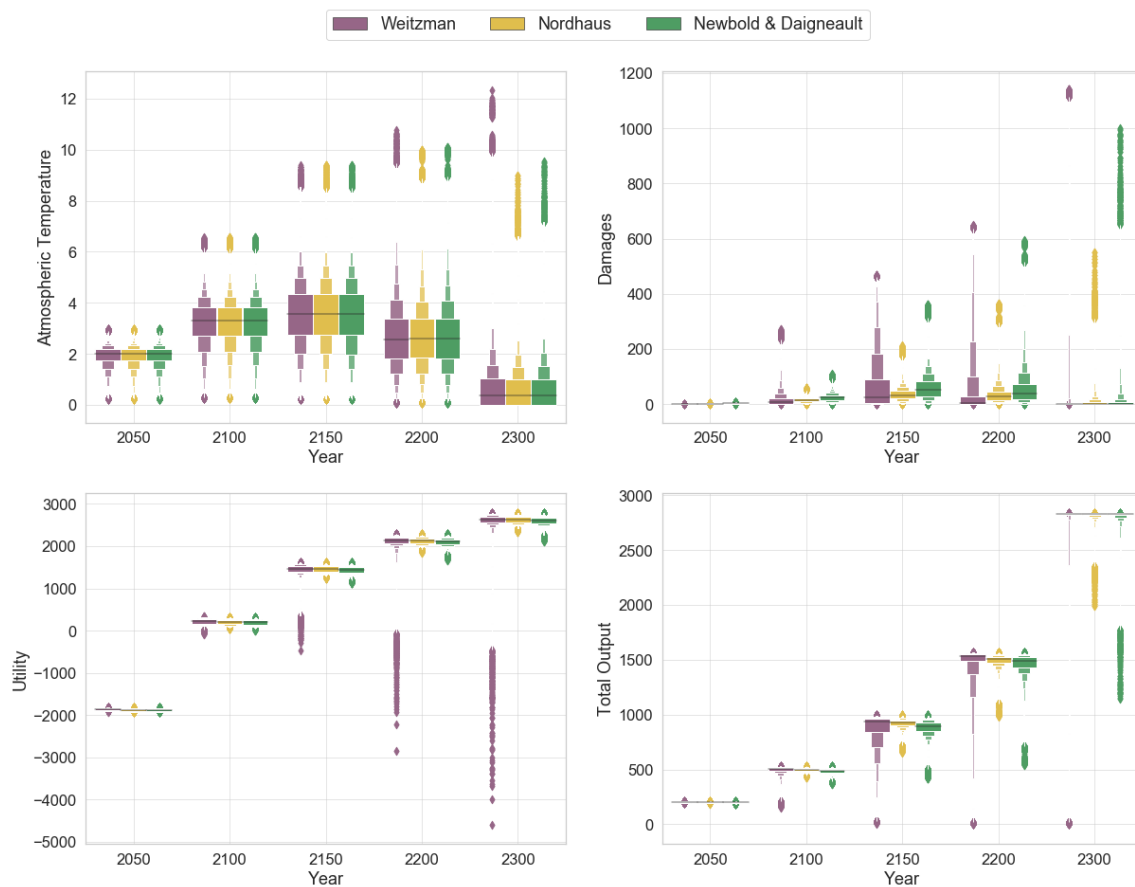


**Figure 9.5:** Distributions of the simulation outcomes for the three damage functions at the time points 2050, 2100, 2150, 2200 and 2300 are illustrated in boxenplots.

### Utility

Similar to the total outcome, table D.2d) shows that the average cumulative discounted utility is almost identical for all three damage function. A noteworthy difference between the different treatment in damage function has not been found for the 5% value at risk. However, the case is different for the 1% value at risk. Here, the 1% risk of total output for Weitzman is 31% lower (-\$754 trillion) than for Nordhaus, and only 3% lower than for Newbold.

### 9.2.3 Effect of Damage Function and Fat-Tailed ECS Parameter in Combination

At last, the effect of the distribution types in combination with the damage functions is analyzed by utilizing the tables D.3, D.4, D.5 and D.6, and the figure 9.6. The boxenplots in figure 9.6 demonstrates clearly that the risk in the outcomes are the product of the damage function and probability function of the ECS parameter. In other words, the larger the kurtosis of the ECS parameter and the greater the impact of the damage function, the higher is the risk of experiencing an unprecedented event.

Therefore, the highest risk is carried by scenarios with Weitzman damage function and Cauchy distributed ECS parameter.

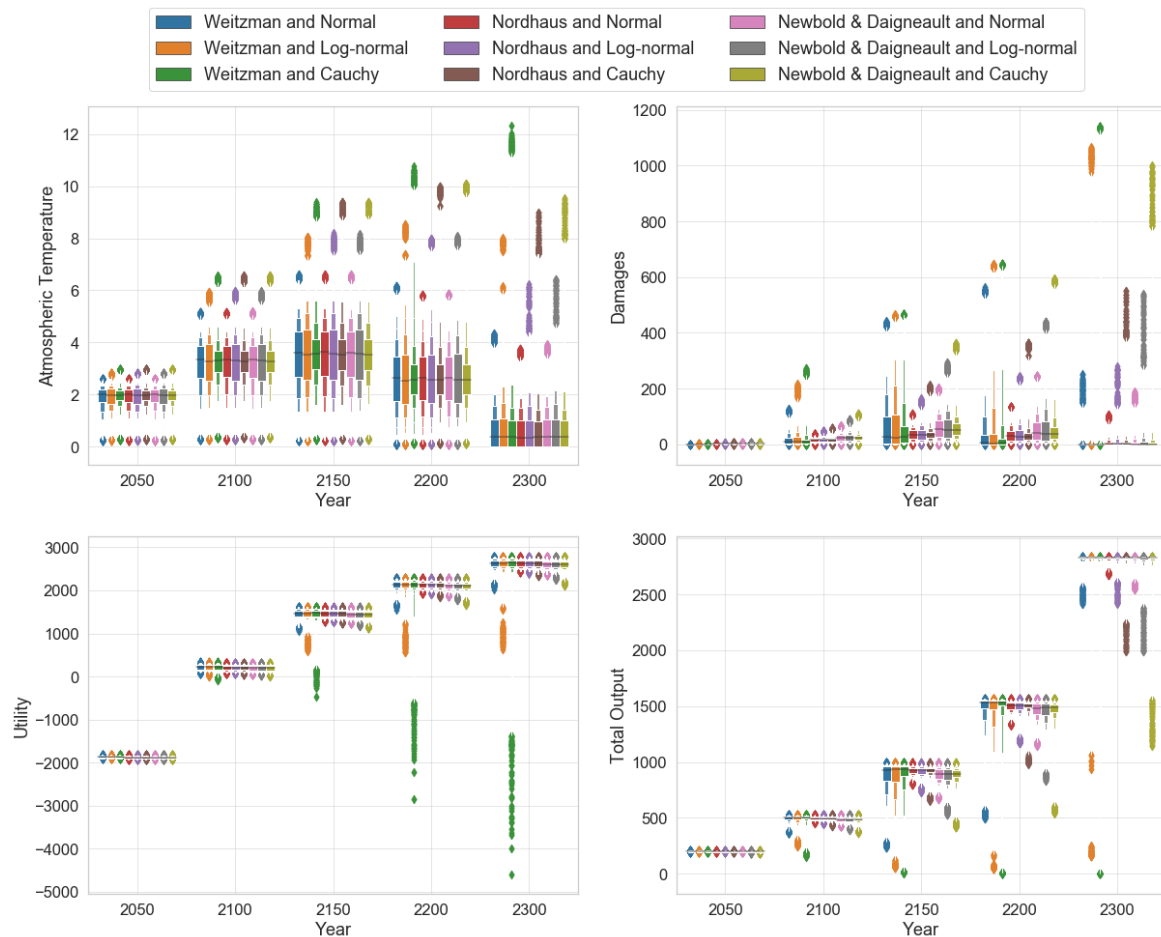


**Figure 9.6:** Distributions of the simulation outcomes for the nine different combinations between the three damage functions and the three ECS distribution types at the time points 2050, 2100, 2150, 2200 and 2300 are illustrated in boxenplots.

### Total Output

Table D.5 reveals that the average outcome of the total output parameter is for all nine combinations of damage function and distribution type about the same size, except for the year 2150. Here the average value of combination with Weitzman was around 6% lower than the combination of Nordhaus and Normal. Moreover, substantial differences between the combinations is found for the 1% and 5% value at risk. For instance, in 2150, the 5% risk of total output for Weitzman and Cauchy is 53% lower than for Nordhaus and Normal. In 2200, the 1% risk of total output for Weitzman and Cauchy is 96% lower than for Nordhaus and Normal. Further combinations that have significant lower 1% value at risk than the Nordhaus and Normal combination are Weitzman and Log-normal (up to 68% lower (2150)), Weitzman and Normal (up to 55% lower (2150)) and Newbold and Cauchy (up to 38% lower (2200)).

### ***Utility***

Table D.6 shows that the average cumulative discounted utility is almost identical for all combinations. A noteworthy difference for the 5% cumulative discounted utility value at risk has only been found for the combination Weitzman and Cauchy. In contrast to the conventional combination of Nordhaus and Normal, the 5% value at risk for the cumulative discounted utility is around 7% lower (-\$180 trillion) for the combination Weitzman and Cauchy. A far more significant impact is found for 1% value at risk. Here, the utility at 2300 for the combination Weitzman and Cauchy is 69% (-\$1705 trillion) lower than the conventional combination. Other combinations that have noticeable lower cumulative discounted utility than the combination Nordhaus and Normal are Weitzman and Log-normal (14% lower), Weitzman and Normal (7% lower) and Newbold and Cauchy (6% lower).

### **Summary**

The statistical analysis has shown that the 1% value at risk for the outcomes, total output and cumulative discounted utility, distinguish significantly depending on the ECS distribution. Moreover, these differences in risk are disproportionately amplified by the damage function, so that substantial differences have been observed at the 5% value at risk. Furthermore, from the findings above, it can be deduced that the risk for extreme events are at first instance carried by the damage function (in the following order: Weitzman, Newbold and Daigneault, and Nordhaus) and only subsequently influenced by ECS distribution (in the following order: Cauchy, log-normal, and normal). This verifies the observations from the initial exploration in Section 9.1. By quantifying the difference in the outcomes for the 1% and 5% value at risk, the significance of fat-tailed ECS parameter and damage functions similar to Weitzman on the outcomes has been demonstrated.

## 9.3 SCENARIO DISCOVERY

After the initial statistical analysis and exploration of the outcome space, in this section, scenario discovery in form of time series clustering and directed scenario search is applied to describe regions in the database, that have particular properties of interest. The time series clustering is conducted over an experiment set of 30000 scenarios. A relatively smaller number of scenarios has been chosen to not only avoid extremely lengthy computation but also to reduce the carbon footprint of this thesis [Strubell et al., 2019].

### 9.3.1 Time Series Clustering

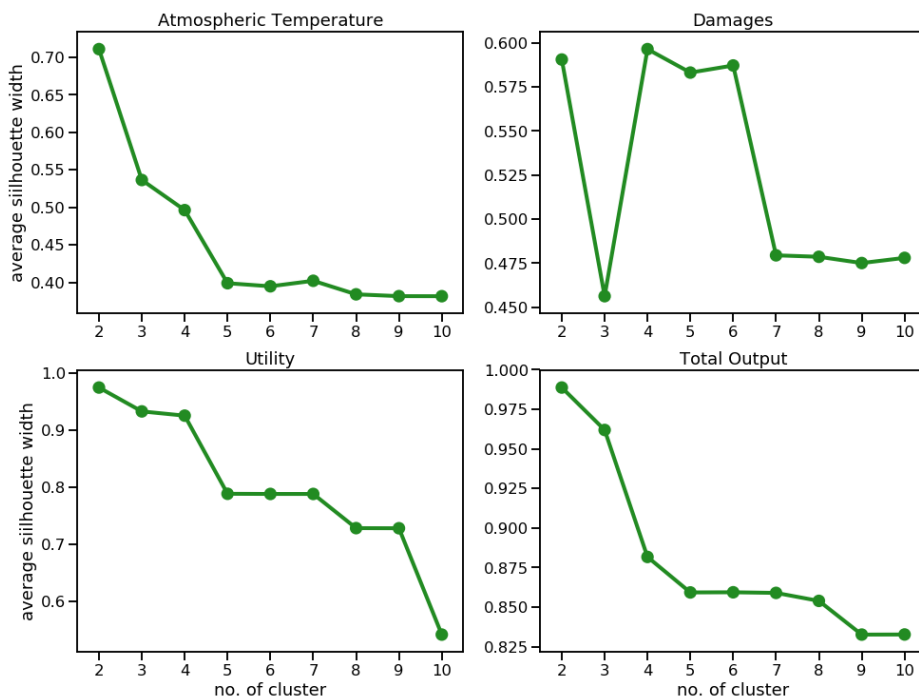


**Figure 9.7:** The average silhouette widths of CID-generated for  $k$  amount of clusters ( $k = [2, 13]$ ).

Before time series of the outcome parameter are aggregated into clusters, one has to determine the number of clusters which satisfy the two main criteria: separability and compactness. This is important as policies based on insufficient time series clustering can unintentionally aim outcomes from different input spaces. The number of clusters is determined by calculating the silhouette width. The concept of silhouette width is explained in more detail in Section 6.2. In principle, the cluster number with the highest silhouette width is chosen. But even though the silhouette width is a good indicator for choosing the “right” number of clusters, the final decision relies upon the analyst after visual inspection.

Based on the silhouette width (see Figure 9.7) and a visual inspection, the following cluster number are chosen for the outcome parameters:

**Table 9.2:** Number of chosen clusters for the outcome parameter

Atmospheric Temperature	Damages	Total Output	Cumulative Discounted Utility
3	4	4	3

In the following, for each outcome variable, the generated clusters are investigated with the goal to identify vulnerable regions. Therefore, the uncertainty space for the least “favourable” clusters is also illustrated in a parallel coordinate plot.

### *Atmospheric Temperature*

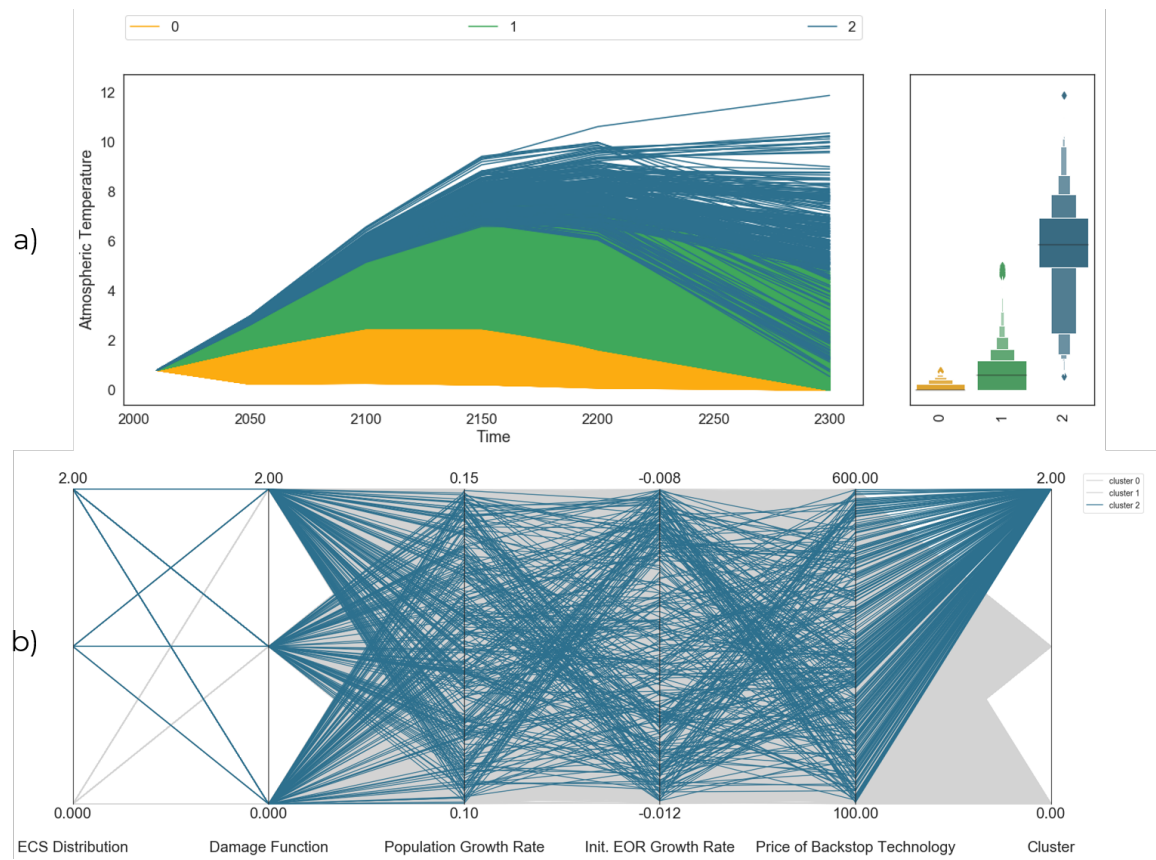


**Figure 9.8:** For the outcome atmospheric temperature: a) Time Series Clustering; b) Input space of the undesired cluster.

The outcomes of the atmospheric temperature are aggregated into three different clusters. Figure 9.8a, shows that each cluster can be examined by their behaviour:

- Blue Cluster: The temperature in the atmosphere grows rapidly until the year 2150. Afterwards, the atmospheric temperature follows three different trajectories. Some few scenarios still rise up to 12°C, others start to stabilize between 6°C and 8°C, whereas, in few other scenarios, the atmospheric temperature drops down to 2°C.

- Green Cluster: The atmospheric temperature rises until 2150 up to 6°C. It stays stable for another 50 years and then sharply declines for most cases to temperatures between 0°C and 2°C. However, some outliers terminated at 6°C.
- Yellow Cluster: Until the year 2100, the atmospheric temperature increases slowly up to 2°C. It stays stable for another 50 years and then declines to a temperature between 0°C and 1°C.

Lower temperatures are desirable outcomes and therefore the clusters can be ranked (from undesirable to desirable) as follows: blue, green and yellow. In order to investigate the root cause for those outcomes, the uncertainty space of the green cluster (305 scenarios), is plotted in a parallel coordinates plot (see Figure 9.8b). This visualization is often utilized to understand the trade-offs/relationship between variables. Hereby every uncertainty is placed at an axis parallel to others. Uncertainty values are plotted as a series of lines, representing the analyzed set of scenarios. The highlighted lines reflects the input space of the undesired cluster. Thus, from figure 9.8b, it can be deduced that high atmospheric temperatures are only obtained in scenarios with ECS parameter that underlies a fat-tailed distribution. Furthermore, many scenarios in the blue cluster, a trade-off between the population growth rate and the initial growth rate of the emission to output ratio as well as the price of back stop technology and the initial growth rate of the emission to output ratio is discernible.

### *Damages*

The annual damage outcomes are aggregated into four different clusters. Figure 9.9a, shows that each cluster can be classified by their behaviour:

- Yellow Cluster: The annual damages starts to grow after the year 2050. Afterwards, it follows various different trajectories. The boxenplot at the end of the time series plot shows that around 75% of all scenarios terminates about \$0, many of the remaining scenario between \$0 - \$200 trillion and some very few scenario are found around \$600 trillion.
- Green Cluster: Here the annual damages remains stable for very low value ( $\approx \$100$  trillion) until 2300.
- Blue Cluster: Similar to the yellow cluster, the annual damages starts also to grow after the year 2050. Afterwards, the scenarios follows various different growth trajectories. 50% of all scenarios in the blue cluster ends up between \$700 - \$1100 trillion. Further, 25% of the scenario have caused a damage between \$1100 - \$1200 trillion for the year 2300, whereas the remaining 25% have caused only damages between \$300 - \$700 trillion.
- Purple Cluster: Here the annual damages remains stable for very low value ( $\approx \$0$ ) until 2300.

As higher damages are undesirable outcomes, the clusters can be ranked (from undesirable to desirable) as follows: blue, yellow, green and purple. Thus, the 156 scenarios in the blue cluster are examined in detail (see Figure9.9b). It can be inferred that

high damages are never obtained for scenarios which consist of the Nordhaus damage function and/or a thin-tailed ECS parameter. Furthermore, none of the scenarios in the blue cluster contains log-normal distributed ECS parameter and the damage function of Newbold and Daigneault, at the same time.

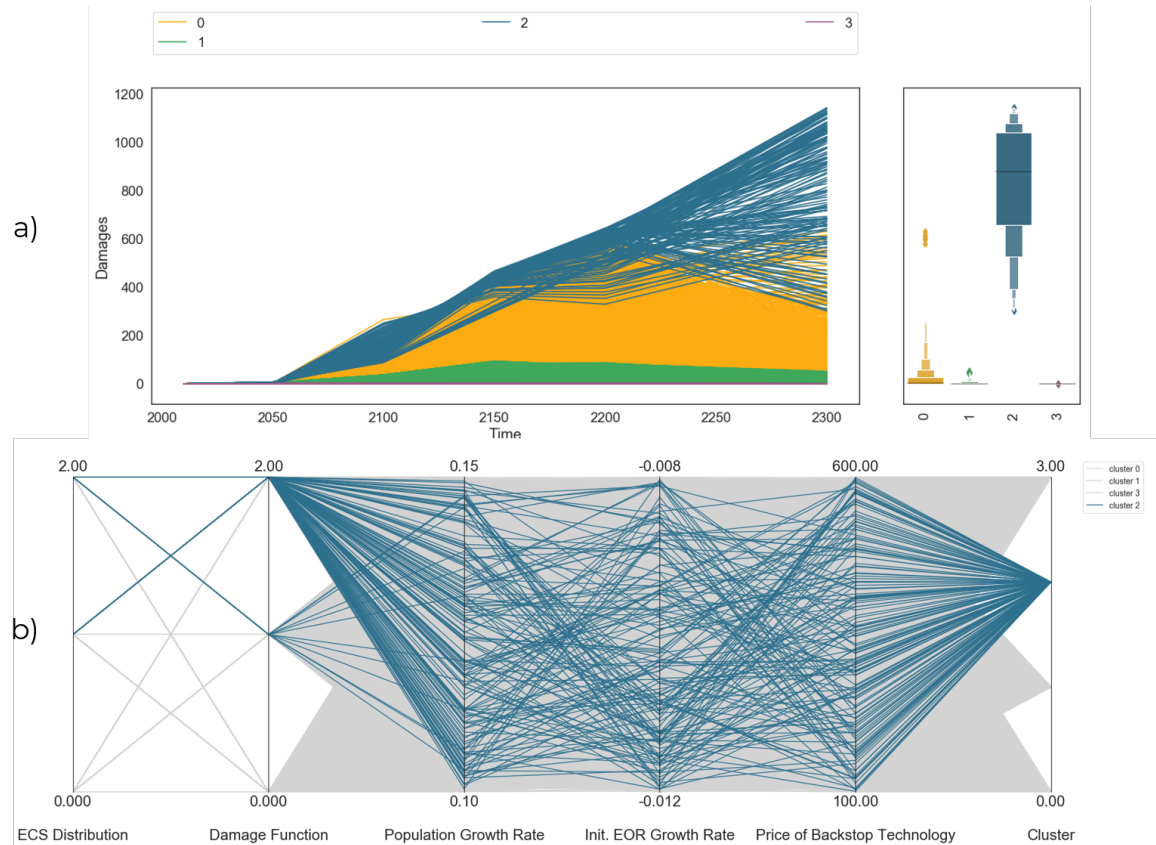


**Figure 9.9:** Clustered space of the outcome damages: a) Time Series Clustering; b) Input space of the undesired cluster.

### Total Output

The outcomes of total output are aggregated into four different clusters. Figure 9.10a, shows that each cluster can be classified by their behaviour:

- **Yellow Cluster:** Whereas for some scenarios in this cluster, total output grows steadily over time, others decline between 2100 and 2150 just to rise again. In most cases, the total output terminates around \$2700 trillion. Some few outliers end up around \$1900 and \$2300 trillion.
- **Green Cluster:** After the total output increases slowly for the first 90 years, it stagnates between 2100 and 2200. For the last 100 years, the total output rises again to terminate between \$500 and \$1000 trillion in 2300.
- **Blue Cluster:** Total output increases until 2050. From here, two trajectories are observed. In the first trajectory, the total output declines steadily over time until it reaches zero total output whereas, in the second trajectory, the output declines until 2200, just to rise again and to terminate around \$400 trillion.

- Purple Cluster: Similar, to the yellow cluster, total output increases until 2100. From here, two different trajectories can be found. One set of scenarios decline between 2100 and 2150 in total output and has stagnated until 2200, whereas the other scenarios has experienced a creeping total output growth until 2200. From 2200, the total output for all scenarios rises again and they finally terminate between \$1200 - \$2300 trillion.

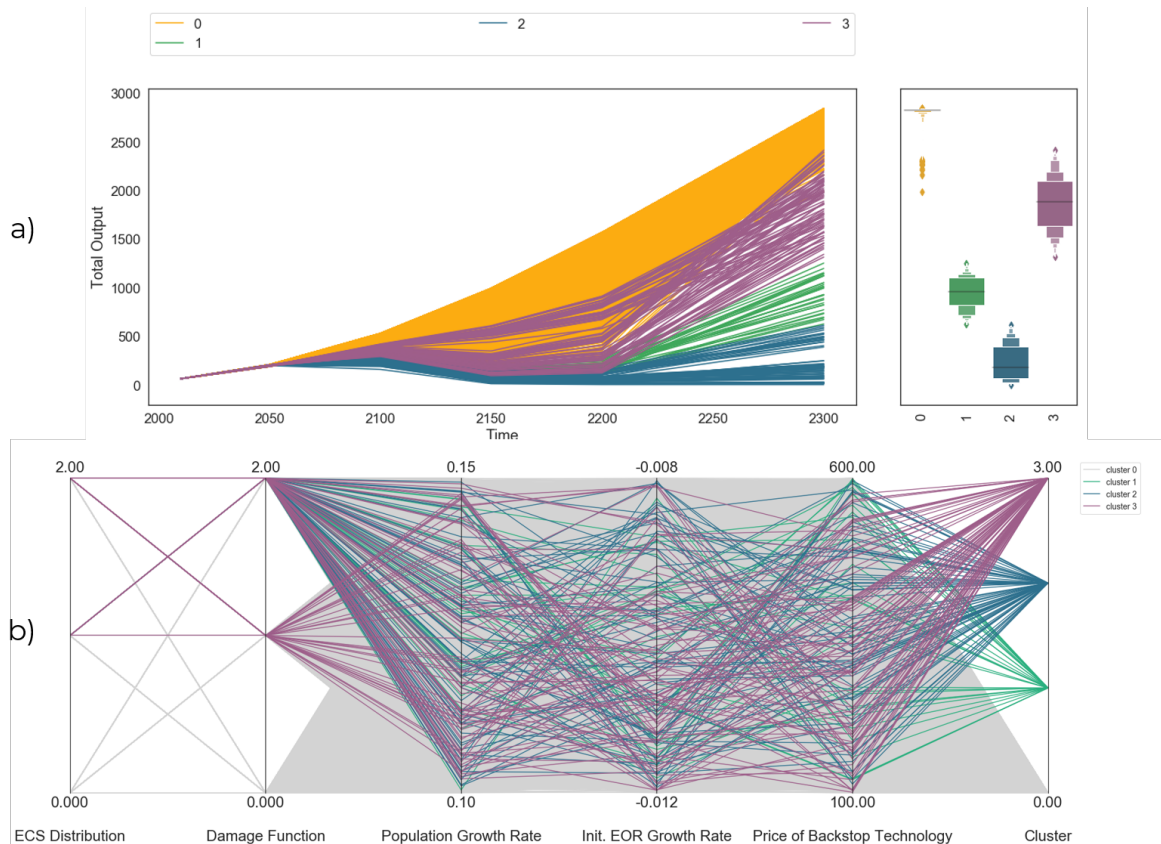


**Figure 9.10:** For the outcome total output: a) Time Series Clustering; b) Input space of the undesired cluster.

As higher total output is desired, the clusters can be ranked (from undesirable to desirable) as follows: blue, green, purple and yellow. From the parallel coordinate plot in Figure 9.10b, one can deduct that the outcomes from the blue, green and purple clusters are only reached for scenarios that comprise of the damage function of Weitzman or Newbold and a fat-tailed ECS parameter. Trade-off or other interesting relationship between the other uncertainty parameters has not been found. These three clusters contains 184 scenarios.

### Cumulative Discounted Utility

The discounted utility outcomes are aggregated into three different clusters. Figure 9.9a, shows that each cluster can be examined by their behaviour:

- Blue Cluster: The utility grows over the time period and closes around \$2700 in 2300.

- Yellow Cluster: Around 75% of the scenarios in the yellow cluster has shown exactly the same behaviours as the scenarios in blue cluster, but for a lower growth rate. Therefore, those scenarios have a cumulative discounted utility between \$300 - \$1500 trillion. The other 25% of the scenarios has experienced a decline after 2100, so that the cumulative discounted utility for these scenarios are between \$300 - \$-1500 trillion.
- Green Cluster: Interestingly, on the basis of the complex-invariant distance metrics, a time series has been clustered into an own cluster. Thus, one can deduce that this outcome illustrates a very extreme event. In this scenario, the cumulative discounted utility is at \$-3800 trillion.

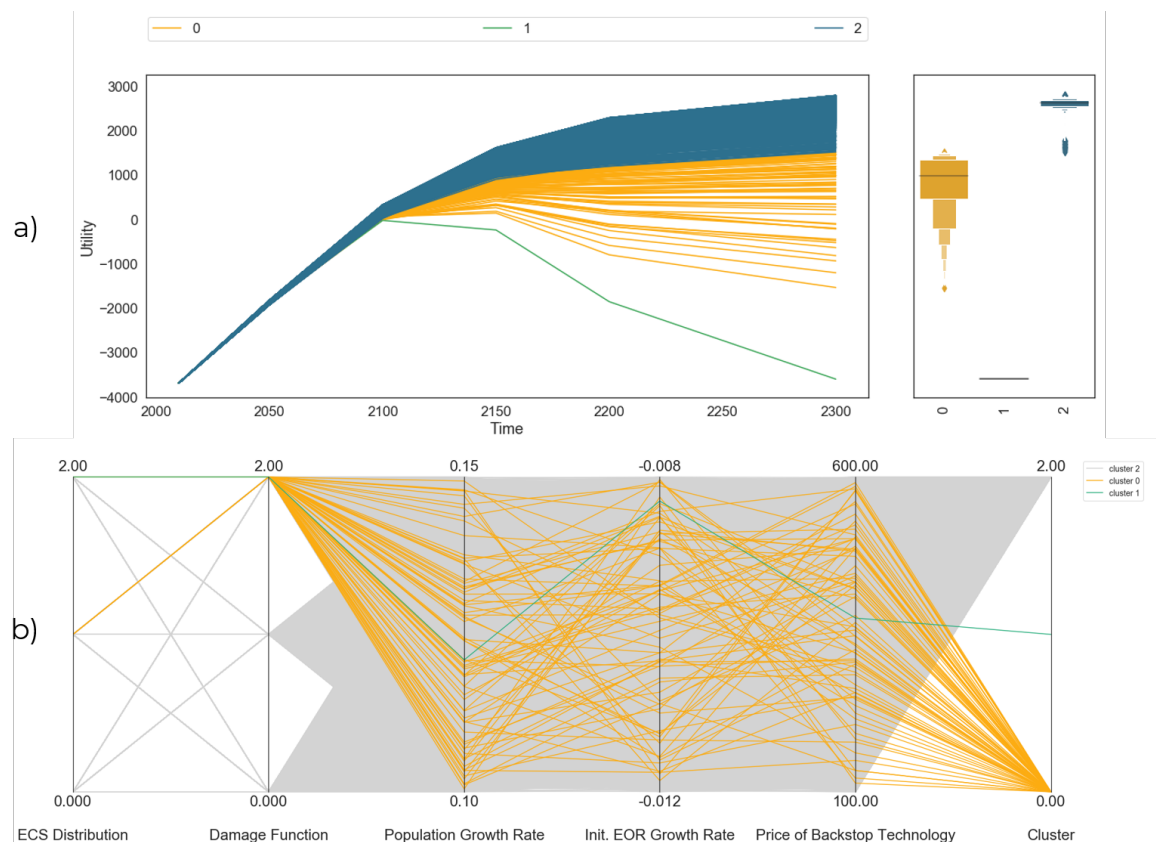


**Figure 9.11:** For the outcome cumulative discounted utility: a) Time Series Clustering; b) Input space of the undesired cluster.

High cumulative discounted utility is preferred and therefore the clusters are ranked (from undesirable to desirable) as follows: green, yellow and blue. From the Figure 9.8b, it can be concluded that for the outcomes for a yellow and green clusters are only attained for scenarios which consist of the damage function of Weitzman and fat-tailed distributed ECS parameter. The green and yellow cluster comprises of 76 scenarios.

## Summary

The bottom line of this analysis is to a large extent comparable to the insights found in the statistical analysis and the initial exploration of the output space (see Sections 9.2 and 9.1). But in contrast to prior analysis, the time series clustering allows the researcher to take a relatively unbiased approach in identifying unfavourable scenarios. Firstly, this analysis has shown that undesirable outcomes can never be attained for scenarios that consist of normal distributed ECS parameter. Moreover, under the discovered set of undesirable scenarios, Nordhaus damage function has only been found in scenarios which led to high atmospheric temperature. Lastly, the scenario discovery demonstrates that the outcomes, damages, total output and utility are only vulnerable to scenarios with a damage function of Weitzman or Newbold and a fat-tailed ECS parameter. Furthermore, the prior findings of the statistical analysis and the initial exploration can be verified as this investigation has shown that that the disproportional risks in the tail of Cauchy and log-normal distribution can only be translated into catastrophic outcomes by damage functions akin to Weitzman or Newbold and Daigneault. Lastly, this analysis has also shown that the optimal policy of Nordhaus is vulnerable for 328 out of 30000 ( $\approx 1.1\%$ ) scenarios.

### 9.3.2 Directed Scenario Search

To overcome the pitfall of using Latin Hypercube sampled data set for the scenario discovery, it is complemented by the directed search technique over uncertainties (see Section 6.3 for an in-depth explanation). Hereby, the many-objective evolutionary algorithm (MOEA),  $\epsilon$ -NSGA-II, is applied to search over the set of uncertainties (see Table 4.3) in finding scenarios which worsens the objectives of this study (see Table 4.1). For 100000 number of function executions, 414 scenarios have been found. Furthermore, it can be noted, that these 414 scenarios are different to the discovered scenarios from time-series clustering. The uncertainty space of those scenarios is presented in 10.1.

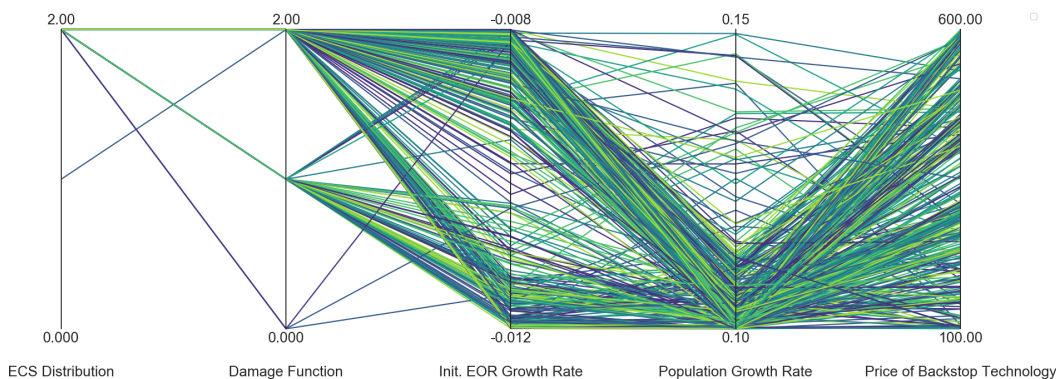


**Figure 9.12:** Uncertainty space of the worst case scenarios from the directed scenario search.

It is noted that the uncertainty space of the worst-case scenarios (see Figure 10.1) corresponds to a large extent with the uncertainty space of the discovered vulnerable scenarios using time series clustering. Undesirable outcomes are in particular attained for scenarios which comprise either of the Weitzman damage function and a fat-tailed ECS parameter or one of the three damage functions and a Cauchy distributed ECS parameter. Furthermore, many of the worst-case scenarios consist of a slow population growth rate. In Section 8.2, the global sensitivity analysis has demonstrated that this particular parameter can have a significant impact on the utility (see Figure 8.5).

# 10 | POLICY DISCOVERY

In Section 9.3, vulnerable scenarios for Nordhaus optimal policy have been determined using time series clustering and directed scenario search. In this chapter, these scenarios are used to determine policy alternatives. To this end, in Section 10.1 four maximal diverse scenarios are selected from the identified vulnerable scenarios by utilizing [Carlsen et al. \[2016\]](#) diversity criterion. Next, Section 10.2 uses  $\epsilon$ -NSGA-II algorithm to identify alternative candidate strategies for each of the four maximum diverse scenarios. Lastly, Section 10.3 uses the signal-to-noise ratio criterion and the minimax regret criterion on the identified candidate strategies from Section 10.2 to determine the ten most robust candidate strategies.

## 10.1 SCENARIO SELECTION

Although a very large set of scenarios could generate a more pronounced set of robust policies, only a limited number of scenarios can be used in the context of MOEA algorithm due to computational limitations. Therefore, a small number of scenarios from a policy-relevant ensemble of scenarios are selected based on the diversity maximization approach of [Carlsen et al. \[2016\]](#) (see Section 6.4).

**Table 10.1:** Selected scenario based on diversity and policy relevance for alternative policy determination.

Scenario No.	Price of Backstop Technology	Damage Function	Population Growth Rate	Initial Growth Rate of Carbon Intensity	Equilibrium Climate Sensitivity Distribution
<b>102</b>	103.0	Weitzman	0.100000	-0.011898	Truncated Cauchy
<b>354</b>	143.0	Nordhaus	0.103253	-0.008141	Truncated Cauchy
<b>467</b>	290.0	Weitzman	0.149353	-0.009790	Truncated Cauchy
<b>473</b>	376.0	Weitzman	0.120957	-0.008306	Truncated Cauchy

A policy-relevant of 742 scenarios are deduced from the findings of scenario discovery in Section 9.3. As this represents still a large set of scenarios, a subset of scenarios are selected by prioritizing the results from directed search scenario and the time series clustering over the outcomes of cumulative discounted utility. This results in a subset of 490 scenarios. From the set of policy-relevant scenarios, four ( $K = 4$ ) maximally

diverse scenarios regarding their outcomes are selected. This diversity selection is done by using Carlsen et al. [2016] diversity criterion over 2.37 billion subsets with size 4 (see Section 6.4). The findings of this selection procedure are presented in Table 10.1.

Figure 10.1 illustrates the policy-relevant scenario space of 490 scenarios in pairwise scatter plots. This figure validates that the chosen four scenarios (coloured in yellow, green, blue, purple) are indeed located in distant edges of the policy-relevant scenario space.

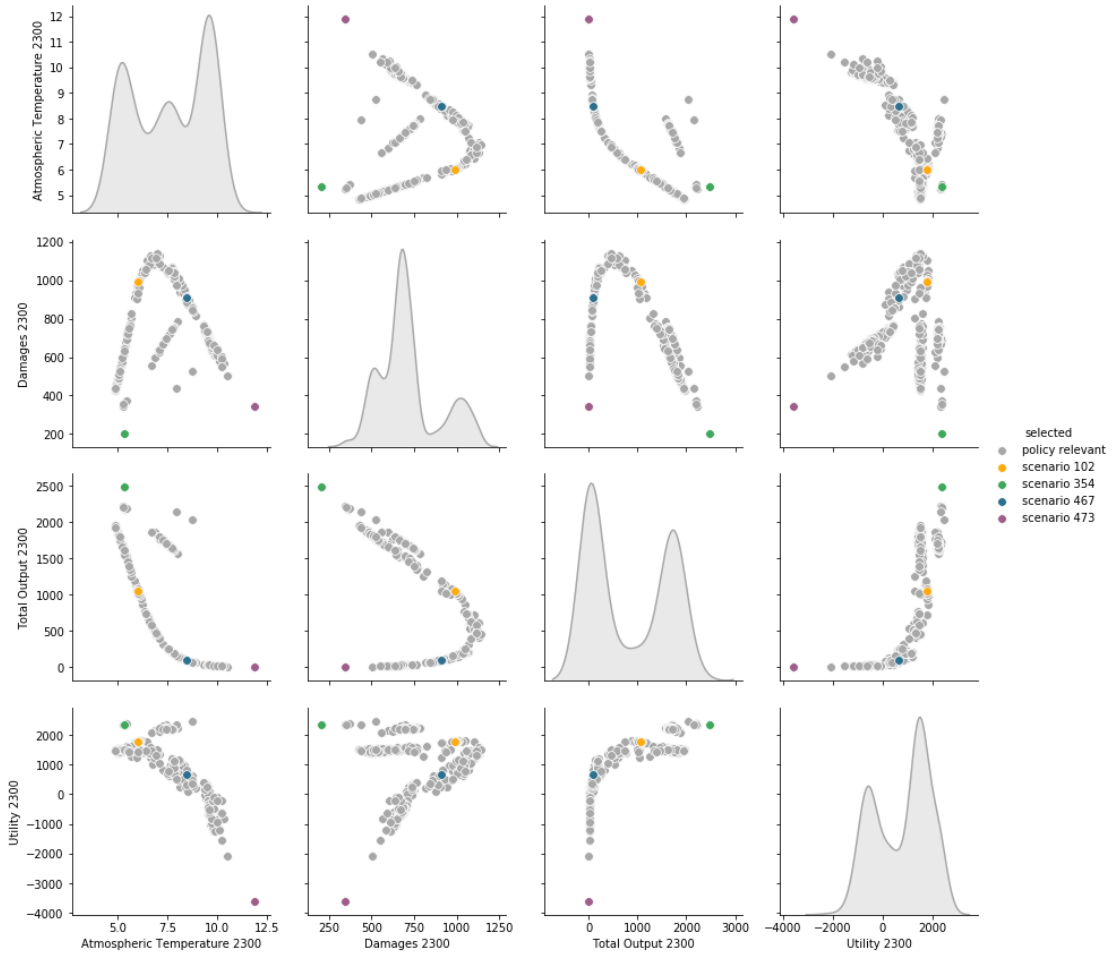


**Figure 10.1:** Results of the scenario selection algorithm illustrating the K=4 maximum diverse scenarios (coloured in yellow, green, blue, purple) from N=490 policy relevant scenarios (light grey).

## 10.2 DIRECTED POLICY SEARCH

In this section, the four selected scenarios are now utilized to generate candidate strategies. These non-dominated set of candidate strategies are identified by using the  $\epsilon$ -NSGA-II algorithm over each chosen scenario individually. Furthermore, a constraint is put on the outcome space, assuming that the global community prioritizes a

positive cumulative discounted utility and an atmospheric temperature below  $4^{\circ}\text{C}$  at all time. Even with the constraints, the MOEA algorithm has found 49, 16, 36 and 12 alternative candidate strategies for the scenarios 102, 354, 467 and 473 respectively. The convergence of the algorithms for each scenario is presented in Figure 10.2.

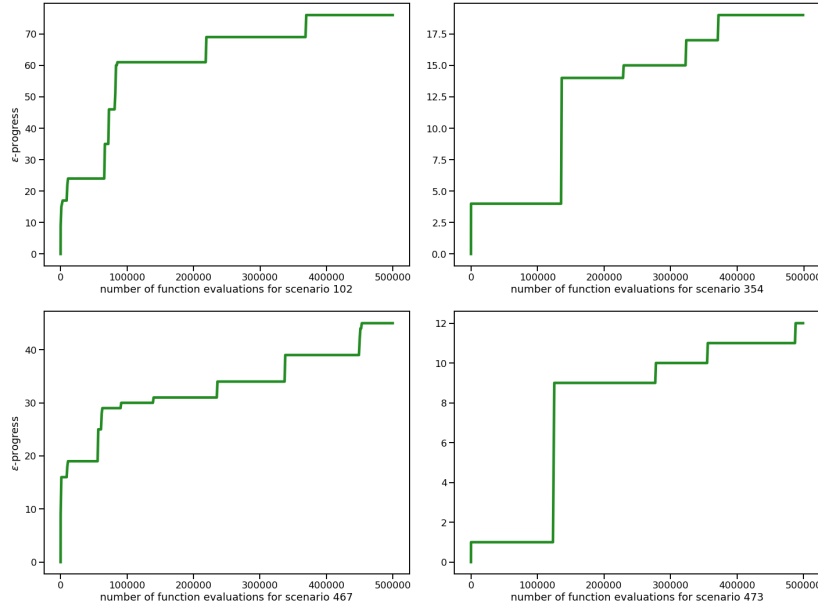


**Figure 10.2:** Epsilon progress for each maximum identified scenarios.

Moreover, Figure 10.3 illustrates the trade-off within the candidate solution for each scenario. There are considerable differences in number but also in the trade-off for each scenario. This is mainly due to the diversity between the scenarios. For instance, for scenario 473 (see Figure 10.3d), which can be considered as the worst case scenario among the four chosen scenarios, only 12 candidate strategies have been found.

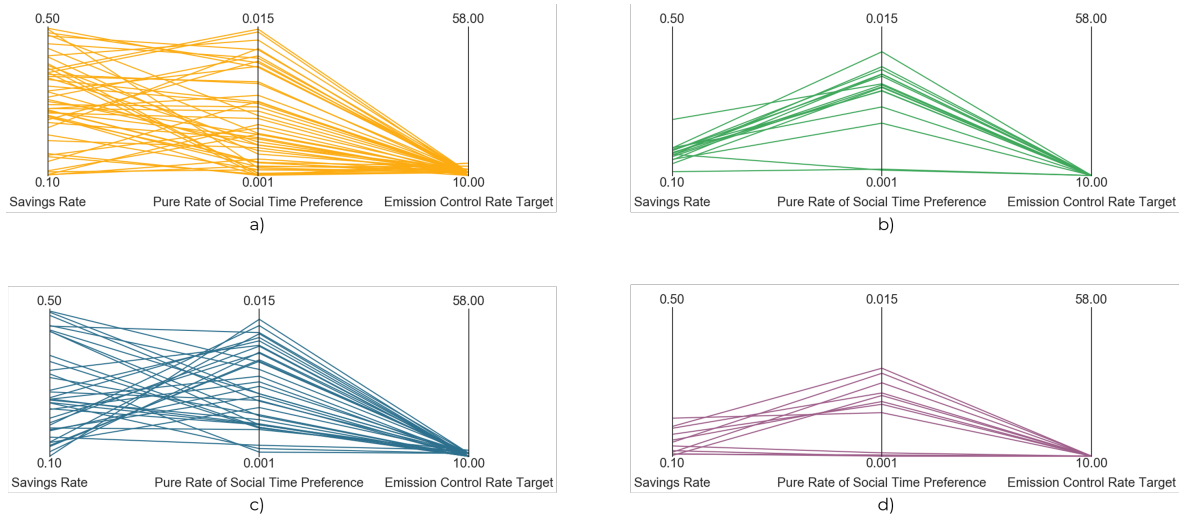


**Figure 10.3:** Candidate strategies generated for the a) scenario 102, b) scenario 354, c) scenario 467, d) scenario 473.

Here, the policy set comprises of very low savings rate (SR), very low to medium pure rate of social time preference (IRSTP) and a very early emission control rate target (ECRT) at 2060. Similarly for the scenario 354 (see Figure 10.3b), which can be considered as the best case, the MOEA has only found 16 candidate strategies which comprise of low SR, relatively high IRSTP and an ECRT for 2060. In contrast, candidate strategies for the scenarios 102 and 476 cover the full range for the policy levers SR and IRSTP. But then again, these candidate strategies impose, similar to the other policies, the ECRT between 2060 and 2080.

Moreover, a trade-off between SR and IRSTP are observed (see Figure 10.3b,d). If a very high IRSTP is chosen by the policy maker, catastrophic outcomes can only be averted if the SR is low. In fact, it implies that the global social planner intends to maximize utility, by setting savings rate low so that consumption can increase. Thereby it sacrifices the growth of the total output, since lower savings rate would mean lower investment and that eventually would lead to a decrease in capital/assets.

## 10.3 UNCERTAINTY ANALYSIS

After having found a Pareto approximated set of 113 candidate strategies, these strategies are evaluated in terms of their robustness against a large number of alternative future states of the world. For this purpose, a data set is generated in which the candidate strategies are simulated over  $N=10000$  different future states of the world. Subsequently, the data set is used to calculate the robustness of the candidate strategies according to the metrics that have been selected (see Section 7.2).

As this study strives to find a robust policy on the basis of the precautionary principle, the minimax regret criterion and signal-to-noise ratio (SNR) criterion are used to determine the robustness Weitzman [2013]. The minimax regret criterion, also known as Savage criterion, is considered within the academic community as a high risk-averse metric McPhail et al. [2018]. It strives to minimize the regret with respect to the worst-case. In contrast, the SNR criterion is a more balanced risk averse metric that examines the mean and variance of the performance of the candidate strategies over multiple scenarios. Moreover, a robustness threshold has been chosen to ensure that only high-performing policies move forward. A subsidiary effect is that the reduction to few policies allows a better interpretation of the candidate strategies for the decision-maker and the analyst. Thus, only the ten most robust policies for each criterion are taken into account.

### *Signal-to-Noise Ratio*

By applying the SNR criterion and subsequently calculating the average SNR over the robustness values of the outcome parameters<sup>1</sup>, a final set of the 10 most robust can-

---

<sup>1</sup> The cumulative discounted utility is weighted by 5 to adjust the overvaluation of the parameters total output, atmospheric temperature and total output.

didate strategies (SNR policies) are derived. These policy alternatives are presented in Figure 10.4 and in Figure E.1.

	0.092	0.034	0.088	0.12	0.13	0.078	0.05	0.15	0.15	0.16
Atmospheric Temperature 2050	0.29	0.26	0.37	0.3	0.37	0.29	0.27	0.37	0.37	0.38
Atmospheric Temperature 2100	0.51	0.73	0.73	0.4	0.53	0.57	0.67	0.46	0.43	0.41
Atmospheric Temperature 2150	1	1	1	1	1	1	1	1	0.99	0.96
Atmospheric Temperature 2200	0.96	1	1	0.81	0.93	0.99	1	0.8	0.7	0.6
Atmospheric Temperature 2300	0.62	0.27	0.52	0.73	0.74	0.55	0.39	0.79	0.81	0.82
Damages 2050	0.67	0.42	0.69	0.76	0.81	0.62	0.5	0.84	0.85	0.86
Damages 2100	0.81	0.89	0.92	0.78	0.87	0.83	0.87	0.85	0.84	0.84
Damages 2150	0.97	1	1	0.89	0.96	0.99	1	0.91	0.87	0.84
Damages 2200	0.97	0.96	0.96	0.97	0.97	0.96	0.96	0.97	0.96	0.91
Damages 2300	0.86	0.86	0.77	0.87	0.78	0.86	0.86	0.78	0.78	0.78
Total Output 2050	0.97	0.96	1	0.98	1	0.97	0.97	1	1	1
Total Output 2100	0.91	0.96	0.97	0.89	0.93	0.93	0.95	0.91	0.9	0.9
Total Output 2150	0.99	1	1	0.97	0.99	1	1	0.98	0.97	0.96
Total Output 2200	1	0.99	0.99	1	1	0.99	0.99	1	1	1
Total Output 2300	0.95	0.99	0.88	0.98	0.94	0.93	0.96	0.96	0.98	0.98
Utility 2300	0.82	0.82	0.82	0.82	0.84	0.81	0.81	0.83	0.83	0.82
Average SNR	2	12	14	33	64	70	88	101	103	104

Figure 10.4: The 10 most robust polices after applying the SNR criterion.

Both figures illustrate clearly that the performance of the 10 candidates strategies for the outcomes, atmospheric temperature, damages and total output, is getting better at each time point. Furthermore, a trade-off between the robustness performance for damages and total output is detected but only for the year 2050. For the remaining time period, Figure E.1 illustrates that the robustness for both metrics can be achieved without sacrificing for either parameter's robustness performance.

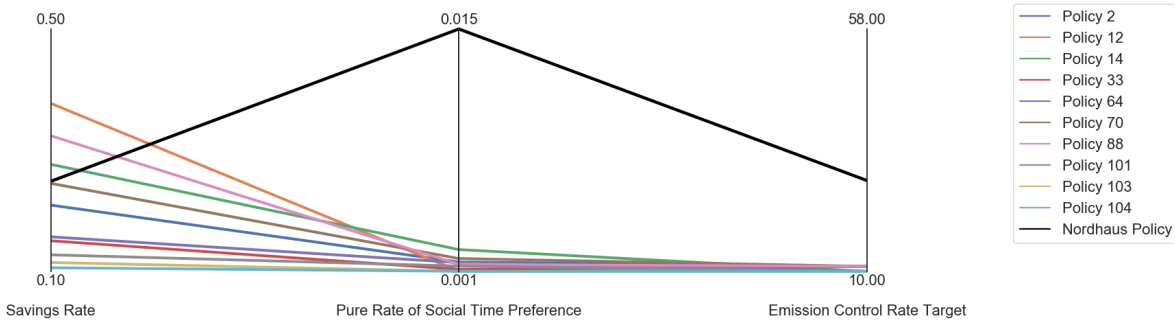


Figure 10.5: Comparison of the SNR policies to Nordhaus optimal policy.

Moreover, a trade-off in robustness is also identified between the parameters total output and cumulative discounted utility. This trade-off especially stands out at the year 2150 when comparing policy 14 and policy 33. Lastly, the Figure 10.4 present that the policies are in average similarly (average SNR: 0.81-0.84) robust.

Recognizing that the chosen policies are robust across many objectives, Nordhaus optimal policy is compared to the identified robust candidate strategies. For a better comparison, the policy space is illustrated in Figure 10.5. The difference in the policy proposal of Nordhaus to the SNR proposed policies is striking. In contrast to Nordhaus optimized policy, the SNR policies have not only a very low rate of social time preference (IRSTP), but also an early emission control rate target (ECRT). To

be more specific, the Nordhaus ECRT (= 2155) is at least 85 years apart from the ECRT of SNR policies. Furthermore, the savings rate for the identified set of robust policies varies between the values 0.10 and 0.38. Moreover, for four SNR policies (12, 14, 70 and 88) higher savings rate relative to Nordhaus has been observed. By examining these four policies in detail, one could observe that these high savings rate are balancing out the effect of either high IRSTP or late ECRT (relative to other SNR policies). As a (relatively) late ECRT will yield higher climate damages and thereby affects the total output negatively, a higher savings rate can have a counter effect by increasing the investment, that again rises the gross output. However, note that high savings rate diminishes the utility, especially when a high IRSTP has been chosen. After applying the minimax regret metric and calculating the average minimax regret over the robustness values of the outcome parameters<sup>2</sup>, the final set of 10 robust candidate strategies are presented in Figure 10.6 and in Figure E.2.

### Minimax Regret

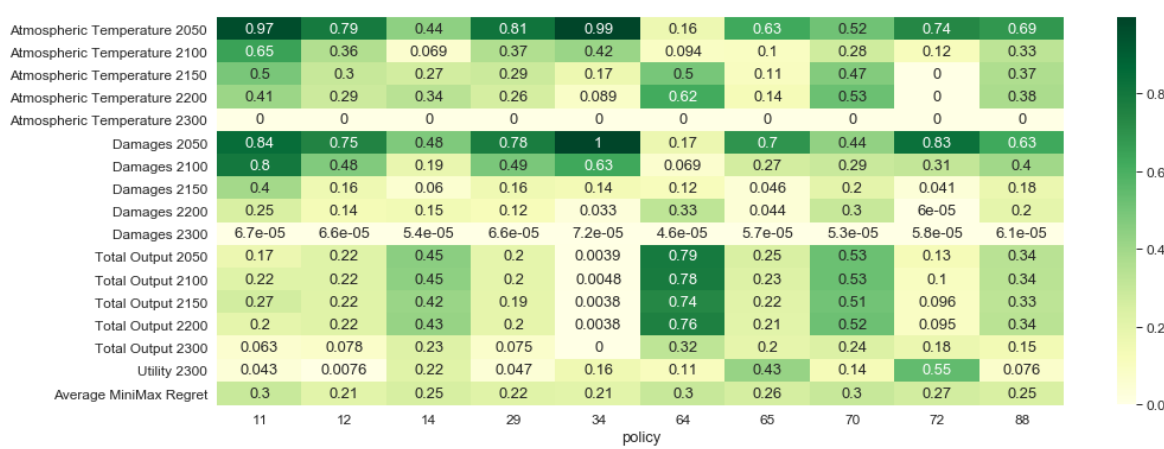


**Figure 10.6:** The 10 most robust polices after applying the minimax regret criterion.

Similar to the robustness scores from the SNR policies, one can observe from both figures that the chosen robust policies in terms of atmospheric temperature, damages and total output are getting closer to zero regrets over time. Moreover, a trade-off between damages and total output is apparent in the first two time points, but in the long run, these trade-off balances out. Another clearly discernible trade-off is between total output and the cumulative discounted utility. In particular, the policies 34, 64, 65, 70 and 72 highlight this trade-off. Other candidate strategies, such as the policies 11, 12, 14 and 29, cancel this trade-off over time. Although all chosen policies are relatively robust, the candidate strategies 12 and 34 are still standing out in the midst of those policies. Whereas policy 12 constitutes minimal compromise on the regret across all outcomes of interest, policy 34 is extremely robust for total output over the whole time period.

<sup>2</sup>The cumulative discounted utility is weighted by 5 to adjust the overvaluation of the parameters total output, atmospheric temperature and total output.

In the following, Nordhaus optimal policy is compared to the identified robust candidate strategies (MiniMax policies). For a better comparison, the policy space is illustrated in Figure 10.7.

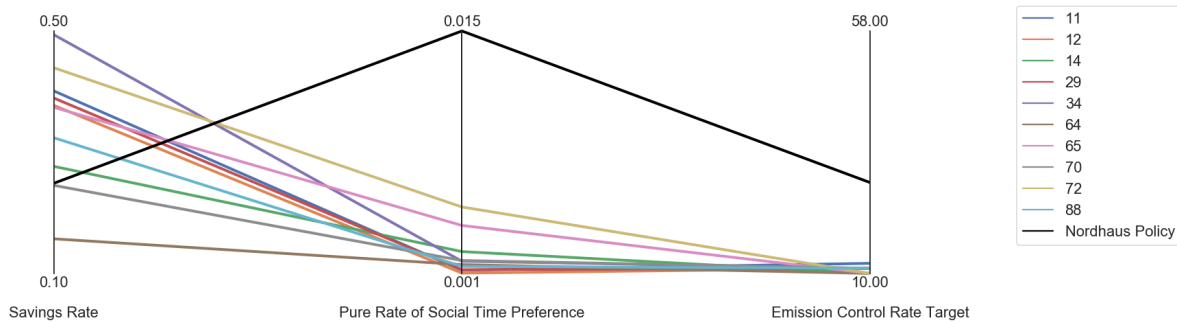


**Figure 10.7:** Comparison of the MiniMax policies to Nordhaus optimal policy.

One can immediately recognize that most MiniMax policies are a mirror image of the Nordhaus optimal policy for all policy levers. However, one should not conclude that this demonstrates a trade-off in policy options. This becomes apparent when taking a closer look at candidate strategy 70. Although it shows a similar SR ( $= 0.245$ ) to the SR ( $= 0.248$ ) of Nordhaus optimal policy, the candidate policy 70 comprises a far lower IRSTP ( $= 0.002405$ ) and sets a very much earlier emission control rate target for 2060. Besides the candidate strategies 64 and 70, the other MiniMax policies have much higher savings rate. A high savings rate implies in the RCK growth model high investment. And as investment increases, capital is accumulated, which again increases the gross output. As discussed earlier, this is essential in the DICE model to sustain high abatement costs and/or damages. However, in return, high savings rate reduces the consumption so that a loss in utility must be accounted for. Furthermore, similar to the SNR policies, all candidate strategies have very low IRSTP. That is justifiable as low IRSTP results in a low discount rate. And the lower the discount rate, the higher is the utility. However, what is even more astonishing is that each candidate strategies sets a target for emission control between 2060 and 2070. In other words, in order to protect the world against disastrous outcomes, a zero-emission target must be reached at the latest by the year 2070.

## Summary

From Figures 10.5 and 10.7, it can be concluded that in contrast to Nordhaus optimal policy, the set of robust policies consist not only of a very low rate of social time preference (IRSTP), but also an early emission control rate target (ECRT). To be more specific, the Nordhaus ECRT (=2155) is at least 85 years apart from the ECRT of the robust policies. Further, a robust policy at maximum consists of an IRSTP of 0.0038, whereas Nordhaus optimal policy is for an IRSTP at 0.015. The difference between the two sets of robust policies is that in general, the SNR strategies suggest a lower savings rate (SR) relative to Nordhaus optimal policy whereas the MiniMax policies propose a higher savings rate. However, both policy sets are clear in their message that the time is running out for effective mitigation against catastrophic outcomes.

# **Part IV**

## **Discussion**

“He knew that all the hazards and perils were now drawing together to a point: the next day would be a day of doom, the day of final effort or disaster, the last gasp.” —

J. R. R. Tolkien

# 11

## CONCLUSION

This voyage has started by illustrating the fundamental issue of Integrated Assessment Models (IAM) of using an optimization approach to find a climate policy in a deeply uncertain system. Furthermore, key concepts around climate economics and decision-making under uncertainty as well as the DICE model has been presented to not only give the reader a general understanding of those concepts, but also to illustrate the multifariousness of this study. In the second part of this study, PyDICE, a simulation version of the DICE model, was conceptualized and implemented. In addition, various methodologies from time series clustering for scenario discovery to multi-objective evolutionary algorithms were introduced to explore the effects of fat-tailed uncertainties on the DICE model and to search for a set of robust policies. Afterwards, these methodologies were applied on PyDICE to generate greater insights about the consequences of fat-tailed uncertainty on Nordhaus optimal policy and subsequently to find robust candidate strategies. This final part is dedicated to bring these strings together and thereby to answer the ensuing main research question:

### Main Research Question

*What are the repercussions of fat-tailed distributions over uncertain parameters on the outcomes and on the robustness of the policy options of the DICE simulation model?*

### 11.1 REVISITING THE SUB-RESEARCH QUESTIONS

The first chapters of this research are summarized and the sub-research questions are addressed to lead the discussion in answering the main research question:

As extensively presented in Chapter 1 and 3, the most crucial shortcoming of IAMs is the deterministic optimization approach to a deeply uncertain future. Deep uncertainties like the damage function or equilibrium climate sensitivity (ECS) is first estimated and then included as a certainty into the model. Many prominent researcher [Pindyck, 2017; Weitzman, 2009a; Heal and Millner, 2014] have pointed out this major issue but have failed to provide an appropriate solution to this problem. Therefore, this research has utilized a multi-scenario MORDM framework to not only illustrate the shortcomings of optimized policies from deterministic assumptions but also to

present an alternative set of robust candidate strategies.

This framework makes use of a variety of methodologies which are summarized under the umbrella term Exploratory Modeling and Analysis. With different methodologies like global sensitivity analysis or scenario discovery, the behaviour of the complex system is explored systematically to deduct vulnerable regions for the development of robust policies. For this, however, a simulation model is mandatory as it allows the integration of various sources of deep uncertainties. But more important, it allows us to run a large number of different scenarios for relatively low computational costs. Thus, the DICE model has been translated into the simulation version PyDICE. Many functional relationships of the DICE model have been maintained in PyDICE. However, as the DICE aims to maximize the welfare function, the optimal values for the two parameters emissions control rate and savings rate are determined a-posterior. Since the underlying structure of the model embodies the Ramsey-Cass-Koopmans growth model, the two parameters are described in PyDICE by functions approximating the trajectory of each from the “optimal” climate policy scenario of DICE.

In the multi-scenario MORDM framework, the model is further organized into policy levers, outcomes of interest and exogenous uncertainties. It is assumed that the four main objectives of the decision-makers are to minimize atmospheric temperature and damages and to maximize total output and utility. Furthermore, the savings rate, emission control rate target and pure rate of social time preference are considered as policy levers. Lastly, on the basis of literature review and the sensitivity analysis on the DICE model, the following seven uncertainties have been integrated into the PyDICE: total availability of fossil fuel, total factor productivity growth rate, population growth rate, initial growth rate of emission to output ratio, price of backstop technology, equilibrium climate sensitivity (ECS) and the damage function. Although the experts in the field of climate economics have confidence in the rough ECS estimation of the IPCC, it is difficult to judge how fat the tail of the distribution is. Therefore, the following sub-research question has been posed:

**SQ1: Which fat-tailed distributions are used to describe the uncertain parameter and how are they integrated into the DICE simulation model?**

Distributions are identified as fat-tailed if the kurtosis is leptokurtic:  $Kurt[X] > 3$ . Since this study aims to answer the question of what are the repercussions of applying fat-tailed distribution over uncertain parameters, the ECS parameter is modelled for two fat-tailed distributions, namely log-normal distribution and Cauchy distribution, and compared to a normal distribution using a statistical analysis and scenario discovery (see Sections 9.2 and 9.3).

The probability density function (PDF) of these three ECS distributions were created by the following three steps:

1. Data points for the cumulative density function (CDF) are generated by using the ECS estimation of the IPCC AR5 and Knutti (2012) (see Table 4.4).

2. CDF of the distribution is fitted over the data points from step 1. R-squared is calculated to assess the goodness of fit.
3. If the R-squared is above 0.95, the CDF is translated into a PDF using the corresponding statistical sizes such as mean, variance or shape.

Subsequently, the fat-tailed distributions and the normal distribution are integrated into PyDICE. During a simulation run, one of these three distributions is uniformly chosen to describe the ECS parameter. In order to prevent absurd extreme cases during the sampling phase like an ECS value of 500°C, the rejection sampling method was used to create a truncated distribution between 0°C and 20°C. Moreover, the generated three distributions are enumerated from 0 to 2 (see Table 4.3), so that during the stochastic simulation run, it is already translated into a computer understandable form.

**SQ2:** *How sensitive are the outcomes of the DICE simulation model to the identified uncertainties?*

To assess the sensitivity of the outcome parameter on the defined uncertainties, a variance-based global sensitivity analysis (GSA), i.e. Sobol method, has been utilized due to its non-linearity and fast run time<sup>1</sup> of the PyDICE (see Figure 5.3). Multiple interesting insights have been obtained. First, the atmospheric temperature, the damages, and the total output are mainly sensitive to the ECS distribution and its sampled data, and the damage function. This is as expected since those exogenous uncertainties are directly linked to atmospheric temperature and damages. This confirms the prior assumption of this study that fat-tailed distributions have a substantial impact on the outcomes of interest. Furthermore, the utility is dominated by the rate of population growth. This can be explained by the fact that a higher population growth rate reduces the steady-state level of capital and output per labour force in the system. Thus, it reduces per capita factors such as the consumption per capita parameter in the social welfare function of the RCK model. This has naturally a significant effect on the utility. It was also observed that the initial growth rate of carbon intensity is substantially higher across all outcomes in 2300 than in the preceding years. The obvious implication of this observation is that a faster improvement in carbon efficiency could decrease the atmospheric temperature on earth and thus reduce the damages. The two uncertain parameters, total availability of fossil fuels and TFP growth rate do not affect any of the four outcomes. The latter is, in particular, surprising because [Nordhaus, 2008b] believed it to be one of the most critical uncertainties as it should be one of the main drivers of long-run economic growth.

Knowing that the system is highly sensitive to the various uncertainties of the model based on sub-research question 1, this study has also aimed at understanding the implication of deep uncertainties on the outcomes under Nordhaus optimal policy:

---

<sup>1</sup> One model run takes around 2.7ms for a computer with 8 virtual processors of 2.8GHz and 16GB of RAM.

**SQ3:** *Under which scenarios/conditions is the optimal policy from the DICE optimization model vulnerable?*

To answer this sub research question, a two-stage analysis has been conducted. In the first stage, the output space of the model was explored for the optimal policy of Nordhaus. Hereto, an experiment set is generated by simulating over 540000 different scenarios. The output space was visualized using pair plots for the several time points. The most intriguing insight from this exploration was that catastrophic outputs in any of the four outcomes are only attained for scenarios which comprise of Weitzman damage function and fat-tailed ECS parameter. This visual analysis has been complemented by a statistical analysis on the outcomes, total output and utility. The statistical analysis has shown that the 1% value at risk for the outcomes distinguishes significantly depending on the ECS distribution. For instance, the 1% risk threshold for the total output for Cauchy distributed scenarios is 80% lower than for normally distributed scenarios at 2200. Moreover, these differences in risk are disproportionately amplified by the damage function, so that substantial differences have even been observed at the 5% value at risk. Similar to the visual analysis, it can be concluded from the statistical analysis that the outcomes for the 1% and 5% value at risk are significantly lower for scenarios with fat-tailed ECS parameter and damage functions similar to Weitzman.

The second stage comprises of scenario discovery in the form of time series clustering and directed scenario search. The analysis has illuminated the relationship between the outcomes and the uncertainties in great detail. In contrast to the statistical and visual analysis, the introduced scenario techniques allow the researchers to take a relatively unbiased approach in identifying unfavourable scenarios. This analysis has shown that undesirable outcomes can never be attained for scenarios that consist of normally distributed ECS parameter. Moreover, under the discovered set of undesirable scenarios, Nordhaus damage function has only been found for scenarios which lead to high atmospheric temperature. Further, the scenario discovery has revealed that the outcomes, damages, total output and utility are only vulnerable to scenarios with a damage function akin to Weitzman or Newbold and fat-tailed ECS parameter. Lastly, the time series clustering has indicated that the optimal policy of Nordhaus is vulnerable for 328 out of 30000 scenarios. In other words, Nordhaus optimal policy fails for around 1.1% of all cases.

Moreover, all three analysis has unanimously demonstrated that the effect of fat-tailed uncertainty can be significant. However, the disproportional risks in the tail of Cauchy and log-normal distribution can only be translated into catastrophic outcomes by damage functions akin to Weitzman or Newbold and Daigneault.

Nordhaus optimal policy is vulnerable for 1% of the cases that consist of scenarios with fat-tailed ECS parameter and damage function similar to Weitzman or Newbold. Thus, under the precautionary principle the following sub-research question has been answered:

**SQ4:** *What are the robust set of policies for the DICE simulation model and how do they differ to the optimal policy of the DICE optimization model?*

From the scenarios that have been identified as vulnerable using scenario discovery, four maximally diverse scenarios ( $K = 4$ ) have been selected based on the diversity criterion of [Carlsen et al., 2016]. With these four scenarios, candidate strategies were generated by utilizing the  $\epsilon$ -NSGA-II algorithm over each chosen scenario individually. Even with constraints on the outcome parameter, utility and atmospheric temperature, 113 alternative candidate strategies to Nordhaus optimal policy were found. These candidate strategies are evaluated on their robustness against a large number of alternative future states by using two different robustness criterion's, namely minimax regret and signal-to-noise ratio. For each criterion, a final set of 10 robust strategies (SNR policies and MiniMax policies) has been identified.

From Figures 10.5 and 10.7, one can immediately observe that the difference between the identified robust policies and Nordhaus optimal policy is striking. In contrast to Nordhaus proposed strategy, the set of robust policies have not only a very low rate of social time preference (IRSTP), but also an early emission control rate target (ECRT). To be more specific, the Nordhaus ECRT ( $= 2155$ ) is at least 85 years apart from the ECRT of the robust policies. Further, a robust policy at maximum consists of an IRSTP of 0.0038. For instance, although the candidate policy 70 shows a similar SR ( $= 0.245$ ) to the SR ( $= 0.248$ ) of Nordhaus optimal policy, it comprises of a far lower IRSTP ( $= 0.002405$ ) and sets a very much earlier ECRT for 2060.

The difference between the two sets of robust policies is that in general, the SNR strategies suggest a low savings rate (SR) relative to Nordhaus optimal policy whereas the MiniMax policies propose a higher savings rate. By examining the policies with higher savings rate in more detail, one could observe that these high savings rates are balancing out the effect of either high IRSTP or late ECRT (relative to other SNR policies). As a (relatively) late ECRT will yield higher climate damages and thereby affects the total output negatively, a higher SR can have a counter effect by increasing the investment, that again raises the gross output. However, note that high SR diminishes the utility, especially when a high IRSTP has been chosen. This conclusion is also justified by assessing the policies with a lower SR. Here, these policies exhibit lower ECRT as well as lower IRSTP relative to high SR policies.

In all this discussion, it should not be forgotten that the main message of this analysis is that in order to protect the world against disastrous outcomes, a zero-emission target must be reached at the latest by the year 2070. What is further worrisome is that the ECRT of the robust policies is at the edge of the policy space. This could actually mean that robust policies could have been found with ECRT earlier to 2065. Therefore, it is recommended to widen the policy window to generate potential further findings.

## 11.2 ANSWERING THE MAIN RESEARCH QUESTIONS

The answers and discussions to each sub-research question can be utilized to answer the main research question of this study.

### Main Research Question

*What are the repercussions of fat-tailed distributions over uncertain parameters on the outcomes and on the robustness of the policy options of the DICE simulation model?*

The results of this study have shown that the effect of fat-tailed distribution is significant. The prior hypothesis of Weitzman [2009a] has been proven by conducting a variety of different analysis over the data set generated by the stochastic simulation version of DICE, PyDICE.

The variance-based GSA has shown that the outcomes are highly sensitive to the distribution type of the ECS parameter, but also to other deep uncertainties such as the damage function or the population growth rate. From the statistical analysis, it has been deduced that the 1% value at risk for the outcomes, utility and total output, distinguish significantly depending on the distribution type for Nordhaus optimal policy (up to 80%). Moreover, if the future states of the world comprise of a damage function akin to Weitzman and a fat-tailed ECS parameter, a significant difference to scenarios with normally distributed ECS parameter and Nordhaus damage function has been found for the 5% value at risk for the total output (up to 53% lower). The scenario discovery has shown that the optimal policy of Nordhaus fails in around 1% of the generated scenarios, in which the failure scenarios comprises of either a Cauchy distributed or log-normal distributed ECS parameter. The high impact of fat-tailed distribution has also been found in the global sensitivity analysis. However, the analysis shows also that these disastrous outcomes are only obtained for scenarios with damage function similar to Weitzman. All analysis has unanimously illustrated that as fatter the tail becomes the risk is getting higher, but it becomes only significant in combination with damage function similar to Weitzman. In addition, this analysis has also shown that Nordhaus optimal policy is not robust enough to protect the world against catastrophic events.

Therefore, an alternative set of robust strategies to Nordhaus optimal policy is illustrated in this study. It is shown that the Pareto optimized set of robust policies suggest a very low pure rate of social time preference and a far earlier emission control rate target between 2060 and 2070. Moreover, the savings rate depends on the emission control rate target as well as the pure rate of social time preference. That means when the global community decides a course of action which consists of an early emission control rate target and the decision to sacrifice current consumption for the benefit of the future generation, a lower savings rate (lower investment) can be chosen. Vice versa, the same principle applies: a high savings rate (= high investment) is necessary for policies with relatively late emission control rate target and a

high pure rate of social time preference. The relationship between the savings rate and the other two parameters is anything but linear. In addition to this point, it has also been observed that robust policies are located at the edges of the defined policy space. This means to avoid catastrophic outcomes from deep uncertainties (incl. fat-tailed distribution and damage functions), policies must be put in place that is far more radical than suggested by Nordhaus, but much closer to the demands of climate scientists.

It can be concluded that as long as not more knowledge is generated for deep uncertainties such as the equilibrium climate sensitivity parameter or the damage function, one has to explore all possible alternatives to deduct a robust set of policies. The implications of using the traditional method for risk and decision analysis (optimization) instead of methods like multi-scenario MORDM (robust optimization) is that disastrous events in future will be considered in hindsight as “Black Swans” although they were predictable “Grey Swans” all the time

# 12 | DEBATE

All the effort and endeavour of conducting an extensive analysis is of little value without a vivid discussion about the implication of the findings in a bigger picture. The main intention of this chapter is to start a debate, respond to doubts, answer potential criticism, and illustrate a code of conduct. Thus, this chapter consists of individual section each standing for itself.

## 12.1 POLICY ADVICE

Since climate change is a global challenge that is not bound to any borders, it can not be solved by any individual country alone. If climate change is to be tackled effectively, the global community must negotiate and agree on a global green new deal (GND). Hereto, policy recommendations, from IAMs such as the PyDICE, can support decision-makers around the world to decide on some overarching targets, such as the emission control rate target or the investment cost. Based on the precautionary principle, this study has proposed a set of robust policies. Taking all potential future states of the world into account, we show that a very early emission control rate target between 2060 and 2070 and a low pure rate of social time preference is the safest strategy in the face of existential risk. Moreover, the more we are willing to sacrifice our consumption for future generations, the less is the investment costs. However, we should keep in mind that these policies are a result of a stylized model, which is essentially only a reflection of the real system. “Letting go of the phantastic mathematical objects and achievables of [...] model-land may not always be comfortable, but it is necessary if we are to make better decisions.” [Thompson and Smith, 2019]. Hence, the implications and the feasibility of these robust policies in the real world is discussed in more detail below.

In terms of early emission control rate target, the robust policy recommendations from PyDICE coincides with the demands of climate scientist to reach net-zero emission target in the next three decades. On the one hand, 17 countries (e.g., UK and France) and 34 major corporations are preparing or already have committed to reach net-zero in the next three decades. However, on the other hand, 159 countries have set targets in the latter half of the century (e.g., Japan) or have yet to put such a target (e.g., US, China and Australia) [Edmond, 2019]. Thus, one can conclude, if a GND that legally binds the global community to reach a net-zero emission target before 2070, is not reached soon, there is no realistic way to protect the world against

the catastrophic scenario of the PyDICE model.

Even if the international community manages to set an early emission control rate target to mitigate the catastrophic climate damages, they still have to agree on an annual investment sum which depends, in PyDICE, highly on the pure rate of social time preference (IRSTP). In general, the IRSTP reflects the societies view on the future. If the global community chooses a very high to medium IRSTP, it means that they do not recognize the urgency for climate mitigation. However, if the international community acknowledges the existence of catastrophic risks, as shown in PyDICE, they have no other means than choosing a relatively low IRSTP since any medium to high IRSTP will lead to annual investment costs beyond the global income. However, by weighing future generations equal to the present generation, a low IRSTP will produce a higher social cost of carbon. This sacrifice in the welfare of the current generation is the price of robustness. If we are fully committed to radically reduce carbon emissions to prevent future catastrophes, this price has to be paid, at least according to the neoclassical growth theory .

Moreover, the trade-off between consumption of current generation versus consumption of future generations does only exist if we assume that financial intermediaries are organized in a loanable funds market. But in reality, banks can create money. Instead of waiting for a raise in savings, central banks could issue new money by buying bonds from intergovernmental institutions such as the World Bank or the Green Climate Fund to cover the large investment costs due to the social discount rate. The fact that this is possible was seen during the financial crisis when central banks bailed out private banks as well as governments by buying up private and public bonds. This would also allow us to shift the discussion from damage cost to the cost of emission reduction, which is far more critical.

## 12.2 SALVATION OF INTEGRATED ASSESSMENT MODELS

This section is aimed at responding to Pindyck [2017] question whether IAMs can be salvaged as a tool for policy analysis if we somehow can account for the lack of knowledge about key relationships and parameter values. In his manuscript, he advocates for an approach in which expert opinions are translated into probabilities and implemented into a simple model. What he is trying to describe sounds like a stochastic model. Indeed, this is a much better approach than the use of estimates, assumptions, and beliefs as deterministic inputs of models to determine the social cost of carbon or the cumulative discounted utility. However, the literature review of this study has shown that various researchers have applied stochasticity into IAMs. However, this alone will not make any substantial difference in the outcomes of the model, and more importantly, this will not change how IAMs will be perceived or utilized. To support this statement, in the following, three arguments are presented in detail.

### ***Decision-Making under Ignorance***

The first exhibit starts with the claim that many researchers in the field of climate economics simply ignore the ontological difference between risk and uncertainty. As mentioned in the introduction part of this manuscript, [Knight \[1921\]](#) describes “risk” as known probabilities and “uncertainty” as unknown probabilities. But despite this strict difference, [Nordhaus \[2016\]](#) and others have applied quasi-random distributions on variables which are by nature deeply uncertain, such as the growth rate of total factor productivity or the growth rate of carbon intensity. This utterly wrong treatment of uncertainties actually could lead to severe consequences in the sense that a scientific investigation reconfirms false perceptions. Beyond parametric uncertainties, the integrated system of climate, carbon and economics consists of a variety of other deep uncertainties. This thesis, among others, has shown that there is deep uncertainty about the distribution type of the equilibrium climate sensitivity parameter. However, the two research groups, [Hwang et al. \[2013\]](#) and [Ackerman et al. \[2010\]](#) who have also studied the implication of fat-tailed distribution on the DICE model, have only utilized a log-normal distribution. But what about a Cauchy distribution or a Pareto distribution?

Both probability distributions have a much higher kurtosis. This neglection perfectly exemplifies the ignorance of many researchers in the field. Even though there is awareness for uncertainties, they still turn a blind eye on other eventualities. Moreover, if one would look deeper into their experiment design, one will observe that many deep uncertainties have been described by normal distributions. Although, [Hwang et al. \[2013\]](#) reasons for many of his choices why certain distributions have been chosen, [Ackerman et al. \[2010\]](#) choices are opaque to the reader.

### ***Optimality vs. Robustness***

This ignorance also has direct consequences on how IAMs are perceived and utilized. In general, IAMs are utilized as an optimization model to identify optimal climate policies based on the given constraints. However, even if the deterministic parameters are turned into probability distributions, a single set of scenarios and a single set of probability distribution will still generate a single best outcome [[Lempert et al., 2006](#)]. Stochastic optimization is well suited to determine the best possible strategy when the uncertainties are well characterized (i.e., risks) and the structure of the system is well known.

IAMs describe a system that is largely complex in nature. With increasing complexity, the system is not only more difficult to understand, but it is also more challenging to find an optimal policy. Any estimates about the future will be inaccurate. When strategies are optimized for the most likely future, they may fail for events that lie at the realm of our expectations. Even the assessment of well-elaborated scenarios, such as the Shared Socio-Economic Pathways SSPs, will fail to cover the vital granularity between different future pathways. This becomes in particular troublesome, when models such as IAMs are used to find an optimal policy for a long time-horizon. Therefore, it can be stated with certainty that the prescriptive value of the optimal

strategy is lost in climate economic systems.

Hence, in line with the principle 15 of the 1992 Rio Declaration and the principle 7 of the Global Impact, it is urged that “where there are threats of serious or irreversible damage” [UN, 1992; Compact, 2016], the precautionary principle must be applied as long as scientific knowledge is incomplete. This is also recognized within the scientific community that in a complex system, policy recommendations must be robust in regards to the manifold of deep uncertainties [Lempert and Collins, 2007; Giuliani and Castelletti, 2016; Kwakkel et al., 2016a; Herman et al., 2015]. In order to find robust policies, IAMs must be translated into a simulation model. With this in hand, it is now possible to answer the ”what-if” question and to systematically explore the behaviour of the climate economic systems under an ensemble of prior specified uncertainties in response to different policy settings. The deep uncertainties are given as a range between two values. How the ranges should be chosen is discussed in great detail in section 12.3. Moreover, this simulation model can be used to determine the worst case scenario, so that a robust policy can be determined. Thus, I propose to redefine IAMs, not as a stochastic optimization model but to take it one step further and turn it into a robust optimization model. This study is an excellent example of how this could be attained.

### *Experts or Opinions*

In my last exhibit, I want to discuss the benefits and pitfalls of the involvement of experts opinions. In traditional model building, the involvement of expert opinion during the model process is of utmost importance. Based on the conceptual model, experts validate whether the model reasonably represents the real system. Therefore, it is effortless to use the experts from the model development process to support the modeller in determining the inputs of the model.

However, what Pindyck proposes from here on is at the least questionable. He suggests not only to further simplify IAMs but also to use expert opinions to attach probabilities on events such as the GDP or consumption decline regarding catastrophic outcomes. By this, he completely discards feedback loops between the three subsystems carbon, climate and economics and suggests to create a simple and very linear model representing the opinion of experts. First of all, determining policies in complex systems regardless of the intrinsic non-linear behaviour is like trying to forecast the weather for the next 100 years based on a simple extrapolation over the observations of the last year. But even if we disregard this aspect and only focus on the second point, that of attaching probabilities on deep uncertain parameters based on expert opinion, it is still controversial.

On the one hand, if expert opinions are used to instigate a critical discourse to challenges their internal beliefs and biases, this would be of high value. However, if scientific ambiguity is only addressed by summarizing the different opinions of experts, it can motivate shortcuts in reasoning and hidden biases. Moreover, such enforced consensus-building can lead to overconfidence and belief polarization [Curry, 2011].

[Kelly \[2008\]](#) illustrates that as more and more experts are weighing on a given issue, at some point when the number of peers exceeds a specific threshold, the total order evidence will completely swamp the first-order evidence. This can lead to increasing confirmation bias that would eventually peripheralize critical voices. But is not a healthy amount of skepticism and disagreement the key driver in science to find an alternative way that could potentially lead to actually solving the problem at hand.

The question of Pindyck, whether IAMs can be salvaged as a tool for policy analysis if we somehow can account for the lack of knowledge about key relationships and parameter values can be still answered with a yes. I certainly believe that IAMs can be salvaged as a policy analysis tool or at least for storytelling, but only if the creators of IAMs abdicate their ontological ignorance and re-shift their mindset from optimality to robustness in light of existential risks for humanity.

### 12.3 UNBIASED BIASED CHOICES

As we have seen in this study, forecasting is hampered subject to the modeller's blind spots and biases. Models are just a reflection of reality. Thus "all models are essentially wrong, but some are useful." [\[Box and Draper, 1987\]](#). However, the usefulness of those models is diminished by the misuse of statistical distributions like thin-tail distributions in a highly complex and uncertain environment, that exclude the (low) probability of high impact events.

But even the use of fat-tailed distribution can be subject to biases. The question is here where to set the boundaries so that low probability high impact events (Grey Swans) are incorporated but do not lead to the naive fallacy of infinite costs. Although statistical tools to estimate the boundaries exists, there is no golden bullet to solve this issue. At the end of the day, setting the boundaries for fat-tailed distributions lies in the hands of modellers. This can lead to errors as the mind uses simplifying schemes to confirm their biases, so-called "confirmation bias". Moreover, as they become overconfident about their ideas about the right bound, they succumb to "epistemic arrogance". This moral dilemma screams for an ethical reflection.

Let us start this discussion by applying the three main ethical theories on the aforementioned dilemma [\[Annas, 2009; Mill, 2009; O'Neill, 1993\]](#). First off: consequentialism, deontological ethics and virtue ethics are offering arguments why modellers, in practice, should strive to integrate Grey Swan events even if the modeller him-/herself has to set the boundaries for the distribution. Consequentialism requires the modeller to predict the likely results of an act and weigh the good it will produce against the harm it would cause. In other words, if the integration of Grey Swan events leads to "good consequences" or "outcomes of higher quality", it is desirable to conceptualize and formalize the model reflecting those uncertainties. This can be defended with the harm principle of Mill [\[Mill, 2009\]](#).

In contrast, deontological ethics focus on the purpose of the model. Within Kantian ethics as a paradigmatic example, the model must be used to illuminate rather than deceive perceptions [O'Neill, 1993]. Therefore, modellers must add additional tools to their model if it produces a more accurate model with elucidating outcomes.

At last, the virtue ethics focus on the people who suffer due to the inaccuracy in models caused by the disregard of the Grey Swan events [Annas, 2009]. For instance, if the integration of Grey Swan events into economic models could have indicated the financial crisis in 2008, one could have set policies to prevent it. However, due to the inability to predict the severity and the far-reaching consequences, millions of households were victims of job loss, home foreclosures and/or debt. All three ethical framework put forward that from an ethical perspective the integration of Grey Swan events is of utmost importance.

However, this still does not give modellers an ethical guideline on how to set the boundaries on fat-tailed distribution in computer simulations. When dealing with deep uncertainties or Grey Swan events, we are not able to fully express the effect of the risks and thus to objectively set the boundaries of fat-tailed distributions during the simulation. To deal with this challenge, the precautionary principle, as shown in this study, is proposed. The maxim states that preventive measures must be taken if there are indications of certain risks and even if the risks cannot be entirely scientifically proven. In other words, “if there is a threat, which is uncertain, then some kind of action is mandatory” [Sandin, 1999]. For our case, the precautionary principle translates to setting the boundaries sufficiently large, so that all potential risks even outside of the realm of expectations are also sufficiently covered. Admittedly, this approach does not answer the aforementioned issue of confirmation bias. This issue can perhaps only be overcome when modellers challenge his/her biases with stakeholders, experts and/or laymen. Moreover, one should be aware that this approach can lead to overestimation of low probability high impact events. Although one would have a hard time to forecast the next occurrence of a Grey Swan event, the solution to deal with Grey Swan events is to restructure institutions and rethink strategies to be more robust in the face of deep uncertainties. The robustness can be achieved through flexibility. To describe it differently, let the system absorb the shock.

After all, the key to a good model is to maintain a mindset of humility as a modeller. A model of a messy and a complex system will never be easy to model and thus will be most certainly wrong. However, if there is a simple answer on how to incorporate Grey Swan events into the model without overestimating or underestimating, there would not be such a polarizing discussion in different scientific fields.

# 13 | FUTURE AVENUES

As this study was only limited to five months, I had to discipline myself to only focus on a certain number of research pathways and to accept some of the limitations of my thesis. However, the limitations of one research can be exciting avenues for future studies.

## *Design Limitations*

One significant limitation of this study is the fact that this study was conducted without the counseling of experts from the field of climate economics. Value ranges for many of the identified uncertainties relied entirely on desk research. In a best practice approach, one would have gathered a panel of experts/proponents from each of the four discourses on climate stabilization not only to identify the min-max ranges of the deep uncertainties but also to validate the simulation version of the DICE model, PyDICE [Storm, 2017].

Although, we have acknowledged in the literature review of this thesis that there is still substantial uncertainty around the equilibrium climate sensitivity parameter, this research has only focused on the uncertainty around the distribution type. However, in future work one can/should add an additional uncertainty dimension to cover scientific ambiguity around the median cumulative probability value.

Moreover, an effective net-zero carbon target can only be reached when every nation in the world actively join this effort at the soonest possible time. In the DICE and PyDICE model, full participation of all countries is assumed. In reality, however, only 175 countries accounting for 88.75% of global emissions ratified the Paris Agreement, and if the Trump administration is going to withdraw from the Paris agreement at the end of 2019, the global emission under control will drop down to 70.86%. Thus, in a future analysis, the policy levers can include the already existing “full participation target” parameter in PyDICE.

## *Methodological Improvements*

From the modellers perspective, the time series clustering in the scenario discovery chapter was limited to “only” 30000 scenarios due to memory issues and computational efforts. Thus, in future research one could test other techniques such as BIRCH [Zhang et al., 1996] or PAM [Kaufman and Rousseeuw, 2009].

Another limitation of this study is that the output of stochastic simulation models, such as the PyDICE, emerges as the results of one “quasi”-random trajectory of po-

tential internal model states. Traditionally, the likelihood function in these models is approximated by an extremely large sample set or by running multiple replications and comparing the outcome based on their descriptive statistics. However, since simulated data are an output of various distributions, traditional practices are insufficient. Thus, in a future study, one should estimate the likelihood function by using methodologies such as approximate Bayesian computing or pattern-oriented modelling [Hartig et al., 2011].

### *Directions for further Exploration*

In this study, we have tested the implications of Weitzman Dismal Theorem by utilizing the multi-scenario MORDM framework on a simulation version of the DICE model. However, the DICE is model considered as simple IAM. Thus, it would be highly interesting to explore the effects of deep uncertainties in a more complex model such as the Model for Energy Supply Strategy Alternatives and their General Environmental Impact (MESSAGE), developed by the International Institute for Applied Systems Analysis (IIASA) or the Integrated Model to Assess the Global Environment (IMAGE), developed by the Netherlands Environmental Assessment Agency (PBL).

Lastly, another exciting future avenue would also be to integrate a monetary system into the DICE model and to analyze the effect of pure rate of social time preference on the outcomes. If we would deduct from such an analysis that the effect of social discount rate is negligible, one could shift the discussion from Pigouvian taxes to other policy alternatives such as climate bonds.

## BIBLIOGRAPHY

- Ackerman, F., Stanton, E. A., and Bueno, R. (2010). Fat tails, exponents, extreme uncertainty: Simulating catastrophe in DICE. *Ecological Economics*, 69(8):1657–1665.
- Annas, J. E. (2009). Virtue ethics. In *The Oxford handbook of ethical theory*. Oxford University Press.
- Bankes, S., Walker, W. E., and Kwakkel, J. H. (2013). Exploratory Modeling and Analysis. In *Encyclopedia of Operations Research and Management Science*, pages 532–537. Springer US, Boston, MA.
- Bartholomew, E. (2018). ROBUST DECISION SUPPORT METHODS: A COMPARATIVE ANALYSIS. *Delft University of Technology*.
- Batista, G. E. A. P. A., Keogh, E. J., Tataw, O. M., and De Souza, V. M. A. (2014). CID: An efficient complexity-invariant distance for time series. *Data Mining and Knowledge Discovery*, 28(3):634–669.
- Bell, R. and Callan, D. (2011). More than meets the eye the social cost of carbon in u.s. climate policy, in plain english. *Policy Brief: World Resources Institute and Environmental Law Institute*.
- Bertsimas, D. and Sim, M. (2004). The price of robustness. *Operations research*, 52(1):35–53.
- Better, M., Glover, F., Kochenberger, G., and Wang, H. (2008). SIMULATION OPTIMIZATION: APPLICATIONS IN RISK MANAGEMENT. 7(4):571–587.
- Borunda, A. (2019). A heat wave is turning greenland’s ice to slush. that’s bad news.
- Box, G. E. and Draper, N. R. (1987). *Empirical model-building and response surfaces*. John Wiley & Sons.
- Boyce, J. K. (2017). The humble economist: What economics can – and can’t – tell us about climate change.
- Breiman, L. (2001). (impo)Random forests(book). *Machine learning*.
- Bruckner, T., Bashmakov, I. A., Mulugetta, Y., Chum, H., Navarro, A. d. l. V., Edmonds, J., Faaij, A., Fungtammasan, B., Garg, A., Hertwich, E., Honnery, D., Infield, D., Kainuma, M., Khennas, S., Kim, S., Nimir, H. B., Riahi, K., Strachan, N., Wiser, R., and Zhang, X. (2014). Energy Systems. *Climate Change 2014: Mitigation of Climate Change. Contribution of Working Group III to the Fifth Assessment Report of the Intergovernmental Panel on Climate Change*, pages 511–598.

- Buchheit, K., Fullmer, W., Gel, A., Jordan, T., Meredith, M., Nicoletti, P., and Van Esendelft, D. (2019). Doe methods.
- Butler, M. P., Reed, P. M., Fisher-Vanden, K., Keller, K., and Wagener, T. (2014). Identifying parametric controls and dependencies in integrated assessment models using global sensitivity analysis. *Environmental Modelling and Software*.
- Carbon Brief (2018). Q&A: How integrated assessment models are used to study climate change.
- Carbon Brief (2019). In-depth Q&A: The UK becomes first major economy to set net-zero climate goal.
- Cariboni, J., Gatelli, D., Liska, R., and Saltelli, A. (2007). The role of sensitivity analysis in ecological modelling. *Ecological modelling*, 203(1-2):167–182.
- Carlsen, H., Lempert, R., Wikman-Svahn, P., and Schweizer, V. (2016). Choosing small sets of policy-relevant scenarios by combining vulnerability and diversity approaches. *Environmental Modelling and Software*, 84:155–164.
- Chang, C. W. (2014). DICESC: Optimal Policy in a Stochastic Control Framework Charles.
- Charney, J. (1979). Carbon Dioxide and Climate: A Scientific Assessment. Technical report.
- Compact, U. G. (2016).
- Costello, C. J., Neubert, M. G., Polasky, S. A., and Solow, A. R. (2010). Bounded uncertainty and climate change economics. *Proceedings of the National Academy of Sciences*, 107(18):8108–8110.
- Curry, J. (2011). Reasoning about climate uncertainty. *Climatic Change*, 108(4):723.
- Dalal, S., Han, B., Lempert, R., Jaycocks, A., and Hackbarth, A. (2013). Improving scenario discovery using orthogonal rotations. *Environmental Modelling and Software*.
- Dietz, S. (2011). High impact, low probability? An empirical analysis of risk in the economics of climate change. *Climatic Change*, 108(3):519–541.
- Dietz, S. and Stern, N. (2015). Endogenous growth, convexity of damage and climate risk: How Nordhaus' framework supports deep cuts in carbon emissions. *Economic Journal*, 125(583):574–620.
- Edmond, C. (2019). Zero by 2050: How the world's economy has planned to battle climate change.
- Eker, S. and Kwakkel, J. H. (2018). Including robustness considerations in the search phase of Many-Objective Robust Decision Making. *Environmental Modelling and Software*, 105:201–216.

- Emmerich, M. T. and Deutz, A. H. (2018). A tutorial on multiobjective optimization: fundamentals and evolutionary methods. *Natural Computing*, 17(3):585–609.
- Giuliani, M. and Castelletti, A. (2016). Is robustness really robust? How different definitions of robustness impact decision-making under climate change. *Climatic Change*, 135(3-4):409–424.
- Golub, A., Narita, D., and Schmidt, M. G. (2014). Uncertainty in Integrated Assessment Models of Climate Change: Alternative Analytical Approaches. *Environmental Modeling and Assessment*, 19(2):99–109.
- Hadka, D., Herman, J., Reed, P., and Keller, K. (2015). An open source framework for many-objective robust decision making. *Environmental Modelling & Software*, 74:114–129.
- Hartig, F., Calabrese, J. M., Reineking, B., Wiegand, T., and Huth, A. (2011). Statistical inference for stochastic simulation models—theory and application. *Ecology letters*, 14(8):816–827.
- Heal, G. and Millner, A. (2014). Uncertainty and decision making in climate change economics. *Review of Environmental Economics and Policy*, 8(1):120–137.
- Herman, J. D., Reed, P. M., Zeff, H. B., and Characklis, G. W. (2015). How Should Robustness Be Defined for Water Systems Planning under Change? *Journal of Water Resources Planning and Management*, 141(10):04015012.
- Herman, J. D., Zeff, H. B., Reed, P. M., and Characklis, G. W. (2014). Beyond optimality: Multistakeholder robustness tradeoffs for regional water portfolio planning under deep uncertainty. *Water Resources Research*, 50(10):7692–7713.
- Hwang, C., Reynes, F., and Tol, R. (2014). The effect of learning on climate policy under fat-tailed uncertainty.
- Hwang, I. C., Reynès, F., and Tol, R. S. J. (2013). Climate Policy Under Fat-Tailed Risk: An Application of Dice. *Environmental and Resource Economics*, 56(3):415–436.
- Ikefuji, M., Laeven, R. J. A., Magnus, J., and Muris, C. (2014). Expected Utility and Catastrophic Risk.
- IPCC (2014). Climate Change 2014: Synthesis Report. Contribution of Working Groups I, II and III to the Fifth Assessment Report of the Intergovernmental Panel on Climate Change. Technical report.
- IPCC (2018). Global warming of 1.5C. An IPCC Special Report on the impacts of global warming of 1.5C above pre-industrial levels and related global greenhouse gas emission pathways, in the context of strengthening the global response to the threat of climate change. Technical report, World Meteorological Organization, Geneva, Switzerland.

- Jaxa-Rozen, M. and Kwakkel, J. (2018). Tree-based ensemble methods for sensitivity analysis of environmental models: A performance comparison with Sobol and Morris techniques. *Environmental Modelling and Software*, 107(October 2017):245–266.
- Kasprzyk, J. R., Nataraj, S., Reed, P. M., and Lempert, R. J. (2013). Many objective robust decision making for complex environmental systems undergoing change. *Environmental Modelling & Software*, 42:55–71.
- Kaufman, L. and Rousseeuw, P. J. (2009). *Finding groups in data: an introduction to cluster analysis*, volume 344. John Wiley & Sons.
- Kelly, T. (2008). Disagreement, dogmatism, and belief polarization. *The Journal of Philosophy*, 105(10):611–633.
- Knight, F. H. (1921). *Risk, uncertainty and profit*.
- Knutti, R. and Hegerl, G. (2008). The equilibrium sensitivity of the Earth's temperature to radiation changes. *Nature Geoscience*, 1:735 – 743.
- Kwakkel, J. H. (2017). The Exploratory Modeling Workbench: An open source toolkit for exploratory modeling, scenario discovery, and (multi-objective) robust decision making. *Environmental Modelling and Software*, 96:239–250.
- Kwakkel, J. H., Auping, W. L., and Pruyt, E. (2013). Dynamic scenario discovery under deep uncertainty: The future of copper. *Technological Forecasting and Social Change*, 80(4):789–800.
- Kwakkel, J. H., Eker, S., and Pruyt, E. (2016a). How robust is a robust policy? Comparing alternative robustness metrics for robust decision-making. In *International Series in Operations Research and Management Science*.
- Kwakkel, J. H., Haasnoot, M., and Walker, W. E. (2016b). Comparing Robust Decision-Making and Dynamic Adaptive Policy Pathways for model-based decision support under deep uncertainty. *Environmental Modelling & Software*, 86:168–183.
- Lempert, R. J. and Collins, M. T. (2007). Managing the Risk of Uncertain Threshold Responses: Comparison of Robust, Optimum, and Precautionary Approaches. *Risk Analysis*, 27(4):1009–1026.
- Lempert, R. J., Groves, D. G., Popper, S. W., and Bankes, S. C. (2006). A General, Analytic Method for Generating Robust Strategies and Narrative Scenarios. *Management Science*, 52(4):514–528.
- Mandelbrot, B. B. (1997). *Fractals and Scaling in Finance. Discontinuity, Concentration, Risk. Selecta Volume E*. Springer-Verlag New York.
- McPhail, C., Maier, H. R., Kwakkel, J. H., Giuliani, M., Castelletti, A., and Westra, S. (2018). Robustness Metrics: How Are They Calculated, When Should They Be Used and Why Do They Give Different Results? *Earth's Future*, 6(2):169–191.

- Metcalf, G. and Stock, J. (2015). The Role of Integrated Assessment Models in Climate Policy: A User's Guide and Assessment. *The Harvard Project on Climate Agreements March*.
- Mill, J. S. (2009). *Utilitarismus*, volume 581. Felix Meiner Verlag.
- Millner, A. (2013). On welfare frameworks and catastrophic climate risks. *Journal of Environmental Economics and Management*, 65(2):310–325.
- Moore, F. C. and Diaz, D. B. (2015). Temperature impacts on economic growth warrant stringent mitigation policy. *Nature Climate Change*, 5(2):127–131.
- Nature (2018). The costs of climate inaction.
- Newbold, S. C. and Daigneault, A. (2009). Climate response uncertainty and the benefits of greenhouse gas emissions reductions. *Environmental and Resource Economics*, 44(3):351–377.
- Nordhaus, W. (2007). The Stern Review on the Economics of Climate Change. *Review Literature And Arts Of The Americas*, pages 1–40.
- Nordhaus, W. (2008a). *A Question of Balance: Weighing the Options on Global Warming Policies*. Yale University Press, New Haven & London.
- Nordhaus, W. (2014). Estimates of the social cost of carbon: concepts and results from the DICE-2013R model and alternative approaches. *Journal of the Association of Environmental and Resource Economists*, 1(1/2):273–312.
- Nordhaus, W. D. (1992). An optimal transition path for controlling greenhouse gases. *Science (New York, N.Y.)*, 258(5086):1315–9.
- Nordhaus, W. D. (2008b). *A Question of Balance: Weighing the Options on Global Warming Policies*. Yale University Press, New Haven, Conn.
- Nordhaus, W. D. (2013). DICE 2013R: Introduction and User's Manual. *Yale University Press*, (October):102.
- Nordhaus, W. D. (2016). Projections and uncertainties about climate change in an era of minimal climate policies.
- O'Neill, O. (1993). Kantian ethics. *A companion to ethics*, 29:175–85.
- Pachauri, R. K. and Mayer, L., editors (2014). *Climate Change 2014: Synthesis Report. Contribution of Working Groups I, II and III to the Fifth Assessment Report of the Intergovernmental Panel on Climate Change*. Intergovernmental Panel on Climate Change, Geneva, Switzerland.
- Pindyck, R. S. (2011). Fat tails, thin tails, and climate change policy. *Review of Environmental Economics and Policy*, 5(2):258–274.
- Pindyck, R. S. (2013). Climate Change Policy: What Do the Models Tell Us? *Journal of Economic Literature*, 51(3):860–872.

- Pindyck, R. S. (2017). The use and misuse of models for climate policy. *Review of Environmental Economics and Policy*, 11(1):100–114.
- Quade, E. S. and Carter, G. M. (1989). *Analysis for public decisions*. MIT Press.
- Reed, P. M., Hadka, D., Herman, J. D., Kasprzyk, J. R., and Kollat, J. B. (2013). Evolutionary multiobjective optimization in water resources: The past, present, and future. *Advances in Water Resources*, 51:438–456.
- Rezai, A. and Van Der Ploeg, F. (2017). Abandoning Fossil Fuel: How Fast and How Much. *Manchester School*, 85:e16–e44.
- Roe, G. H. and Baker, M. B. (2007). Why Is Climate Sensitivity So Unpredictable? *Science*, (OCTOBER):277–313.
- Rogelj, J., Meinshausen, M., and Knutti, R. (2012). Global warming under old and new scenarios using ipcc climate sensitivity range estimates. *Nature climate change*, 2(4):248.
- Rosen, R. A. and Guenther, E. (2015). The economics of mitigating climate change: What can we know? *Technological Forecasting and Social Change*, 91:93–106.
- Rousseeuw, P. J. (1987). Silhouettes: A graphical aid to the interpretation and validation of cluster analysis. *Journal of Computational and Applied Mathematics*.
- Saltelli, A. A. (2008). *Global sensitivity analysis : the primer*. John Wiley.
- Sandin, P. (1999). Dimensions of the precautionary principle. *Human and Ecological Risk Assessment: An International Journal*, 5(5):889–907.
- Sargent, R. G. (2013). Verification and validation of simulation models. *Journal of simulation*, 7(1):12–24.
- Shayegh, S. and Thomas, V. M. (2015). Adaptive stochastic integrated assessment modeling of optimal greenhouse gas emission reductions. *Climatic Change*, 128(1-2):1–15.
- Stanton, E. A., Ackerman, F., and Kartha, S. (2009). Inside the integrated assessment models: Four issues in climate economics. *Climate and Development*, 1(2):166–184.
- Steinmann, P. (2018). Behavior-Based Scenario Discovery.
- Stern, N. (2006). The Economics of Climate Change: The Stern Review.
- Storm, S. (2017). How the Invisible Hand is Supposed to Adjust the Natural Thermostat: A Guide for the Perplexed. *Science and Engineering Ethics*, 23(5):1307–1331.
- Straub, S. (2018). Natural catastrophe review: Series of hurricanes makes 2017 year of highest insured losses ever.

- Strubell, E., Ganesh, A., and McCallum, A. (2019). Energy and policy considerations for deep learning in nlp. *arXiv preprint arXiv:1906.02243*.
- Taleb, N. N. (2006). Fat Tails , Asymmetric Knowledge , and Decision Making. *Wal-mott magazine*, pages 56–59.
- Taleb, N. N. (2010). *The Black Swan. The Impact of the highly improbable*. Random House Trade Paperbacks, 2 edition.
- Taleb, N. N. (2015). *Silent Risk*, volume 1.
- Taleb, N. N., Cirillo, P., Douady, R., Fontanari, A., Geman, H., Geman, D., and Haug, E. (2019). *The Statistical Consequences of Fat Tails (Technical Incerto Collection)*.
- Thompson, E. L. and Smith, L. A. (2019). Escape from model-land.
- Tol, R. S. J. (2003). Is the uncertainty about climate change too large for expected cost-benefit analysis? *Climatic change*, 56(3):265–289.
- Traeger, C. P. (2014). A 4-Stated DICE: Quantitatively Addressing Uncertainty Effects in Climate Change. *Environmental and Resource Economics*, 59(1):1–37.
- Trindade, B., Reed, P., Herman, J., Zeff, H., and Characklis, G. (2017). Reducing regional drought vulnerabilities and multi-city robustness conflicts using many-objective optimization under deep uncertainty. *Advances in Water Resources*, 104:195–209.
- UN (1992). United nations conference on environment and development: Rio declaration on environment and development. *International Legal Materials*, 31(4):874–880.
- uncertainty. (n.d.). uncertainty — meaning in the cambridge english dictionary.
- United Nations (2018). World ‘Nearing Critical Point of No Return’ on Climate Change, Delegate Warns, as Second Committee Debates Sustainable Development.
- United Nations (2019). Business leaders urged to set more ambitious climate targets in effort to limit global temperature rise to 1.5c.
- Vautard, R., van Aalst, M., Stott, P., Boucher, O., Vogel, M. M., Seneviratne, S. I., Otto, F., Haustein, K., van Oldenborgh, G. J., Soubeyroux, J.-M., Schneider, M., Drouin, A., Ribes, A., and Kreienkamp, F. (2019). Human contribution to the record-breaking July 2019 heat wave in Western Europe. Technical Report July.
- Wagner, G. and Weitzman, M. L. (2018). Potentially large equilibrium climate sensitivity tail uncertainty. *Economics Letters*, 168:144–146.
- Walker, W. E., Lempert, R. J., and Kwakkel, J. H. (2013). Deep uncertainty. *Encyclopedia of operations research and management science*, pages 395–402.

- Walker, W. E., Rahman, S. A., and Cave, J. (2001). Adaptive policies, policy analysis, and policy-making. *European Journal of Operational Research*, 128(2):282–289.
- Ward, V. L., Singh, R., Reed, P. M., and Keller, K. (2015). Confronting tipping points: Can multi-objective evolutionary algorithms discover pollution control tradeoffs given environmental thresholds? *Environmental Modelling and Software*, 73:27–43.
- Watson, A. A. and Kasprzyk, J. R. (2017). Incorporating deeply uncertain factors into the many objective search process. *Environmental Modelling & Software*, 89:159–171.
- Weitzman, M. L. (2009a). ON MODELING AND INTERPRETING THE ECONOMICS OF CATASTROPHIC CLIMATE CHANGE. *The Review of Economics and Statistics*, 91(February):1–19.
- Weitzman, M. L. (2009b). Reactions to the Nordhaus critique. *Harward University, Cambridge, {MA}*, 91:1–19.
- Weitzman, M. L. (2011). Fat-tailed uncertainty in the economics of catastrophic climate change. *Review of Environmental Economics and Policy*, 5(2):275–292.
- Weitzman, M. L. (2013). Tail-Hedge Discounting and the Social Cost of Carbon. *Journal of Economic Literature*, 51(3):873–882.
- Weyant, J. (2014). Integrated assessment of climate change: state of the literature. *Journal of Benefit-Cost Analysis*, 5(03):377–409.
- Weyant, J. (2017). Some Contributions of Integrated Assessment Models of Global Climate Change. *Review of Environmental Economics and Policy*, 11(1):115–137.
- Woodruff, M. and Herman, J. (2013). Nondominated sorting for multi-objective problems.
- Zhang, T., Ramakrishnan, R., and Livny, M. (1996). Birch: an efficient data clustering method for very large databases. In *ACM Sigmod Record*, volume 25, pages 103–114. ACM.
- Zhang, X. Y., Trame, M. N., Lesko, L. J., and Schmidt, S. (2015). Sobol sensitivity analysis: A tool to guide the development and evaluation of systems pharmacology models.

# **Appendices**

# A | VERIFICATION

In the following, values for the the Figures 4.2 and 4.3 from the verification section 4.2 is given in the following tables A.1 and A.2. Note that, the jupyter notebook file “*PyDICE\_V4\_Validation\_Part1.ipynb*” and “*PyDICE\_V4\_Validation\_Part2.ipynb*” in the folder “*1\_Model*” of the author’s GitHub repository offers the reader the possibility to not only verify these outcomes but also to test other parameters.

**Table A.1:** Comparison of the PyDICE and the DICE on the parameters emission control rate, per period utility, emission, atmospheric temperature, damage and total output with the optimized outcome of Nordhaus optimal policy for the parameter control rate  $t$  and savings rate  $sr_t$

	Emission Control Rate		Per Period Utility		Emission		Atmospheric Temperature		Damage		Total Output	
	DICE	PyDICE	DICE	PyDICE	DICE	PyDICE	DICE	PyDICE	DICE	PyDICE	DICE	PyDICE
2010	0.039	0.039	1976.827	1976.827	36.853	36.853	0.800	0.800	0.109	0.109	63.473	63.473
2015	0.195	0.195	2279.402	2279.402	34.544	34.544	0.925	0.925	0.174	0.174	75.679	75.679
2020	0.218	0.218	2526.326	2526.326	36.937	36.937	1.055	1.055	0.266	0.266	89.319	89.319
2025	0.243	0.243	2718.121	2718.121	39.236	39.236	1.187	1.187	0.395	0.395	104.388	104.388
2030	0.269	0.269	2858.021	2858.021	41.352	41.352	1.323	1.323	0.568	0.568	120.891	120.891
2035	0.297	0.297	2950.785	2950.785	43.210	43.210	1.460	1.460	0.796	0.796	138.829	138.829
2040	0.327	0.327	3001.913	3001.913	44.744	44.744	1.600	1.600	1.091	1.091	158.200	158.200
2045	0.357	0.357	3017.112	3017.112	45.898	45.898	1.740	1.740	1.463	1.463	178.998	178.998
2050	0.390	0.390	3001.953	3001.953	46.625	46.625	1.881	1.881	1.924	1.924	201.215	201.215
2055	0.423	0.423	2961.670	2961.670	46.884	46.884	2.021	2.021	2.487	2.487	224.840	224.840
2060	0.459	0.459	2901.032	2901.032	46.646	46.646	2.159	2.159	3.161	3.161	249.859	249.859
2065	0.495	0.495	2824.295	2824.295	45.884	45.884	2.295	2.295	3.956	3.956	276.258	276.258
2070	0.533	0.533	2735.186	2735.186	44.581	44.581	2.427	2.427	4.880	4.880	304.021	304.021
2075	0.573	0.573	2636.923	2636.923	42.726	42.726	2.554	2.554	5.937	5.937	333.134	333.134
2080	0.614	0.614	2532.244	2532.244	40.312	40.312	2.675	2.675	7.129	7.129	363.580	363.580
2085	0.656	0.656	2423.447	2423.447	37.341	37.341	2.791	2.791	8.454	8.454	395.347	395.347
2090	0.699	0.699	2312.445	2312.445	33.817	33.817	2.898	2.898	9.907	9.907	428.421	428.421
2095	0.744	0.744	2200.803	2200.803	29.752	29.752	2.998	2.998	11.476	11.476	462.794	462.794
2100	0.790	0.790	2089.794	2089.794	25.162	25.162	3.088	3.088	13.146	13.146	498.455	498.455
2105	0.837	0.837	1980.438	1980.438	20.065	20.065	3.165	3.165	14.873	14.873	535.415	535.415
2110	0.886	0.886	1873.538	1873.538	14.487	14.487	3.230	3.230	16.627	16.627	573.673	573.673
2115	0.935	0.935	1769.715	1769.715	8.462	8.462	3.281	3.281	18.370	18.370	613.211	613.211
2120	0.985	0.985	1669.444	1669.444	2.034	2.034	3.317	3.317	20.061	20.061	653.991	653.991
2125	1.000	1.000	1573.092	1573.092	0.019	0.019	3.338	3.338	21.650	21.650	696.861	696.861
2130	1.000	1.000	1480.763	1480.763	0.016	0.016	3.346	3.346	23.137	23.137	741.696	741.696
2135	1.000	1.000	1392.475	1392.475	0.012	0.012	3.344	3.344	24.535	24.535	788.201	788.201
2140	1.000	1.000	1308.224	1308.224	0.010	0.010	3.334	3.334	25.853	25.853	836.315	836.315
2145	1.000	1.000	1227.976	1227.976	0.008	0.008	3.318	3.318	27.104	27.104	886.034	886.034
2150	1.000	1.000	1151.654	1151.654	0.006	0.006	3.298	3.298	28.304	28.304	937.436	937.436
2155	1.200	1.200	1079.284	1079.284	-29.196	-29.196	3.275	3.275	29.471	29.471	985.015	985.015
2160	1.200	1.200	1010.989	1010.989	-29.402	-29.402	3.231	3.231	30.159	30.159	1037.616	1037.616
2165	1.200	1.200	946.561	946.561	-29.583	-29.583	3.170	3.170	30.484	30.484	1092.049	1092.049
2170	1.200	1.200	885.821	885.821	-29.736	-29.736	3.094	3.094	30.478	30.478	1148.126	1148.126
2175	1.200	1.200	828.599	828.599	-29.858	-29.858	3.008	3.008	30.178	30.178	1205.678	1205.678
2180	1.200	1.200	774.735	774.735	-29.948	-29.948	2.913	2.913	29.619	29.619	1264.550	1264.550
2185	1.200	1.200	724.071	724.071	-30.007	-30.007	2.812	2.812	28.836	28.836	1324.597	1324.597
2190	1.200	1.200	676.455	676.455	-30.034	-30.034	2.705	2.705	27.865	27.865	1385.682	1385.682
2195	1.200	1.200	631.737	631.737	-30.029	-30.029	2.595	2.595	26.736	26.736	1447.674	1447.674
2200	1.200	1.200	589.772	589.772	-29.993	-29.993	2.483	2.483	25.480	25.480	1510.448	1510.448
2205	1.200	1.200	550.416	550.416	-29.927	-29.927	2.369	2.369	24.124	24.124	1573.886	1573.886
2210	1.200	1.200	513.531	513.531	-29.831	-29.831	2.255	2.255	22.693	22.693	1637.872	1637.872
2215	1.200	1.200	478.982	478.982	-29.707	-29.707	2.140	2.140	21.210	21.210	1702.297	1702.297
2220	1.200	1.200	446.641	446.641	-29.557	-29.557	2.026	2.026	19.694	19.694	1767.051	1767.051
2225	1.200	1.200	416.382	416.382	-29.380	-29.380	1.912	1.912	18.164	18.164	1832.027	1832.027
2230	1.200	1.200	388.085	388.085	-29.178	-29.178	1.800	1.800	16.636	16.636	1897.108	1897.108
2235	1.200	1.200	361.637	361.637	-28.952	-28.952	1.689	1.689	15.124	15.124	1962.161	1962.161
2240	1.200	1.200	336.929	336.929	-28.702	-28.702	1.579	1.579	13.640	13.640	2027.019	2027.019
2245	1.200	1.200	313.858	313.858	-28.427	-28.427	1.470	1.470	12.196	12.196	2091.447	2091.447
2250	1.200	1.200	292.330	292.330	-28.127	-28.127	1.364	1.364	10.801	10.801	2155.082	2155.082
2255	1.200	1.200	272.258	272.258	-27.795	-27.795	1.259	1.259	9.462	9.462	2217.319	2217.319
2260	1.200	1.200	252.906	252.906	-27.425	-27.425	1.156	1.156	8.187	8.187	2277.111	2277.111
2265	1.200	1.200	235.580	235.580	-27.268	-27.268	1.055	1.055	7.051	7.051	2355.909	2355.909
2270	1.200	1.200	219.364	219.364	-27.042	-27.042	0.956	0.956	5.967	5.967	2430.433	2430.433
2275	1.183	1.183	204.211	204.211	-24.528	-24.528	0.859	0.859	4.948	4.948	2502.005	2502.005
2280	1.057	1.057	190.073	190.073	-7.594	-7.594	0.766	0.766	4.040	4.040	2572.593	2572.593
2285	0.910	0.910	176.880	176.880	11.742	11.742	0.700	0.700	3.460	3.460	2640.916	2640.916
2290	0.741	0.741	164.573	164.573	33.335	33.335	0.679	0.679	3.341	3.341	2706.961	2706.961
2295	0.549	0.549	153.097	153.097	57.264	57.264	0.717	0.717	3.814	3.814	2770.668	2770.668
2300	0.328	0.328	142.399	142.399	83.998	83.998	0.820	0.820	5.098	5.098	2831.871	2831.871
2305	0.000	0.000	132.428	132.428	122.903	122.903	0.989	0.989	7.570	7.570	2890.270	2890.270

**Table A.2:** Comparison of the PyDICE and the DICE on the parameters emission control rate, per period utility, emission, atmospheric temperature, damage and total output with the integrated functions (4.1) and (4.2) for emission control rate 4.2 and savings rate 4.2

	Emission Control Rate		Per Period Utility		Emission		Atmospheric Temperature		Damage		Total Output	
	DICE	PyDICE	DICE	PyDICE	DICE	PyDICE	DICE	PyDICE	DICE	PyDICE	DICE	PyDICE
2010	0.039	0.030	1976.827	2015.481	36.853	36.853	0.800	0.800	0.109	0.109	63.473	63.473
2015	0.195	0.071	2279.402	2290.805	34.544	38.898	0.925	0.925	0.174	0.173	75.679	75.273
2020	0.218	0.113	2526.326	2523.872	36.937	40.965	1.055	1.058	0.266	0.266	89.319	88.660
2025	0.243	0.154	2718.121	2709.637	39.236	42.933	1.187	1.196	0.395	0.398	104.388	103.625
2030	0.269	0.196	2858.021	2847.792	41.352	44.701	1.323	1.339	0.568	0.578	120.891	120.157
2035	0.297	0.237	2950.785	2940.970	43.210	46.189	1.460	1.484	0.796	0.819	138.829	138.234
2040	0.327	0.278	3001.913	2993.455	44.744	47.332	1.600	1.631	1.091	1.131	158.200	157.836
2045	0.357	0.320	3017.112	3010.292	45.898	48.084	1.740	1.779	1.463	1.527	178.998	178.937
2050	0.390	0.361	3001.953	2996.727	46.625	48.410	1.881	1.926	1.924	2.020	201.215	201.510
2055	0.423	0.402	2961.670	2957.847	46.884	48.288	2.021	2.071	2.487	2.621	224.840	225.529
2060	0.459	0.444	2901.032	2898.380	46.646	47.703	2.159	2.214	3.161	3.339	249.859	250.966
2065	0.495	0.485	2824.295	2822.588	45.884	46.651	2.295	2.353	3.956	4.185	276.258	277.795
2070	0.533	0.527	2735.186	2734.227	44.581	45.134	2.427	2.487	4.880	5.164	304.021	305.990
2075	0.573	0.568	2636.923	2636.547	42.726	43.160	2.554	2.616	5.937	6.280	333.134	335.528
2080	0.614	0.609	2532.244	2532.317	40.312	40.742	2.675	2.739	7.129	7.534	363.580	366.388
2085	0.656	0.651	2423.447	2423.865	37.341	37.895	2.791	2.854	8.454	8.923	395.347	398.551
2090	0.699	0.692	2312.445	2313.121	33.817	34.640	2.898	2.962	9.907	10.442	428.421	432.001
2095	0.744	0.733	2200.803	2201.665	29.752	30.999	2.998	3.061	11.476	12.080	462.794	466.728
2100	0.790	0.775	2089.794	2090.775	25.162	26.996	3.088	3.152	13.146	13.822	498.455	502.723
2105	0.837	0.816	1980.438	1981.487	20.065	22.657	3.165	3.230	14.873	15.628	535.415	540.005
2110	0.886	0.858	1873.538	1874.590	14.487	18.008	3.230	3.297	16.627	17.471	573.673	578.580
2115	0.935	0.899	1769.715	1770.686	8.462	13.077	3.281	3.350	18.370	19.321	613.211	618.457
2120	0.985	0.940	1669.444	1670.221	2.034	7.890	3.317	3.391	20.061	21.147	653.991	659.648
2125	1.000	0.982	1573.092	1573.513	0.019	2.475	3.338	3.420	21.650	22.911	696.861	702.167
2130	1.000	1.023	1480.763	1480.775	0.016	-3.141	3.346	3.434	23.137	24.575	741.696	746.031
2135	1.000	1.064	1392.475	1392.132	0.012	-8.933	3.344	3.435	24.535	26.096	788.201	791.259
2140	1.000	1.106	1308.224	1307.642	0.010	-14.874	3.334	3.422	25.853	27.430	836.315	837.871
2145	1.000	1.147	1227.976	1227.307	0.008	-20.939	3.318	3.394	27.104	28.529	886.034	885.889
2150	1.000	1.189	1151.654	1151.085	0.006	-27.104	3.298	3.351	28.304	29.345	937.436	935.337
2155	1.200	1.200	1079.284	1079.083	-29.196	-28.995	3.275	3.291	29.471	29.828	985.015	987.257
2160	1.200	1.200	1010.989	1011.043	-29.402	-29.218	3.231	3.217	30.159	29.991	1037.616	1041.155
2165	1.200	1.200	946.561	946.761	-29.583	-29.408	3.170	3.132	30.484	29.866	1092.049	1096.590
2170	1.200	1.200	885.821	886.098	-29.736	-29.565	3.094	3.038	30.478	29.485	1148.126	1153.435
2175	1.200	1.200	828.599	828.908	-29.858	-29.688	3.008	2.937	30.178	28.881	1205.678	1211.563
2180	1.200	1.200	774.735	775.049	-29.948	-29.777	2.913	2.832	29.619	28.083	1264.550	1270.852
2185	1.200	1.200	724.071	724.373	-30.007	-29.833	2.812	2.722	28.836	27.121	1324.597	1331.181
2190	1.200	1.200	676.455	676.736	-30.034	-29.856	2.705	2.610	27.865	26.022	1385.682	1392.434
2195	1.200	1.200	631.737	631.992	-30.029	-29.847	2.595	2.496	26.736	24.812	1447.674	1454.499
2200	1.200	1.200	589.772	589.998	-29.993	-29.806	2.483	2.382	25.480	23.514	1510.448	1517.268
2205	1.200	1.200	550.416	550.615	-29.927	-29.735	2.369	2.267	24.124	22.148	1573.886	1580.637
2210	1.200	1.200	513.531	513.703	-29.831	-29.636	2.255	2.152	22.693	20.736	1637.872	1644.506
2215	1.200	1.200	478.982	479.130	-29.707	-29.508	2.140	2.039	21.210	19.293	1702.297	1708.779
2220	1.200	1.200	446.641	446.765	-29.557	-29.354	2.026	1.926	19.694	17.836	1767.051	1773.366
2225	1.200	1.200	416.382	416.485	-29.380	-29.174	1.912	1.814	18.164	16.380	1832.027	1838.178
2230	1.200	1.200	388.085	388.167	-29.178	-28.971	1.800	1.703	16.636	14.936	1897.108	1903.133
2235	1.200	1.200	361.637	361.697	-28.952	-28.745	1.689	1.595	15.124	13.516	1962.161	1968.149
2240	1.200	1.200	336.929	336.966	-28.702	-28.499	1.579	1.487	13.640	12.132	2027.019	2033.152
2245	1.200	1.200	313.858	313.866	-28.427	-28.232	1.470	1.382	12.196	10.791	2091.447	2098.069
2250	1.200	1.200	292.330	292.299	-28.127	-27.948	1.364	1.278	10.801	9.503	2155.082	2162.831
2255	1.200	1.200	272.258	272.170	-27.795	-27.646	1.259	1.175	9.462	8.275	2217.319	2227.372
2260	1.200	1.200	252.906	253.069	-27.425	-27.329	1.156	1.075	8.187	7.114	2277.111	2291.630
2265	1.200	1.200	235.580	235.688	-27.268	-27.127	1.055	0.976	7.051	6.055	2355.909	2366.724
2270	1.200	1.200	219.364	219.436	-27.042	-26.869	0.956	0.879	5.967	5.055	2430.433	2438.556
2275	1.183	1.200	204.211	204.257	-24.528	-26.572	0.859	0.783	4.948	4.125	2502.005	2507.881
2280	1.057	1.200	190.073	190.092	-7.594	-26.245	0.766	0.689	4.040	3.276	2572.593	2575.228
2285	0.910	1.200	176.880	176.880	11.742	-25.894	0.700	0.596	3.460	2.514	2640.916	2640.960
2290	0.741	1.200	164.573	164.564	33.335	-25.526	0.679	0.505	3.341	1.845	2706.961	2705.331
2295	0.549	1.200	153.097	153.086	57.264	-25.144	0.717	0.415	3.814	1.274	2770.668	2768.511
2300	0.328	1.200	142.399	142.394	83.998	-24.752	0.820	0.326	5.098	0.805	2831.871	2830.614
2305	0.000	1.200	132.428	132.434	122.903	-24.352	0.989	0.239	7.570	0.442	2890.270	2891.714

# B | OPEN EXPLORATION

In this appendix, the results of the open exploration analysis under Nordhaus Optimal Policy is given for the time points 2050, 2100, 2150, 2200 and 2300 in the Figures 4.2, Figures 4.2 and 4.3. These figures expand the shown results from the section 9.1 is given in the following tables A.1 and A.2. Note that, the corresponding Jupyter notebook file “*Statistical Analysis\_NordhausOpt\_V4Util2300.ipynb*” can be found in the folder “*3\_Nordhaus\_Optimal\_Policy\_Exploration*” of the author’s GitHub repository.

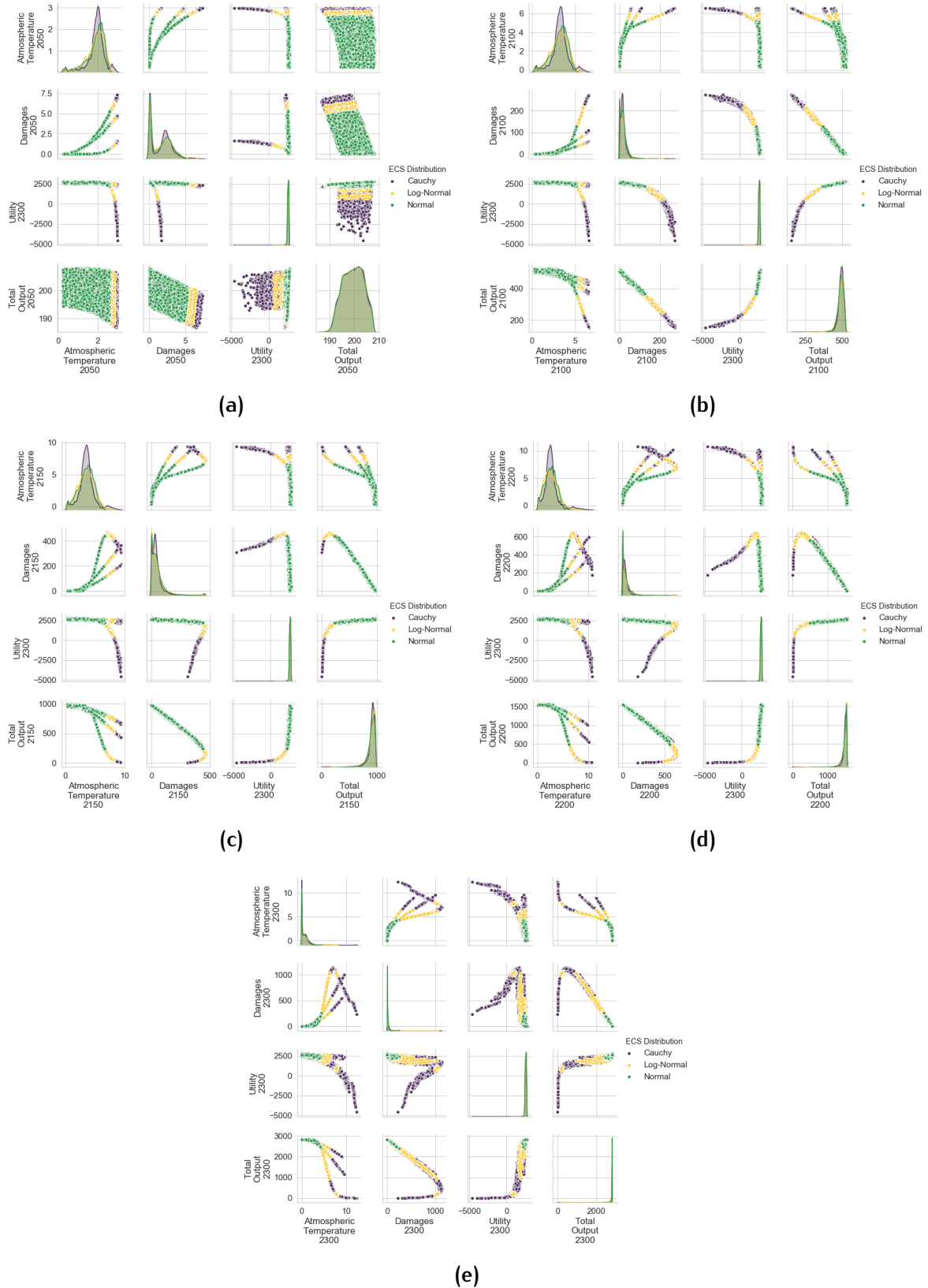


**Figure B.1:** For the years 2050(a), 2100(b), 2150(c), 2200(d) and 2300(e), pair plot over the outcome variable is presented with the third dimension describing ECS distribution types.

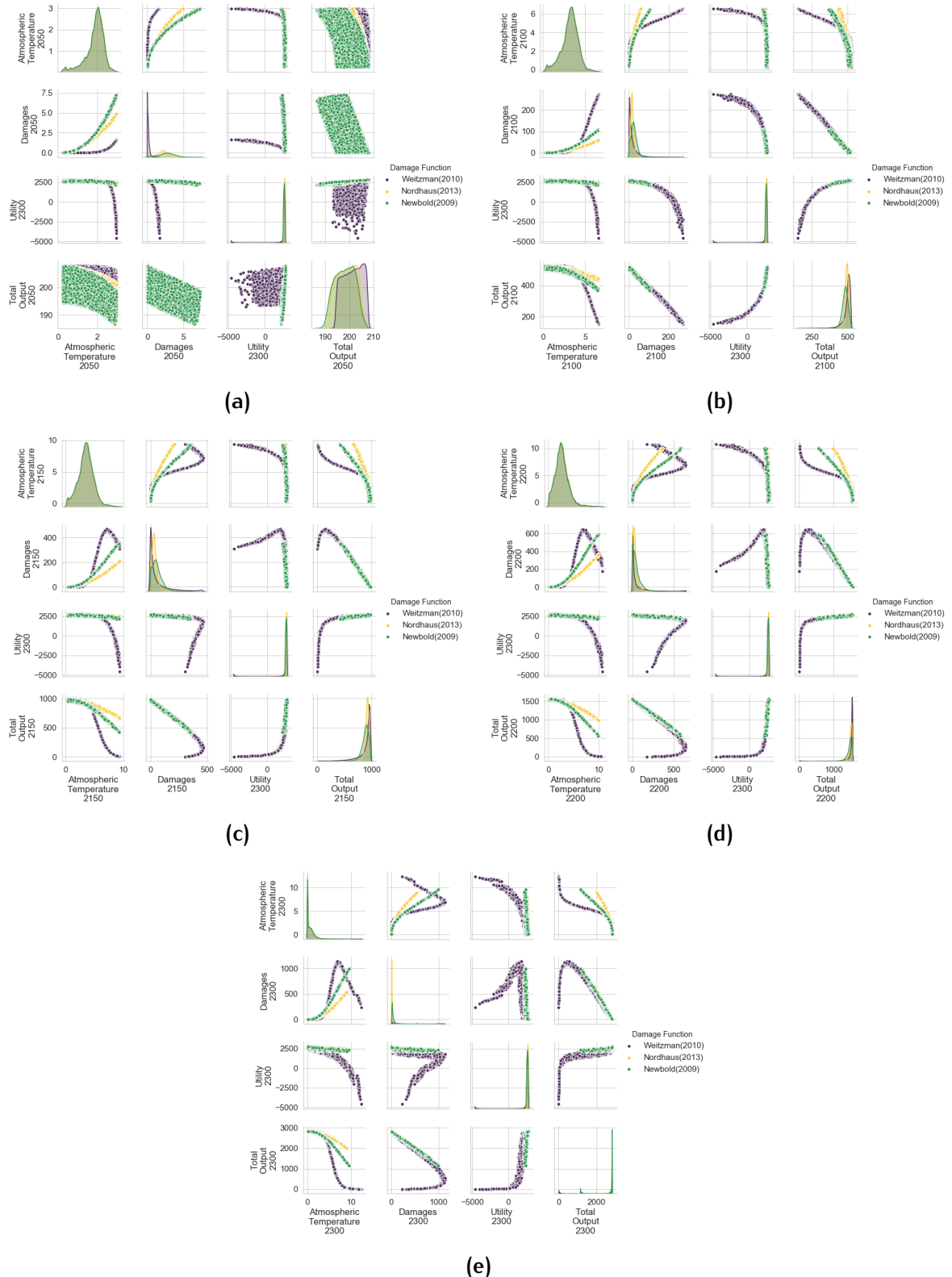


**Figure B.2:** For the years 2050(a), 2100(b), 2150(c), 2200(d) and 2300(e), pair plot over the outcome variable is presented with the third dimension describing the damage functions.

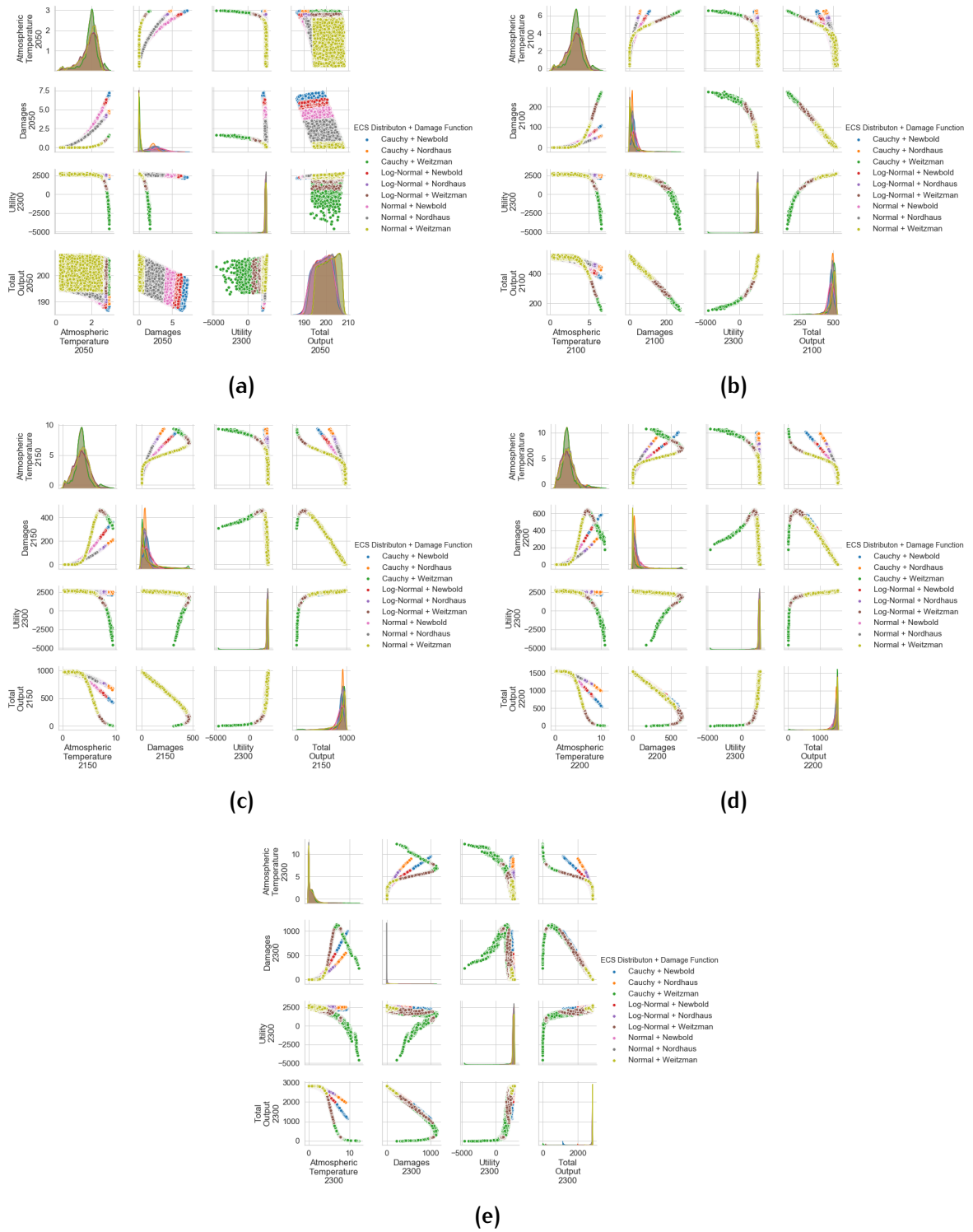


**Figure B.3:** For the years 2050(a), 2100(b), 2150(c), 2200(d) and 2300(e), pair plot over the outcome variable is presented with the third dimension describing the combination of damage function and ECS distribution

# C | GLOBAL SENSITIVITY ANALYSIS

As an extension to the outcomes from the global sensitivity analysis (GSA) in Section 8.2, this appendix presents the confidence intervals in barplots in the Figures C.1, C.2, C.3 and C.4. Furthermore, a GSA was also conducted over the identified policy levers of the study to verify their effectiveness on the outcomes of interest. To that end, the Figures C.5 illustrate clearly the sensitivity of the outcomes to the policy levers. Note that, the corresponding Jupyter notebook file “*Open\_Exploration\_SA\_V4.ipynb*” can be found in the folder “*2\_Open\_Exploration*” of the author’s GitHub repository.

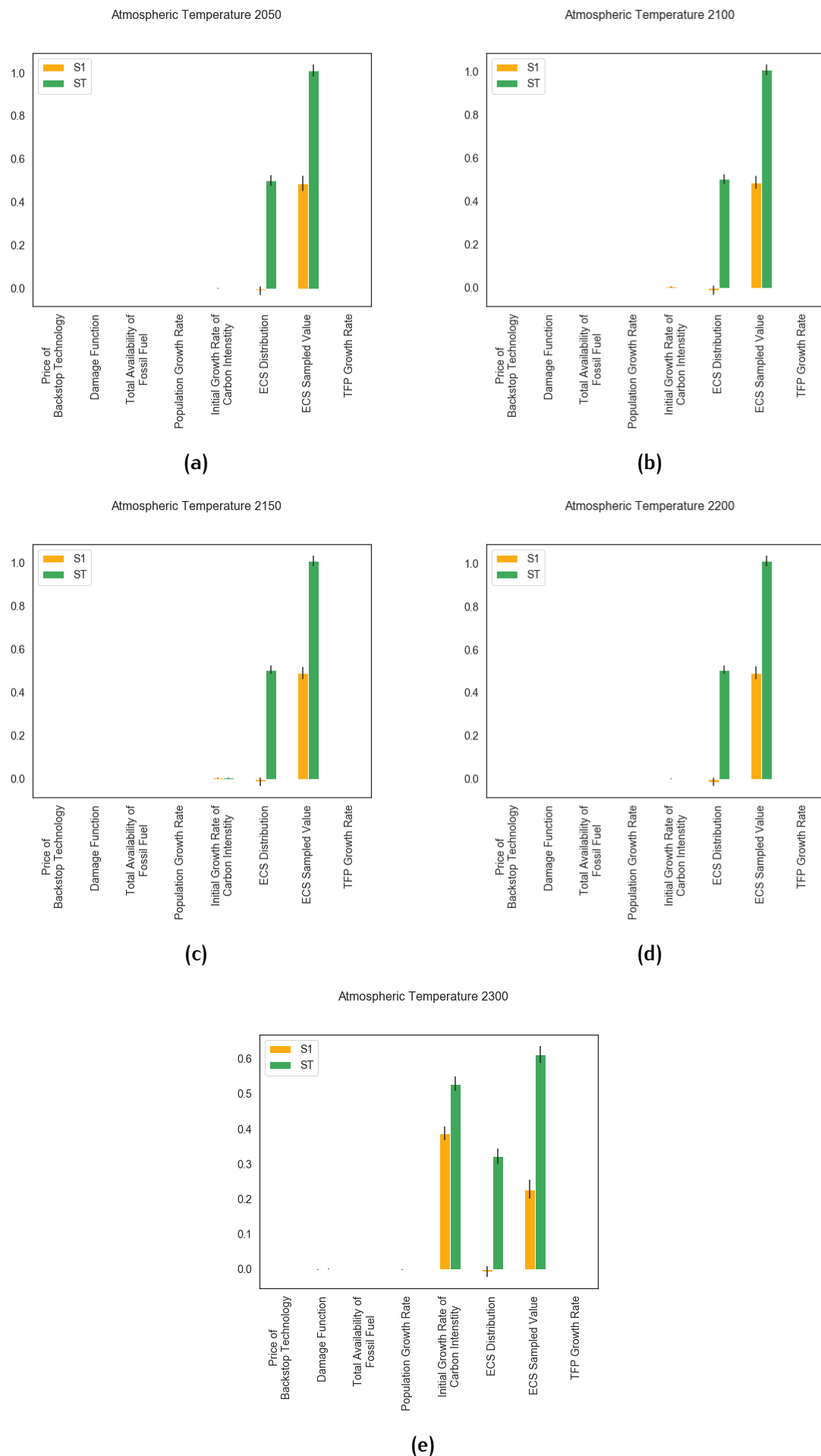


**Figure C.1:** Results of the global sensitivity analysis of the uncertainties on the outcome atmospheric temperature at the time points 2050(a), 2100(b), 2150(c), 2200(d) and 2300(e) (with confidence intervals).

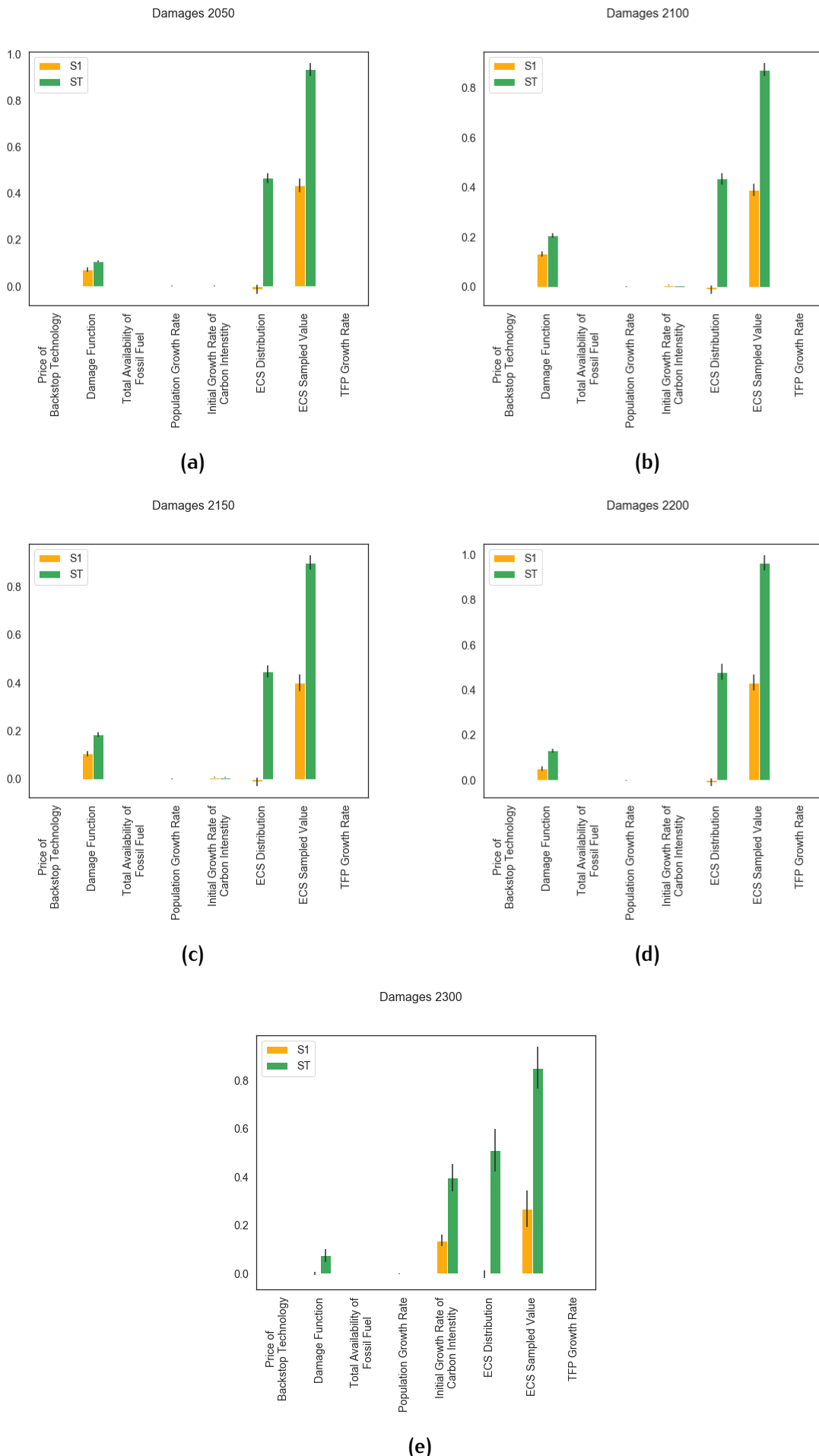


**Figure C.2:** Results of the global sensitivity analysis with confidence intervals of the uncertainties on the the outcome damage at the time points 2050(a), 2100(b), 2150(c), 2200(d) and 2300(e) (with confidence intervals).

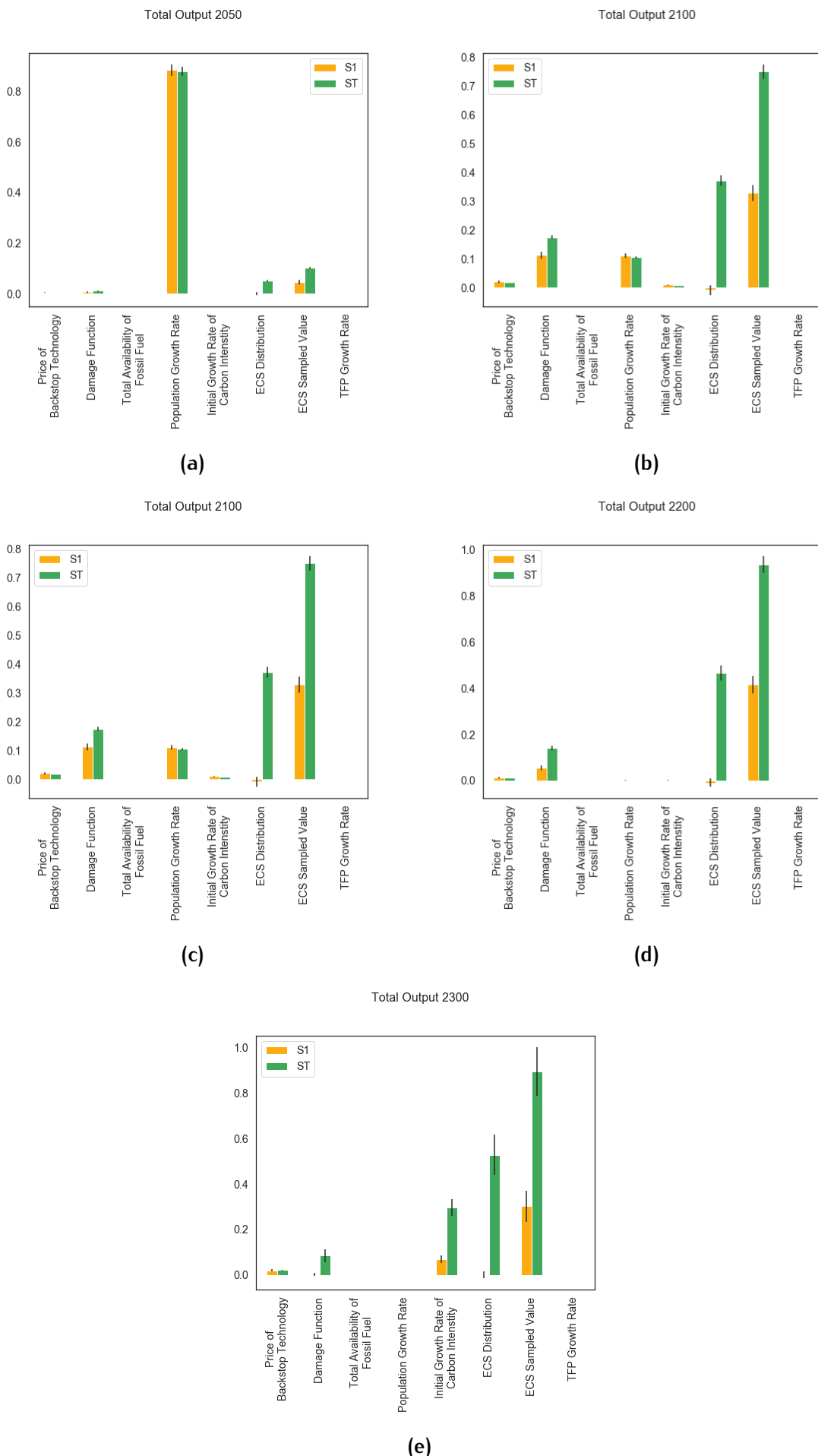


**Figure C.3:** Results of the global sensitivity analysis of the uncertainties on the the total output at the time points 2050(a), 2100(b), 2150(c), 2200(d) and 2300(e) (with confidence intervals).

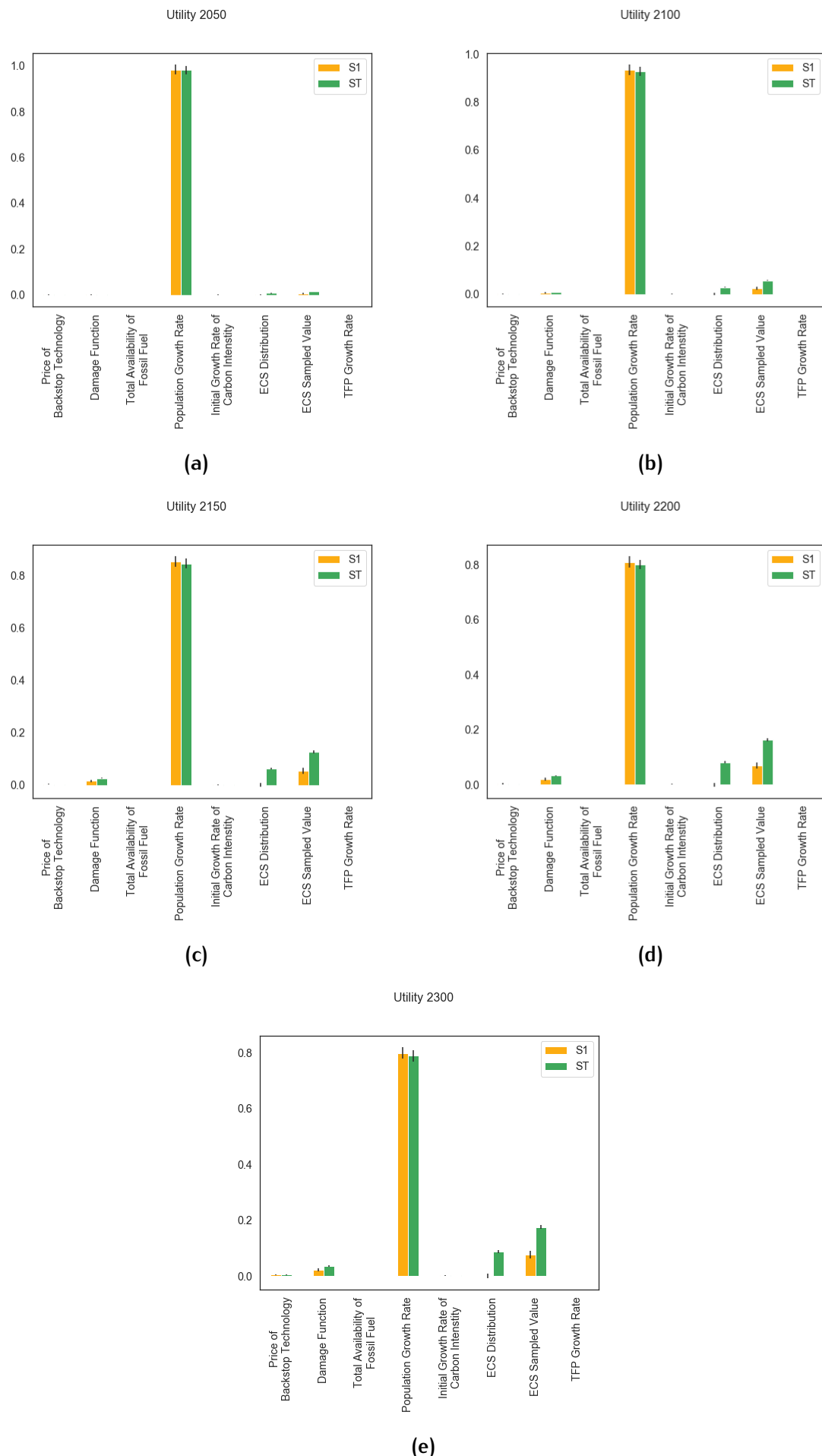
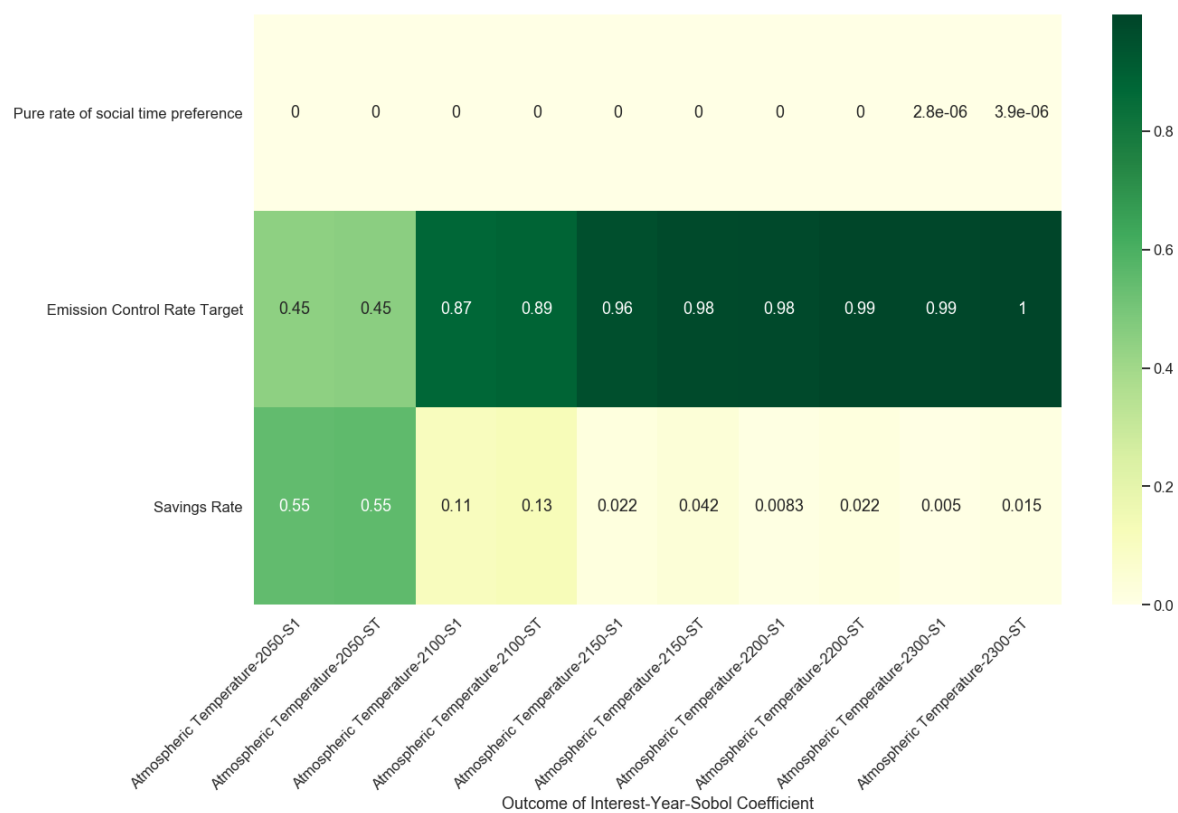
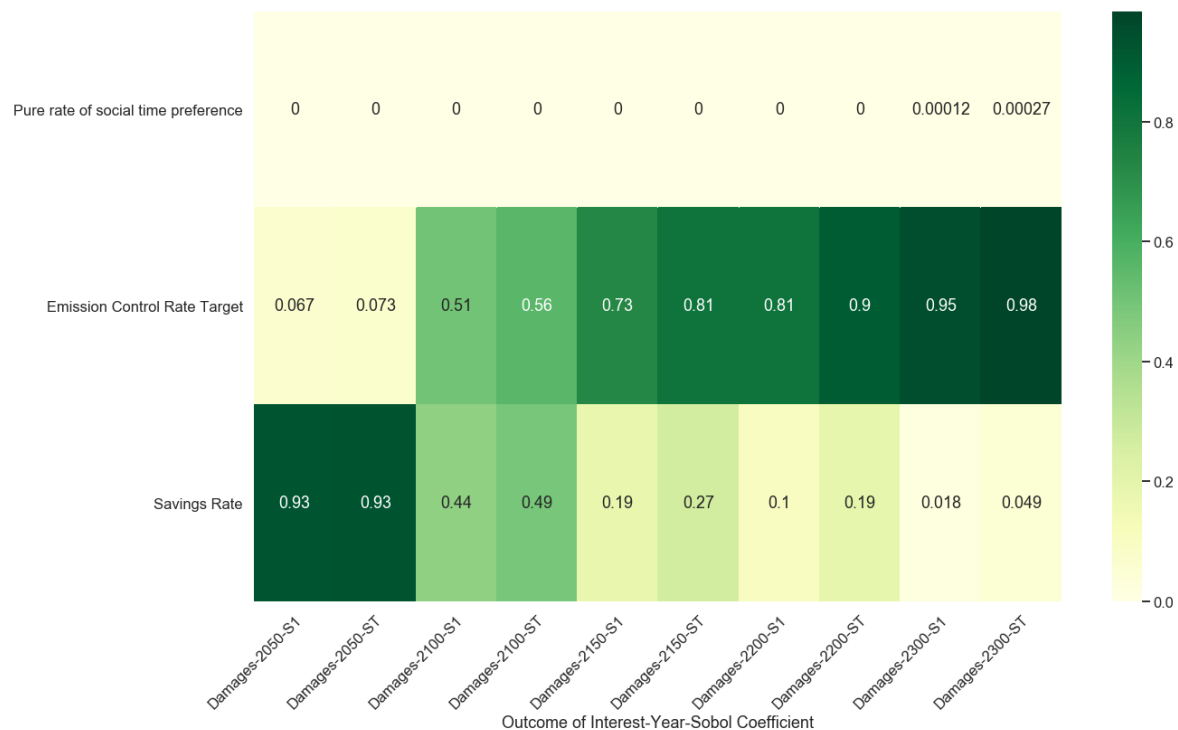


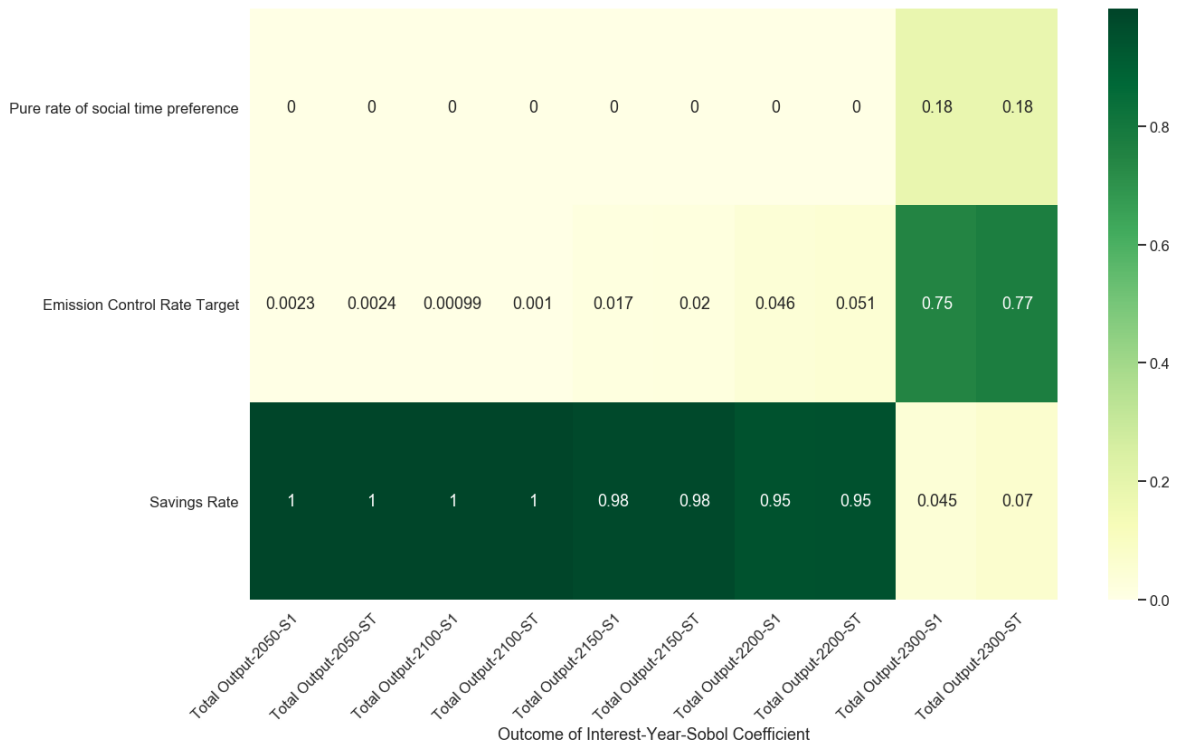
**Figure C.4:** Results of the global sensitivity analysis of the uncertainties on the outcome utility at the time points 2050(a), 2100(b), 2150(c), 2200(d) and 2300(e) (with confidence intervals).



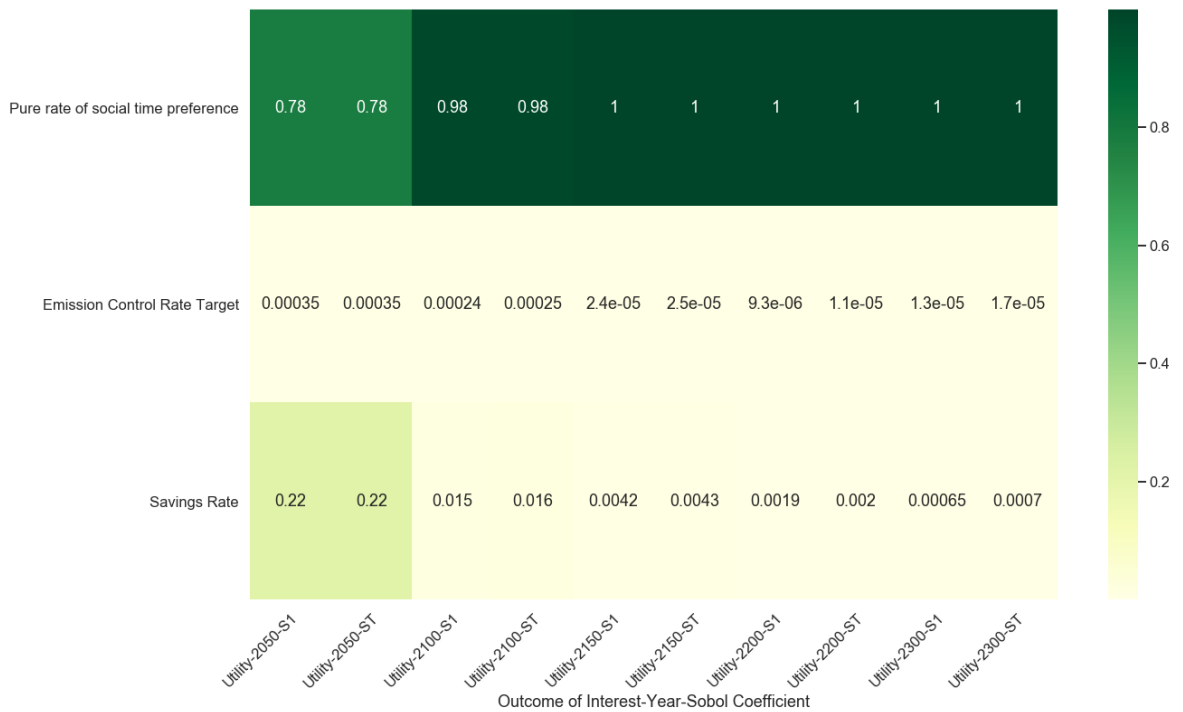
(a)



(b)



(c)



(d)

**Figure C.5:** Results of the global sensitivity analysis of the levers on the outcomes atmospheric temperature(a), damages(b), total output(c), and utility(d).

# D | STATISTICAL ANALYSIS

The descriptive statistics of the simulation outcomes are used for the statistical analysis in Section 5.2. These statistics are illustrated in the following tables. Note that, the corresponding Jupyter notebook file “*Statistical Analysis\_NordhausOpt\_V4Util2300.ipynb*” and the resulting .xlsx files can be found in the folder “*3\_Nordhaus\_Optimal Policy Exploration*” of the author’s GitHub repository.

**Table D.1:** Descriptive statistics of the simulation outcomes for the three ECS distribution functions at the time points 2050, 2100, 2150, 2200 and 2300.

Atmospheric Temperature	2050			2100			2150			2200			2300		
	Cauchy	Log-Normal	Normal	Cauchy	Log-Normal	Normal	Cauchy	Log-Normal	Normal	Cauchy	Log-Normal	Normal	Cauchy	Log-Normal	Normal
count	180000	180000	180000	180000	180000	180000	180000	180000	180000	180000	180000	180000	180000	180000	180000
mean	1.92975	1.89324	1.8926	3.2569	3.1895	3.1827	3.5984	3.5177	3.49906	2.7365	2.6663	2.63206	0.7325	0.6597	0.610419
std	0.41804	0.45679	0.455	0.9365	1.0021	0.9643	1.3256	1.3631	1.27772	1.4079	1.334	1.2063	1.2017	0.8387	0.720694
min	0.2741	0.24113	0.2382	0.3413	0.2673	0.2688	0.2767	0.2115	0.21066	0.1034	0.0795	0.07717	0	0	0
1%	0.39246	0.46667	0.3581	0.5147	0.6008	0.4595	0.4185	0.4985	0.37437	0.2217	0.2465	0.17744	0	0	0
5%	1.10614	0.98932	0.9468	1.5344	1.3667	1.2873	1.3997	1.2256	1.1439	0.7822	0.6795	0.62761	0	0	0
10%	1.48942	1.26871	1.2745	2.2125	1.8223	1.8244	2.1548	1.7086	1.71227	1.3321	1.0072	1.00229	0	0	0
25%	1.79811	1.65132	1.7058	2.8517	2.5392	2.6432	2.95	2.5502	2.68149	2.0034	1.6575	1.76753	0	0	0
50%	1.98392	1.98321	2.0046	3.2859	3.2887	3.3408	3.542	3.5453	3.61961	2.5608	2.5572	2.63357	0.3813	0.3576	0.357717
75%	2.13867	2.22459	2.2074	3.6898	3.9234	3.8793	4.1301	4.488	4.41964	3.1512	3.544	3.46262	0.9863	1.0414	1.019543
90%	2.33049	2.39073	2.3476	4.2359	4.4151	4.2838	4.9869	5.2826	5.06573	4.0936	4.4671	4.2033	1.6112	1.8006	1.65244
95%	2.50834	2.47719	2.4104	4.8187	4.6793	4.4825	5.9753	5.735	5.39669	5.2839	5.0472	4.58642	2.5681	2.3451	2.052726
99%	2.81369	2.60741	2.5307	5.8433	5.1059	4.8616	7.9232	6.4996	6.05747	8.1642	6.0906	5.46534	6.4697	3.5698	2.900045
max	2.98367	2.82987	2.6072	6.5833	5.9962	5.1839	9.3963	8.1927	6.60979	10.764	8.5502	6.16606	12.308	8.0012	4.350704

a)

Damages	2050			2100			2150			2200			2300		
	Cauchy	Log-Normal	Normal	Cauchy	Log-Normal	Normal	Cauchy	Log-Normal	Normal	Cauchy	Log-Normal	Normal	Cauchy	Log-Normal	Normal
count	180000	180000	180000	180000	180000	180000	180000	180000	180000	180000	180000	180000	180000	180000	180000
mean	1.64817	1.60585	1.6012	20.223	19.538	18.655	55.565	57.923	54.4231	48.335	48.595	42.2282	21.188	8.078	5.132073
std	1.3523	1.36576	1.3315	24.125	18.32	15.242	71.17	70.552	59.8092	90.866	78.812	57.6834	109.87	35.588	13.41431
min	0.00157	0.00157	0.0016	0.0041	0.0041	0.0041	0.0078	0.0078	0.00783	0.0125	0.0079	0.00732	0	0	0
1%	0.00178	0.00181	0.0017	0.0072	0.0077	0.0055	0.0101	0.0105	0.00911	0.0127	0.0127	0.01263	0	0	0
5%	0.03069	0.01024	0.0134	0.7154	0.3151	0.2586	1.0748	0.4324	0.33056	0.1455	0.0406	0.04225	0	0	0
10%	0.06244	0.04030	0.0466	2.57	1.3536	1.46	5.2327	2.3576	2.51322	0.7819	0.3295	0.38168	0	0	0
25%	0.159	0.19963	0.1946	8.4475	6.5805	7.0896	19.615	13.263	14.9606	6.5518	4.8996	5.38688	0.0226	0.0228	0.018099
50%	0.86228	1.56987	1.6724	15.6	15.671	16.336	36.76	36.827	39.2128	23.857	23.316	25.2307	0.0338	0.0379	0.034952
75%	2.56794	2.67174	2.6683	23.982	26.756	26.026	61.362	73.128	70.7529	46.156	60.102	56.4644	3.9894	3.8006	3.533641
90%	3.24425	3.45822	3.3813	36.488	41.461	38.329	112.26	132.22	118.048	93.212	119.09	101.968	15.924	19.039	15.74728
95%	3.81684	3.97273	3.8265	49.983	52.382	46.245	183.61	194.9	167.826	189.79	176.61	136.468	48.476	37.855	27.92289
99%	5.59431	4.81535	4.5128	151.7	88.688	69.981	436.23	376.37	315.923	560.42	424.16	294.435	703.19	114.05	65.37813
max	7.33978	6.47731	5.3402	273.14	216.72	126.32	468.87	466.1	444.593	649.15	647.52	563.107	1141	1068.5	251.347

b)

Total Output	2050			2100			2150			2200			2300		
	Cauchy	Log-Normal	Normal	Cauchy	Log-Normal	Normal	Cauchy	Log-Normal	Normal	Cauchy	Log-Normal	Normal	Cauchy	Log-Normal	Normal
count	180000	180000	180000	180000	180000	180000	180000	180000	180000	180000	180000	180000	180000	180000	180000
mean	199.473	199.500	199.510	490.065	490.993	492.113	889.012	887.854	893.639	1465.089	1469.873	1481.067	287.612	2817.060	2822.531
std	4.089	4.099	4.078	31.492	24.092	20.485	122.813	108.333	89.602	190.623	135.515	97.737	257.165	69.800	21.799
min	186.700	187.905	188.818	152.023	245.425	362.964	6.395	51.611	236.364	0.594	42.688	491.871	0.691	155.991	2410.910
1%	191.121	191.100	191.222	326.517	406.608	429.797	155.335	390.578	500.097	202.338	809.981	1043.597	1276.100	2645.463	2727.050
5%	192.735	192.737	192.780	450.254	447.914	455.285	706.764	689.074	729.741	1251.212	1264.189	1328.632	2749.430	2769.456	2786.721
10%	193.918	193.966	193.995	467.280	461.719	465.592	810.246	781.149	801.471	1400.402	1360.765	1387.215	2806.346	2799.662	2805.921
25%	196.254	196.271	196.288	483.416	480.051	480.932	882.921	866.556	869.614	1475.444	1454.049	1459.202	2821.761	2820.860	2821.346
50%	199.589	199.613	199.616	495.556	495.336	494.835	918.966	918.600	916.018	151.839	150.906	150.285	2828.049	2828.026	2828.130
75%	202.729	202.737	202.728	506.015	507.478	506.827	945.340	952.453	950.263	1536.035	1539.193	1537.945	2832.856	2832.908	2832.901
90%	204.830	204.970	204.939	514.575	516.077	515.757	969.498	968.773	954.670	1551.433	1550.965	1550.899	2835.937	2835.923	2835.923
95%	206.008	206.078	206.088	518.865	520.108	519.908	973.455	976.143	976.143	1555.317	1556.528	1556.195	2837.140	2837.157	2837.150
99%	207.258	207.255	207.271	524.544	525.329	525.248	984.562	986.167	985.924	1562.283	1563.025	1562.876	2838.751	2838.710	2838.724
max	208.080	208.057	208.081	530.728	530.623	530.637	995.340	995.410	995.298	1568.753	1569.133	1568.996	2840.356	2840.359	2840.404

d)

Utility	2050			2100			2150			2200			2300		
	Cauchy	Log-Normal	Normal	Cauchy	Log-Normal	Normal	Cauchy	Log-Normal	Normal	Cauchy	Log-Normal	Normal	Cauchy	Log-Normal	Normal
count	180000	180000	180000	180000	180000	180000	180000	180000	180000	180000	180000	180000	180000	180000	180000
mean	-1873.19	-1873.22	-1873.19	203.23	205.83	204.42	1447.12	1451.45	1454.20	2103.20	2112.63	2117.05	2598.82	2612.43	2617.41
std	26.66	26.69	26.64	63.18											

**Table D.2:** Descriptive statistics of the simulation outcomes for the three damage function at the time points 2050, 2100, 2150, 2200 and 2300.

a)

Atmospheric Temperature	2050			2100			2150			2200			2300		
	Newbold	Nordhaus	Weitzman	Newbold	Nordhaus	Weitzman	Newbold	Nordhaus	Weitzman	Newbold	Nordhaus	Weitzman	Newbold	Nordhaus	Weitzman
count	180000	180000	180000	180000	180000	180000	180000	180000	180000	180000	180000	180000	180000	180000	180000
mean	1.90534	1.90627	1.90397	3.20825	3.21144	3.20937	3.53578	3.54111	3.53828	2.67562	2.66979	2.68941	0.65765	0.63397	0.71101
std	0.44421	0.44326	0.44446	0.96822	0.96692	0.97067	1.32226	1.32180	1.32580	1.30822	1.29684	1.35243	0.88153	0.83747	1.09225
min	0.23882	0.23904	0.23819	0.26882	0.26755	0.26735	0.21066	0.21085	0.21069	0.07717	0.07860	0.07837	0.00000	0.00000	0.00000
1%	0.39023	0.39038	0.39076	0.50782	0.50813	0.41389	0.41412	0.41519	0.21302	0.21204	0.21583	0.00000	0.00000	0.00000	0.00000
5%	0.99182	0.99529	0.99003	1.37179	1.37865	1.37221	1.22966	1.23747	1.23083	0.68320	0.68472	0.67881	0.00000	0.00000	0.00000
10%	1.31776	1.32447	1.31789	1.90744	1.91447	1.90760	1.80341	1.81154	1.80385	1.07142	1.07864	1.06988	0.00000	0.00000	0.00000
25%	1.73240	1.73459	1.73083	2.70245	2.70661	2.70559	2.76176	2.75518	2.83779	1.84179	1.82908	0.00000	0.00000	0.00000	0.00000
50%	1.98842	1.99038	1.98842	3.30009	3.30338	3.30110	3.56089	3.56618	3.56379	2.58282	2.58222	2.57552	0.37052	0.35616	0.37006
75%	2.19291	2.19219	2.19078	3.83251	3.83174	3.83158	4.34629	4.34717	4.34680	3.39272	3.38038	3.39371	1.01785	0.99417	1.02681
90%	2.36196	2.36187	2.36240	4.31810	4.32168	4.32750	5.12177	5.12969	5.13803	4.27819	4.25781	4.33437	1.68467	1.64070	1.74971
95%	2.45881	2.45762	2.45822	4.62134	4.61880	4.62951	5.63346	5.63453	5.64682	4.87984	4.85585	4.98762	2.22143	2.14352	2.41068
99%	2.70223	2.69973	2.70263	5.43323	5.42709	5.44000	7.12053	7.11161	7.11831	6.91464	6.84474	7.20987	4.01737	3.74149	5.80506
max	2.98052	2.98055	2.98367	6.56163	6.55669	6.58333	9.39625	9.39433	9.38267	10.10580	9.99771	10.76359	9.53758	9.00260	12.30763

b)

Damages	2050			2100			2150			2200			2300		
	Newbold	Nordhaus	Weitzman												
count	180000	180000	180000	180000	180000	180000	180000	180000	180000	180000	180000	180000	180000	180000	180000
mean	2.643611	2.059272	0.1523024	24.77103	15.4501	18.19892	61.17608	36.76224	69.97162	56.6641	35.87445	46.61952	12.13699	8.229242	14.031745
std	1.187323	0.798419	0.164916	14.97982	12.82275	14.54719	46.64678	25.00176	101.15878	63.32359	34.68337	109.91383	46.61691	23.7828	104.43551
min	0.014769	0.029959	0.0015726	0.051299	0.097876	0.0040902	0.05404	0.116328	0.0078303	0.007322	0.025626	0.0124761	0	0	0.0228005
1%	0.05054	0.082359	0.0016296	0.247445	0.359813	0.0042517	0.284534	0.452249	0.0079923	0.088568	0.187532	0.0125811	0	0	0.0228301
5%	0.493543	0.532827	0.0025833	2.821896	2.643363	0.0265755	4.080417	4.029341	0.0282865	1.533399	1.955087	0.0131714	0	0	0.0228426
10%	0.98811	0.942332	0.008231	6.267537	5.0771	2.110154	10.35119	8.61454	2.769754	4.60886	4.847199	0.0250819	0	0	0.0228506
25%	1.922979	1.613604	0.0431902	14.51418	10.1048	2.1596894	28.75861	19.91807	46.739906	17.11356	14.06487	4.4800517	0	0	0.0228667
50%	2.694719	2.129209	0.1077029	23.36441	15.03229	8.2561848	52.603	33.0328	27.057412	38.82791	27.54083	4.6992744	0.622558	0.961075	0.0228948
75%	3.413122	2.981999	0.2052835	33.13751	20.15708	21.830696	83.06926	48.74178	88.966399	73.90703	46.90463	29.337064	7.384544	7.475952	0.0409114
90%	4.087495	2.998133	0.3417347	43.66072	25.58038	46.702576	119.3757	67.34752	215.43236	125.6966	73.77226	134.41934	25.19829	20.30608	0.6518115
95%	4.507473	3.248283	0.4460568	50.8625	29.13745	69.141596	146.0801	80.74336	313.12711	168.1173	95.29441	281.4589	49.13462	34.56261	5.4760749
99%	5.649987	3.904091	0.8397971	72.54853	39.98076	154.65205	231.8984	126.1014	444.18787	339.5153	183.3688	592.27604	196.9713	103.9237	699.12854
max	7.339783	4.902693	1.6687806	109.3166	58.55355	273.14285	362.8986	212.4013	468.7441	594.0709	364.9125	649.15107	1002.064	550.5662	1141.0282

c)

Total Output	2050			2100			2150			2200			2300		
	Newbold	Nordhaus	Weitzman												
count	180000	180000	180000	180000	180000	180000	180000	180000	180000	180000	180000	180000	180000	180000	180000
mean	198.2153	198.0909	201.3583	483.3655	495.7258	494.0796	883.9671	919.9979	866.5397	1460.677	1494.915	1460.436	2810.86	2817.848	2798.495
std	3.961643	3.84271	3.773522	20.83766	12.63695	36.19274	68.5937	36.99993	165.2439	99.43865	52.95858	225.6299	75.00073	36.69937	254.9953
min	186.6999	189.0498	193.0337	367.8198	427.1435	152.0226	418.4615	653.6987	6.394505	542.8274	979.223	0.594409	1144.312	1990.781	0.690613
1%	190.327	191.594	194.579	419.794	461.8046	323.7319	633.7914	793.6954	148.5893	1021.553	1275.486	193.242	2515.103	2667.838	1209.276
5%	191.813	192.6998	195.254	447.4518	474.4917	431.6551	760.2303	855.3913	1229.4	148.133	1404.138	1061.691	2751.921	2777.683	2815.605
10%	192.7886	193.5868	195.9921	457.1275	479.7475	458.7497	799.4616	874.6754	658.773	1354.448	1436.906	1312.206	2790.24	2800.061	281.499
25%	195.0354	195.7185	198.1444	471.2534	487.6859	488.4913	851.8229	901.2262	844.2983	1433.191	1476.923	1492.503	2817.784	2818.606	2826.992
50%	198.3345	199.0597	201.5233	484.9988	496.1938	504.3856	896.1836	924.9021	933.9604	1487.32	1506.659	1535.849	2825.938	2825.818	281.505
75%	201.4223	202.214	204.6637	497.7782	504.377	513.7505	931.6656	945.3005	963.324	1522.225	1528.375	1548.842	2831.323	2831.073	2834.987
90%	203.3885	203.9388	206.409	508.6924	511.5432	520.107	957.6182	961.5464	975.7118	1542.107	1543.147	1556.686	2834.808	2834.615	2837.179
95%	204.3344	204.7139	206.9929	514.3413	515.7998	522.9335	967.9497	969.6018	981.2475	1549.731	1549.831	1560.211	2836.257	2836.062	2838.097
99%	206.0292	206.0709	207.5551	521.9887	522.2887	526.7498	981.0617	981.1777	988.5211	1559.22	1558.867	1564.672	2838.028	2837.828	2839.254
max	207.9937	207.9762	208.0809	530.3263	530.2752	530.7276	995.0875	994.4371	995.4101	1568.995	1568.081	1569.133	2840.383	2840.032	2840.404

d)

Utility	2050		
---------	------	--	--

**Table D.3:** Descriptive statistics of the outcome atmospheric temperature for the nine different combinations between the three damage functions and the three ECS distribution functions at the time points 2050, 2100, 2150, 2200 and 2300.

Atmospheric Temperature		2050								
		Newbold & Cauchy	Newbold & Log-Normal	Newbold & Normal	Nordhaus & Cauchy	Nordhaus & Log-Normal	Nordhaus & Normal	Weitzman & Cauchy	Weitzman & Log-Normal	Weitzman & Normal
a)	mean	1.929079	1.894939	1.892074	1.928452	1.893715	1.896595	1.931705	1.891056	1.889099
	std	0.418742	0.455945	0.455876	0.418166	0.4579	0.451904	0.417215	0.456554	0.457206
	min	0.274595	0.241445	0.238821	0.274266	0.241125	0.239045	0.274103	0.241614	0.238191
	1%	0.392184	0.476039	0.355207	0.391994	0.414499	0.358108	0.392886	0.466125	0.360105
	5%	1.104977	0.993122	0.912659	1.103853	0.986604	0.962242	1.107511	0.987745	0.908423
	10%	1.486861	1.266806	1.273266	1.488366	1.26974	1.282878	1.49237	1.270153	1.264175
	25%	1.797444	1.652813	1.704772	1.7973	1.651402	1.714327	1.799835	1.649323	1.696793
	50%	1.983093	1.9847	2.004213	1.982491	1.985491	2.008181	1.985927	1.979284	2.001805
	75%	2.138404	2.226608	2.207511	2.13761	2.225222	2.208518	2.13975	2.22164	2.206101
	90%	2.327963	2.392867	2.346591	2.329645	2.390322	2.348341	2.333309	2.388904	2.348257
	95%	2.50657	2.47861	2.410302	2.505982	2.477626	2.410021	2.512695	2.475174	2.411
	99%	2.813636	2.606925	2.528814	2.812798	2.607798	2.531498	2.814379	2.607652	2.532732
	max	2.98052	2.828546	2.607188	2.980354	2.829866	2.60378	2.983667	2.822254	2.605145
b)			2100							
	Newbold & Cauchy	Newbold & Log-Normal	Newbold & Normal	Nordhaus & Cauchy	Nordhaus & Log-Normal	Nordhaus & Normal	Weitzman & Cauchy	Weitzman & Log-Normal	Weitzman & Normal	
	mean	3.253677	3.191401	3.179803	3.253312	3.190671	3.190279	3.263784	3.186334	3.177881
	std	0.956466	1.001124	0.964179	0.935823	1.003467	0.959113	0.9373	1.001837	0.969527
	min	0.342208	0.268824	0.269525	0.341266	0.267547	0.268872	0.34158	0.267347	0.269057
	1%	0.514317	0.621142	0.453601	0.5142	0.549598	0.460055	0.515424	0.600704	0.46473
	5%	1.533204	1.372821	1.274176	1.532295	1.362749	1.322754	1.537713	1.364241	1.268605
	10%	2.206903	1.818003	1.821467	2.210469	1.821764	1.839011	2.219733	1.827511	1.811198
	25%	2.849721	2.542627	2.640591	2.848054	2.540649	2.658581	2.858179	2.534751	2.631002
	50%	3.282307	3.290058	3.338904	3.282563	3.293301	3.347239	3.293292	3.281858	3.334603
	75%	3.68731	3.926281	3.877937	3.687119	3.924188	3.880725	3.695044	3.919123	3.87925
	90%	4.226339	4.419719	4.276052	4.233352	4.412859	4.285501	4.247487	4.412191	4.289344
	95%	4.802163	4.678409	4.478212	4.811322	4.677276	4.482233	4.830677	4.681643	4.487695
	99%	5.842277	5.096981	4.853474	5.833082	5.109232	4.859097	5.857453	5.107838	4.873113
	max	6.561633	5.982816	5.18388	6.556691	5.996206	5.176558	6.583334	5.943997	5.177188
c)			2150							
	Newbold & Cauchy	Newbold & Log-Normal	Newbold & Normal	Nordhaus & Cauchy	Nordhaus & Log-Normal	Nordhaus & Normal	Weitzman & Cauchy	Weitzman & Log-Normal	Weitzman & Normal	
	mean	3.593399	3.519678	3.494417	3.593887	3.520257	3.509144	3.60795	3.513162	3.493561
	std	1.324903	1.362415	1.275911	1.324842	1.364948	1.272727	1.327009	1.361858	1.284496
	min	0.277349	0.212254	0.210656	0.276743	0.211466	0.210846	0.276879	0.211519	0.210689
	1%	0.418421	0.516163	0.36958	0.417958	0.447557	0.375392	0.419537	0.498822	0.377301
	5%	1.399437	1.23214	1.131899	1.398164	1.221468	1.183138	1.403752	1.223778	1.123456
	10%	2.148487	1.70401	1.708842	2.152666	1.708395	1.727167	2.162521	1.714427	1.697709
	25%	2.947281	2.553781	2.678168	2.94537	2.55141	2.699993	2.958462	2.545462	2.665918
	50%	3.535681	3.546873	3.616565	3.537924	3.552364	3.628765	3.552103	3.536303	3.610935
	75%	4.125477	4.492387	4.415833	4.126668	4.489847	4.422694	4.138756	4.481161	4.420398
	90%	4.972368	5.289864	5.053197	4.985874	5.281569	5.069716	5.005998	5.277117	5.075374
	95%	5.951187	5.733292	5.388504	5.968691	5.734282	5.397672	5.994515	5.737261	5.40368
	99%	7.923358	6.48703	6.041484	7.914167	6.511456	6.057474	7.928593	6.496358	6.068696
	max	9.39625	8.159805	6.609792	9.394326	8.19273	6.608827	9.382669	8.07035	6.592706
d)			2200							
	Newbold & Cauchy	Newbold & Log-Normal	Newbold & Normal	Nordhaus & Cauchy	Nordhaus & Log-Normal	Nordhaus & Normal	Weitzman & Cauchy	Weitzman & Log-Normal	Weitzman & Normal	
	mean	2.730297	2.667932	2.628726	2.719619	2.657551	2.632223	2.759599	2.673238	2.635223
	std	1.389907	1.326631	1.198928	1.374913	1.317099	1.190389	1.457159	1.357772	1.22933
	min	0.103518	0.079452	0.077173	0.103431	0.079724	0.078604	0.103768	0.081515	0.078374
	1%	0.220307	0.258332	0.176732	0.220536	0.240719	0.174907	0.223718	0.246122	0.18109
	5%	0.778406	0.686593	0.622762	0.781091	0.673238	0.643997	0.78655	0.678249	0.617057
	10%	1.326147	1.003677	1.003081	1.33171	1.011055	1.015059	1.337504	1.00631	0.990095
	25%	2.005482	1.665276	1.766125	2.00098	1.656819	1.786765	2.003422	1.65038	1.748691
	50%	2.561891	2.565446	2.634803	2.555405	2.564399	2.643303	2.565779	2.542669	2.623271
	75%	3.152423	3.549115	3.46393	3.139785	3.538698	3.455294	3.161513	3.544616	3.468248
	90%	4.07522	4.45855	4.189284	4.05843	4.434024	4.179906	4.147706	4.507966	4.245486
	95%	5.193364	5.033822	4.562284	5.184233	4.995944	4.539446	5.399549	5.12951	4.650159
	99%	8.055334	6.036702	5.38397	7.98233	6.009689	5.385828	8.474723	6.266986	5.585317
	max	10.1058	8.07604	5.866368	9.997711	7.98788	5.820427	10.76359	8.550198	6.166058
e)			2300							
	Newbold & Cauchy	Newbold & Log-Normal	Newbold & Normal	Nordhaus & Cauchy	Nordhaus & Log-Normal	Nordhaus & Normal	Weitzman & Cauchy	Weitzman & Log-Normal	Weitzman & Normal	
	mean	0.70892	0.654732	0.609371	0.677844	0.629452	0.594672	0.810589	0.694877	0.627293
	std	1.078922	0.811178	0.710842	1.00393	0.779903	0.695989	1.466245	0.917416	0.753772
	min	0	0	0	0	0	0	0	0	0
	1%	0	0	0	0	0	0	0	0	0
	5%	0	0	0	0	0	0	0	0	0
	10%	0	0	0	0	0	0	0	0	0
	25%	0	0	0	0	0	0	0	0	0
	50%	0.389681	0.362921	0.360811	0.374671	0.344487	0.350302	0.380458	0.366404	0.362748
	75%	0.989934	1.046083	1.025135	0.97356	1.01517	1.00141	0.995637	1.061429	1.032348
	90%	1.608216	1.791021	1.65343	1.567818	1.740024	1.610678	1.670235	1.879943	1.699931
	95%	2.514006	2.317521	2.039439	2.344394	2.21685	1.98587	3.008355	2.518149	2.141898
	99%	5.760246	3.371501	2.817184	5.257343	3.227899	2.750898	8.19638	4.069525	3.117309
	max	9.53758	6.437	3.941756	9.002604	6.249984	3.762772	12.30763	8.001211	4.350704

**Table D.4:** Descriptive statistics of the outcome damages for the nine different combinations between the three damage functions and the three ECS distribution functions at the time points 2050, 2100, 2150, 2200 and 2300.

Damages	2050								
	Newbold & Cauchy	Newbold & Log-Normal	Newbold & Normal	Nordhaus & Cauchy	Nordhaus & Log-Normal	Nordhaus & Normal	Weitzman & Cauchy	Weitzman & Log-Normal	Weitzman & Normal
mean	2.694376	2.624255	2.612349	2.093657	2.040551	2.043543	0.160218	0.152472	0.144191
std	1.160919	1.237598	1.159902	0.769568	0.834172	0.789241	0.202668	0.15402	0.128965
min	0.020938	0.01519	0.014769	0.039687	0.030415	0.029959	0.001574	0.001573	0.001573
1%	0.051411	0.081265	0.039917	0.083633	0.093693	0.068602	0.001626	0.001639	0.001623
5%	0.636826	0.494393	0.408437	0.646446	0.522214	0.497583	0.003601	0.002569	0.002191
10%	1.324228	0.898827	0.904138	1.190495	0.867792	0.881181	0.016949	0.006774	0.00661
25%	2.107499	1.718386	1.844202	1.73617	1.468293	1.572532	0.055718	0.031639	0.037949
50%	2.672371	2.680406	2.745773	2.111807	2.119133	2.169643	0.106709	0.10461	0.112749
75%	3.215823	3.54216	3.472292	2.45843	2.662848	2.622314	0.175969	0.226266	0.215953
90%	3.957924	4.223575	4.025487	2.925293	3.07578	2.966697	0.315166	0.36812	0.328359
95%	4.75749	4.596235	4.30733	3.414405	3.293556	3.133252	0.523538	0.467206	0.393172
99%	6.228281	5.18878	4.824433	4.240441	3.651552	3.45689	1.104291	0.660303	0.544809
max	7.339783	6.477312	5.34022	4.902693	4.426659	3.735153	1.668781	1.152675	0.67697

Damages	2100								
	Newbold & Cauchy	Newbold & Log-Normal	Newbold & Normal	Nordhaus & Cauchy	Nordhaus & Log-Normal	Nordhaus & Normal	Weitzman & Cauchy	Weitzman & Log-Normal	Weitzman & Normal
mean	25.29468	24.71824	24.30112	15.73718	15.36394	15.24913	19.65533	18.50031	16.43547
std	15.76979	15.31128	13.76836	8.396069	8.34483	7.596898	37.14184	25.6217	20.05329
min	0.093379	0.051299	0.051437	0.159976	0.097876	0.099468	0.004096	0.004092	0.00409
1%	0.255566	0.406593	0.186147	0.367139	0.421018	0.294041	0.004257	0.004297	0.004222
5%	3.68647	2.828336	2.351707	3.254002	2.582287	2.427079	0.052396	0.025768	0.017383
10%	8.909743	5.592049	5.58902	6.760256	6.411345	4.686022	0.577901	0.159081	0.150036
25%	16.4881	12.55135	13.73773	11.19334	8.924319	9.745168	3.155274	1.412175	1.810308
50%	23.05188	23.20337	24.03411	14.83854	14.93346	15.432	8.111614	7.94248	8.835964
75%	30.34913	35.05282	34.04702	18.6884	21.14442	20.6608	17.33771	25.2328	23.64944
90%	41.52817	45.98326	42.67995	24.53788	26.62575	25.13543	41.67463	52.3042	44.19804
95%	55.48868	52.38847	47.44274	31.58622	29.90714	27.49548	87.48815	73.64672	57.94999
99%	84.9315	63.4875	56.80581	46.09343	35.50657	32.24367	203.5754	116.5016	91.28725
max	109.3166	90.55562	66.91524	58.55355	49.41257	37.0103	273.1428	216.7164	126.3173

Damages	2150								
	Newbold & Cauchy	Newbold & Log-Normal	Newbold & Normal	Nordhaus & Cauchy	Nordhaus & Log-Normal	Nordhaus & Normal	Weitzman & Cauchy	Weitzman & Log-Normal	Weitzman & Normal
mean	62.64839	61.42478	59.45617	37.67261	36.68647	35.92881	66.39449	75.54772	67.97002
std	51.93978	46.67156	40.58829	27.86894	24.89224	21.85636	105.9469	106.5312	89.84147
min	0.10633	0.055134	0.054044	0.200524	0.117311	0.116328	0.007832	0.007834	0.00783
1%	0.291443	0.489276	0.214829	0.45935	0.527428	0.371147	0.007995	0.008029	0.007971
5%	5.59824	4.104921	3.334716	5.139209	9.392768	3.674893	0.057209	0.027577	0.018892
10%	15.80345	9.027138	9.077967	12.14119	7.669322	7.839295	0.922786	0.198553	0.186185
25%	33.72564	23.95946	26.82259	22.62542	17.03343	19.04651	7.525625	2.74755	3.748553
50%	51.73303	52.13222	54.52226	32.49638	32.72737	34.18753	25.19787	24.46493	27.99687
75%	73.81357	89.43338	86.07851	44.01488	51.94427	50.41482	66.28932	106.1048	98.1093
90%	111.8359	128.0428	115.8713	63.66977	71.25934	65.78017	190.8508	242.3472	203.5735
95%	163.4895	151.6819	133.0288	90.08577	83.57148	74.32856	365.5312	329.6373	266.6708
99%	280.015	194.3918	168.8426	154.0737	106.5936	92.79415	456.5706	431.8456	383.0288
max	362.8986	293.7781	203.3488	212.4013	165.4203	110.6047	468.8744	466.0989	444.5926

Damages	2200								
	Newbold & Cauchy	Newbold & Log-Normal	Newbold & Normal	Nordhaus & Cauchy	Nordhaus & Log-Normal	Nordhaus & Normal	Weitzman & Cauchy	Weitzman & Log-Normal	Weitzman & Normal
mean	59.54801	57.2953	53.15058	37.58038	35.88909	34.15715	47.91315	52.52042	39.40378
std	79.33841	58.83873	47.51367	43.20727	32.09306	26.57477	127.9047	113.7492	82.70343
min	0.015051	0.00786	0.007322	0.044597	0.026507	0.025626	0.012476	0.012477	0.012479
1%	0.096007	0.141731	0.055915	0.202749	0.242169	0.127543	0.012581	0.012588	0.012576
5%	2.117126	1.552941	1.222632	2.540489	1.889666	1.730099	0.014151	0.013169	0.012897
10%	7.741179	3.928496	3.922466	7.368728	4.25673	4.292793	0.068974	0.020876	0.020007
25%	21.15361	13.49703	15.55407	16.61103	11.39734	13.2468	0.876487	0.246161	0.35772
50%	38.066	38.2198	40.73923	26.95632	27.17282	28.84081	4.58097	4.320611	5.31672
75%	62.27323	82.12821	77.59797	40.56571	51.30061	48.93077	18.42374	38.87758	33.77002
90%	112.6985	137.8895	119.9058	67.27065	79.82208	71.14235	103.9392	168.0418	119.4373
95%	192.1839	180.0398	145.1422	108.2738	100.6573	83.61806	366.3144	319.4739	198.8663
99%	440.6078	262.5583	207.5292	244.7099	143.5453	116.3548	624.626	577.3042	441.8672
max	594.0709	439.3565	246.655	364.9125	244.6659	135.0985	649.1511	647.5193	563.1074

Damages	2300								
	Newbold & Cauchy	Newbold & Log-Normal	Newbold & Normal	Nordhaus & Cauchy	Nordhaus & Log-Normal	Nordhaus & Normal	Weitzman & Cauchy	Weitzman & Log-Normal	Weitzman & Normal
mean	18.21565	10.39767	7.813166	10.82743	7.546407	6.314072	34.50808	6.282156	1.259894
std	73.68247	27.42575	17.02437	35.92623	16.07584	11.66821	170.8009	52.69262	9.505423
min	0	0	0	0	0	0	0.022807	0.0228	0.022806
1%	0	0	0	0	0	0	0.02283	0.02283	0.02283
5%	0	0	0	0	0	0	0.022843	0.022843	0.022842
10%	0	0	0	0	0	0	0.022851	0.022851	0.02285
25%	0	0	0	0	0	0	0.022867	0.022867	0.022866
50%	0.704693	0.591386	0.583026	1.062798	0.898795	0.929591	0.022897	0.022894	0.022894
75%	6.900254	7.893334	7.514819	7.169649	7.795313	7.584932	0.03684	0.044385	0.040707
90%	22.51325	29.22271	24.07478	18.54938	22.84217	19.57171	0.482422	1.043986	0.540118
95%	66.01391	54.3044	40.04272	41.2634	36.94406	29.71186	23.91522	7.329457	2.481483
99%	430.1779	132.0459	86.78491	200.8637	77.66366	56.68643	104.0264	168.7007	30.35075
max	1002.064	539.8418	190.1589	550.5662	281.1875	105.2314	1141.028	1068.542	251.347

**Table D.5:** Descriptive statistics of the outcome total output for the nine different combinations between the three damage functions and the three ECS distribution functions at the time points 2050, 2100, 2150, 2200 and 2300.

Total Output	2050								
	Newbold & Cauchy	Newbold & Log-Normal	Newbold & Normal	Nordhaus & Cauchy	Nordhaus & Log-Normal	Nordhaus & Normal	Weitzman & Cauchy	Weitzman & Log-Normal	Weitzman & Normal
mean	198.1657	198.2252	198.2547	198.8987	198.9178	198.9134	201.3496	201.3579	201.3674
std	3.955018	3.981464	3.947826	3.841171	3.854259	3.832784	3.770034	3.77671	3.773863
min	186.6999	187.905	188.8175	189.0498	189.9591	190.09	193.0337	193.4327	193.8376
1%	190.1176	190.287	190.5176	191.5654	191.5582	191.6569	194.5784	194.5735	194.5883
5%	191.8299	191.7686	191.8395	192.6999	192.6785	192.7232	195.2528	195.2537	195.2564
10%	192.7583	192.781	192.839	193.5368	193.5804	193.593	195.9656	195.9989	196.007
25%	194.9866	195.0496	195.067	195.7116	195.7232	195.7202	198.1284	198.1429	198.158
50%	198.3045	198.3213	198.3787	199.0521	199.0595	199.0673	201.5273	201.5205	201.5233
75%	201.4162	201.4258	201.4262	202.1236	202.1501	202.1438	204.6362	204.6689	204.6858
90%	203.3287	203.4296	203.4113	203.9327	203.9639	203.9193	206.394	206.4094	206.423
95%	204.1544	204.4637	204.4136	204.6456	204.7925	204.7153	206.9838	206.9945	206.9981
99%	205.8288	206.0749	206.1227	205.9047	206.1227	206.128	207.5494	207.5521	207.5629
max	207.8694	207.9937	207.9797	207.9393	207.8325	207.9762	208.0799	208.0566	208.0809
Total Output	2100								
	Newbold & Cauchy	Newbold & Log-Normal	Newbold & Normal	Nordhaus & Cauchy	Nordhaus & Log-Normal	Nordhaus & Normal	Weitzman & Cauchy	Weitzman & Log-Normal	Weitzman & Normal
mean	482.6734	483.4136	484.0085	495.3942	495.8102	495.9729	492.1035	493.7959	496.3467
std	21.85307	21.22842	19.32714	12.93042	12.88672	12.06963	47.3452	32.16151	25.34647
min	367.8198	395.1323	422.4089	427.1435	445.3932	454.9027	152.0226	245.425	362.9641
1%	403.5001	430.7561	439.5585	453.9789	465.2912	469.0535	259.0967	372.5887	403.6685
5%	441.1008	445.6899	451.4796	471.9187	478.8486	476.2084	408.6489	426.4224	444.7838
10%	459.397	454.3832	458.5283	480.42	478.7643	480.2965	464.4879	451.6813	461.9178
25%	474.2583	469.0473	470.3017	488.7489	486.9277	487.4103	493.1119	484.9878	486.524
50%	485.3871	485.1203	484.3075	496.4518	496.1993	495.8086	504.9135	504.444	503.6854
75%	495.6639	499.7217	498.3692	503.7022	505.122	504.452	513.2874	514.2949	513.7438
90%	505.7827	509.8894	509.6708	510.133	512.49	511.9345	519.3188	520.6784	520.2615
95%	512.5094	514.8833	515.0478	514.3261	516.4117	516.2644	522.1709	523.4041	523.1236
99%	521.5175	521.9188	522.4019	522.0411	522.3682	522.4223	526.1406	527.1209	526.8895
max	529.4351	530.1085	530.3263	529.948	529.3322	530.2752	530.7276	530.6228	530.6375
Total Output	2150								
	Newbold & Cauchy	Newbold & Log-Normal	Newbold & Normal	Nordhaus & Cauchy	Nordhaus & Log-Normal	Nordhaus & Normal	Weitzman & Cauchy	Weitzman & Log-Normal	Weitzman & Normal
mean	881.6244	883.6439	886.6309	918.7284	920.0702	921.1933	866.6645	860.009	872.9638
std	76.82149	68.24308	59.5482	40.89321	36.82802	32.80101	190.2734	165.3357	135.1453
min	418.4615	527.5632	666.1378	653.6987	727.744	796.3557	6.394505	51.61054	236.3643
1%	560.0203	688.4527	726.5659	752.5268	818.9319	838.9385	65.294	265.4082	375.7106
5%	733.2025	752.5258	778.3254	841.774	851.751	863.0762	397.4804	474.9859	578.5743
10%	809.2879	787.1679	804.4587	879.4489	869.3825	876.7805	695.6585	616.3766	677.0674
25%	864.0826	842.949	847.6318	906.9012	897.2736	899.2084	875.6082	820.1284	830.7312
50%	897.4454	896.7891	893.6525	925.6483	925.0778	923.6005	934.8951	935.5088	930.6681
75%	924.5486	937.695	933.752	942.1782	948.1838	945.9751	960.7111	965.4669	963.7194
90%	950.8894	959.9311	959.6178	957.559	963.318	962.65451	973.4166	977.1296	976.2848
95%	964.3216	968.9052	969.4168	966.9115	970.63	970.5109	979.135	982.2969	981.6596
99%	980.3262	980.7879	982.0375	980.6231	981.3528	981.6625	987.327	989.2165	988.9268
max	993.9918	993.7174	995.0875	993.84	993.9777	994.4371	995.3395	995.4101	995.2961
Total Output	2200								
	Newbold & Cauchy	Newbold & Log-Normal	Newbold & Normal	Nordhaus & Cauchy	Nordhaus & Log-Normal	Nordhaus & Normal	Weitzman & Cauchy	Weitzman & Log-Normal	Weitzman & Normal
mean	1455.722	1459.93	1466.376	1492.341	1494.893	1497.506	1447.176	1454.938	1479.255
std	125.566	91.47325	74.075	65.51024	49.15325	41.14717	296.1841	208.1151	145.0191
min	542.8274	828.7457	1147.347	979.223	1167.428	1328.981	0.594409	42.68759	491.871
1%	849.7042	1144.818	1227.169	1180.515	1335.107	1374.171	50.78906	471.3039	776.7302
5%	1250.479	1272.141	1323.474	1381.643	1397.643	1420.487	865.9431	1000.085	1203.456
10%	1372.332	1335.341	1363.326	1445.135	1427.756	1440.188	1363.722	1255.846	1337.411
25%	1450.647	1420.297	1427.428	1485.47	1470.526	1473.717	1511.245	1476.559	1484.35
50%	1488.727	1488.21	1484.324	1507.579	1507.024	1505.019	1536.928	1535.866	1534.479
75%	1515.821	1527.16	1523.989	1525.037	1531.392	1529.069	1548.513	1549.39	1548.646
90%	1537.1	1544.026	1543.6451	1539.429	1544.842	1544.119	1556.091	1557.227	1556.715
95%	1546.833	1550.745	1550.772	1547.375	1550.863	1550.618	1559.659	1560.665	1560.339
99%	1558.57	1559.312	1559.877	1558.314	1559.032	1559.08	1564.122	1564.952	1564.795
max	1568.05	1567.575	1568.995	1568.01	1568.081	1568.008	1568.753	1569.133	1568.996
Total Output	2300								
	Newbold & Cauchy	Newbold & Log-Normal	Newbold & Normal	Nordhaus & Cauchy	Nordhaus & Log-Normal	Nordhaus & Normal	Weitzman & Cauchy	Weitzman & Log-Normal	Weitzman & Normal
mean	2801.084	2813.583	2817.888	2813.849	2818.834	2820.86	2747.956	2818.78	2828.859
std	118.9726	43.36497	26.74348	55.59126	24.65365	17.73688	422.5198	109.9838	18.21782
min	1144.312	1992.6	2544.563	1990.781	2413.064	2673.538	0.690613	155.9905	2410.91
1%	2144.69	2623.591	2695.145	2520.37	2713.113	2744.576	126.5197	2510.12	2765.433
5%	2722.612	2743.339	2767.288	2765.365	2773.789	2785.999	2774.708	2811.051	2818.94
10%	2795.415	2782.808	2792.642	2802.901	2795.665	2801.462	2821.064	2820.851	2822.352
25%	2819.136	2816.602	2817.27	2819.583	2817.747	2818.241	2827.111	2826.656	2827.213
50%	2825.969	2825.925	2825.906	2825.853	2825.831	2825.769	2831.636	2831.344	2831.53
75%	2831.149	2831.446	2831.378	2830.952	2831.215	2831.062	2835.078	2834.91	2834.97
90%	2834.663	2834.92	2834.846	2834.505	2834.698	2834.622	2837.264	2837.136	2837.15
95%	2836.101	2836.369	2836.292	2835.973	2836.135	2836.09	2838.171	2838.046	2838.059
99%	2837.841	2838.118	2838.13	2837.719	2837.894	2837.859	2839.277	2839.225	2839.257
max	2839.979	2839.872	2840.383	2840.005	2840.032	2839.971	2840.356	2840.359	2840.404

**Table D.6:** Descriptive statistics of the outcome utility for the nine different combinations between the three damage functions and the three ECS distribution functions at the time points 2050, 2100, 2150, 2200 and 2300.

Utility	2050								
	Newbold & Cauchy	Newbold & Log-Normal	Newbold & Normal	Nordhaus & Cauchy	Nordhaus & Log-Normal	Nordhaus & Normal	Weitzman & Cauchy	Weitzman & Log-Normal	Weitzman & Normal
mean	-1876.81	-1876.77	-1876.65	-1875.61	-1875.75	-1875.78	-1867.15	-1867.15	-1867.13
std	26.30706	26.34959	26.30799	26.35032	26.31514	26.24373	26.28227	26.33774	26.32449
min	-1932.96	-1930.41	-1928.65	-1928.68	-1926.77	-1926.84	-1915.52	-1915.34	-1915.22
1%	-1923.67	-1923.85	-1923.83	-1922.29	-1922.39	-1922.35	-1913.2	-1913.22	-1913.24
5%	-1918.76	-1918.48	-1918.49	-1917.74	-1917.53	-1917.48	-1909.18	-1909.17	-1909.22
10%	-1913.74	-1913.44	-1913.32	-1912.72	-1912.76	-1912.46	-1904.34	-1904.26	-1904.22
25%	-1899.19	-1899.31	-1899.11	-1898.09	-1898.29	-1898.34	-1889.79	-1889.71	-1889.7
50%	-1876.18	-1876.38	-1875.95	-1874.87	-1875.05	-1875.1	-1866.29	-1866.46	-1866.44
75%	-1854.15	-1854.04	-1854.03	-1852.7	-1852.92	-1853.02	-1844.21	-1844.06	-1844.05
90%	-1841.29	-1841.21	-1841.05	-1840.08	-1840.03	-1840.31	-1831.52	-1831.4	-1831.4
95%	-1836.9	-1836.74	-1836.79	-1835.9	-1835.88	-1835.88	-1827.25	-1827.08	-1827.12
99%	-1831.99	-1830.9	-1830.9	-1831.65	-1831.07	-1831.26	-1823.87	-1823.84	-1823.8
max	-1823.18	-1822.88	-1823.11	-1823.15	-1823.43	-1822.96	-1822.12	-1822.17	-1822.08

Utility	2100								
	Newbold & Cauchy	Newbold & Log-Normal	Newbold & Normal	Nordhaus & Cauchy	Nordhaus & Log-Normal	Nordhaus & Normal	Weitzman & Cauchy	Weitzman & Log-Normal	Weitzman & Normal
mean	191.0138	191.4778	192.1062	201.481	201.3629	201.4089	217.1513	218.6599	219.7695
std	62.08953	62.03804	61.57375	60.68154	60.65574	60.39438	63.9768	61.19554	60.59562
min	4.296142	26.89466	46.56827	48.6026	62.43745	66.00182	-89.6031	-4.07011	62.35708
1%	65.47633	68.4618	71.60796	87.13224	86.78264	87.57827	68.19567	100.0355	105.7515
5%	90.65808	90.48398	91.46452	102.0285	102.527	102.9453	117.9974	120.1543	121.2217
10%	104.7887	105.6563	106.4895	115.2241	115.6198	115.8248	130.1041	132.3623	133.788
25%	140.3018	141.1182	141.3603	150.8752	150.5101	150.4891	165.86	167.7545	169.0396
50%	194.2936	194.215	195.2641	204.8917	204.7516	204.8988	220.946	221.8644	222.9521
75%	243.2979	243.121	243.4597	253.5972	253.3762	253.5203	271.7161	271.2824	272.4177
90%	272.2358	272.3874	272.6386	280.9107	280.745	280.5326	300.4056	299.6869	299.8363
95%	283.4539	286.0436	285.1188	290.6332	291.5576	290.8513	310.4027	310.0416	309.8802
99%	301.7661	305.417	305.6845	304.2894	306.4833	306.2182	320.0372	320.5252	320.6267
max	326.0583	327.4401	327.2277	327.1825	325.8708	327.7221	328.8006	328.4825	328.7491

Utility	2150								
	Newbold & Cauchy	Newbold & Log-Normal	Newbold & Normal	Nordhaus & Cauchy	Nordhaus & Log-Normal	Nordhaus & Normal	Weitzman & Cauchy	Weitzman & Log-Normal	Weitzman & Normal
mean	1436.849	1438.009	1439.434	1457.478	1457.602	1457.876	1447.014	1458.814	1465.287
std	79.0225	77.53118	75.90737	72.6342	72.4416	71.89143	157.6267	95.12971	82.74122
min	1114.925	1172.167	1229.069	1229.381	1262.082	1277.204	-468.048	587.5702	1057.744
1%	1240.777	1270.009	1279.8	1311.413	1313.559	1316.354	697.5022	1165.276	1247.584
5%	1310.039	1310.058	1313.466	1338.229	1338.126	1339.43	1259.183	1299.67	1330.359
10%	1331.964	1333.028	1335.661	1355.239	1355.927	1356.552	1355.937	1350.191	1360.91
25%	1376.955	1378.072	1379.857	1398.365	1398.413	1398.643	1404.52	1400.011	1404.484
50%	1442.021	1440.918	1443.435	1462.456	1462.211	1462.848	1473.814	1467.356	1470.584
75%	1501.019	1499.709	1499.495	1518.894	1518.387	1518.486	1535.729	1531.632	1532.242
90%	1536.95	1539.016	1538.591	1551.17	1551.344	1550.702	1572.603	1572.174	1571.341
95%	1552.676	1558.169	1557.057	1563.796	1565.993	1564.679	1586.406	1587.308	1586.287
99%	1580.387	1585.076	1585.269	1583.567	1586.582	1586.409	1601.214	1603.098	1602.857
max	1611.662	1613.989	1614.15	1613.945	1612.103	1614.751	1615.733	1615.39	1615.533

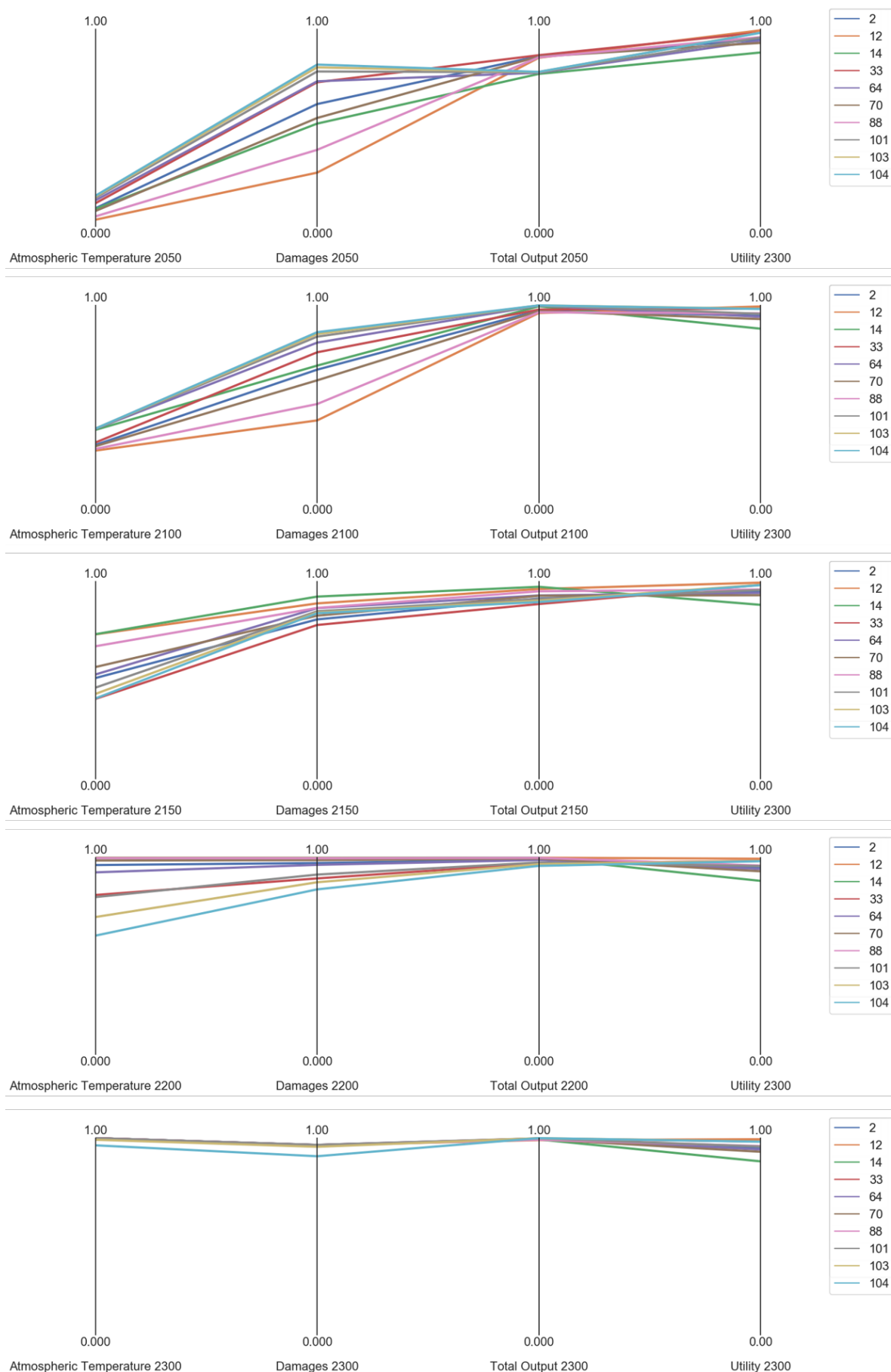
Utility	2200								
	Newbold & Cauchy	Newbold & Log-Normal	Newbold & Normal	Nordhaus & Cauchy	Nordhaus & Log-Normal	Nordhaus & Normal	Weitzman & Cauchy	Weitzman & Log-Normal	Weitzman & Normal
mean	2098.23	2099.97	2101.941	2122.924	2123.243	2123.698	2088.424	2114.765	2098.23
std	86.74489	83.10947	80.56394	76.10605	75.57416	74.81046	276.359	123.5182	86.74489
min	1670.682	1772.98	1862.82	1849.853	1900.439	1925.707	-289.78	554.7888	1670.682
1%	1854.825	1911.727	1927.095	1963.279	1969.465	1973.867	697.8662	1662.852	1854.825
5%	1959.704	1961.896	1967.683	1998.48	1998.274	1999.916	1837.288	1908.045	1959.704
10%	1987.228	1988.788	1992.522	2016.643	2017.706	2018.633	2010.253	1989.77	1987.228
25%	2036.452	2037.618	2040.147	2061.879	2062.338	2062.664	2066.355	2058.577	2036.452
50%	2105.486	2102.914	2105.774	2128.123	2128.173	2129.165	2139.527	2131.092	2105.486
75%	2166.714	2165.553	2164.884	2186.744	2185.812	2185.907	2204.715	2200.046	2166.714
90%	2204.96	2208.182	2207.101	2220.441	2221.006	2220.045	2243.543	2243.366	2204.96
95%	2222.153	2228.788	2227.656	2234.047	2236.738	2235.313	2258.314	2259.523	2222.153
99%	2252.727	2257.638	2257.631	2255.952	2259.078	2259.057	2274.253	2276.464	2252.727
max	2285.509	2288.215	2288.591	2288.285	2286.285	2289.21	2290.086	2289.91	2285.509

Utility	2300								
	Newbold & Cauchy	Newbold & Log-Normal	Newbold & Normal	Nordhaus & Cauchy	Nordhaus & Log-Normal	Nordhaus & Normal	Weitzman & Cauchy	Weitzman & Log-Normal	Weitzman & Normal
mean	2597.587	2599.746	2601.954	2623.29	2623.743	2624.288	2575.586	2613.886	2625.97
std	89.86781	84.65443	81.72026	77.17735	76.36318	75.50596	363.7902	133.1078	98.70358
min	2113.086	2249.727	2355.815	2329.66	2390.667	2421.08	-4605.04	621.4062	2026.532
1%	2332.076	2405.217	2423.203	2457.554	2467.111	2472.13	766.3556	2120.854	2304.394
5%	2455.023	2459.019	2465.666	2497.504	2497.349	2499.229	2319.622	2399.485	2459.525
10%	2485.059	2486.872	2491.135	2515.914	2517.259	2518.345	2509.626	2487.412	2511.355
25%	2535.861	2536.792	2539.577	2561.709	2562.382	2562.936	2566.997	2558.794	2563.978
50%	2605.819	2602.812	2605.848	2628.654	2628.747	2629.931	2641.04	2632.243	2635.139
75%	2667.681	2666.444	2665.569	2687.94	2686.766	2686.861	2706.554	2701.874	2702.092
90%	2706.282	2709.728	2708.529	2721.909	2722.536	2721.579	2745.659	2745.474	2744.405
95%	2723.814	2730.634	2729.531	2735.683	2738.541	2737.017	2760.462	2761.687	2760.679
99%	2754.882	2759.829	2759.8	2758.022	2761.231	2761.231	2776.534	2778.677	2778.435
max	2787.857	2790.668	2791.117	2790.774	2788.74	2791.737	2792.569	2792.459	2792.378

# E | UNCERTAINTY ANALYSIS

In this appendix, the two Figures E.1 and E.2 represents the output space of the selected robust policies from uncertainty analysis by using the criteria, minimax regret and signal-to-noise ratio. These figures are presented here as a complementary visualization to the Figures 10.4 and 10.6 in Section 10.3. Note that, the corresponding Jupyter notebook file “*MORDM Policies\_V4.ipynb*” can be found in the folder “*5\_Policy\_Discovery*” of the author’s GitHub repository.



**Figure E.1:** The output space of the ten most robust polices according to the SNR criterion

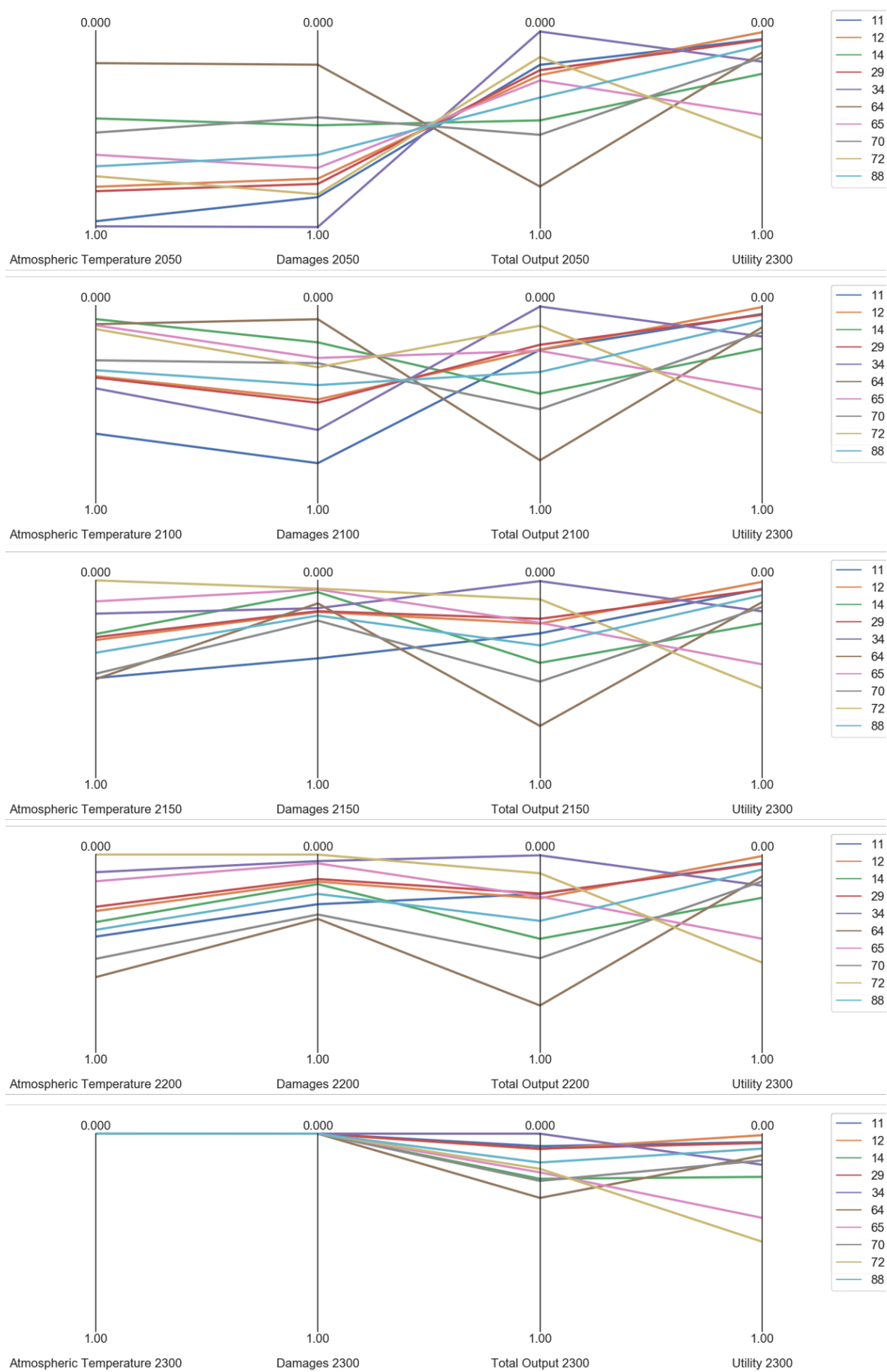


**Figure E.2:** The output space of the ten most robust polices according to the maximum regret criterion